Parametric and Mechanistic Studies of Biomass Conversion to High-Purity
Hydrogen with Integrated Carbon Fixation

Thomas E. Ferguson

Submitted in partial fulfillment of the
requirements for the degree of
Doctor of Philosophy
in the Graduate School of Arts and Sciences

COLUMBIA UNIVERSITY

2014

ABSTRACT

Parametric and Mechanistic Studies of Biomass Conversion
to High-Purity Hydrogen with Integrated Carbon Fixation

Thomas E. Ferguson

Due to the increasingly detrimental impacts of the global fossil fuel-driven energy economy, technological solutions that can mitigate the deleterious emissions from fossil fuel conversion or that can lessen societal dependence on fossil fuels are urgently required. The conversion of biomass, a renewable energy feedstock, into energy and fuels that are fungible with those derived from fossil fuels would help supplant some of the global fossil fuel consumption with sustainable energy generation. However, one of the main disadvantages of biomass as an energy feedstock when compared to fossil fuels is its low energy density. The majority of thermochemical biomass conversion technologies therefore focus on converting a low energy density feedstock in biomass to a higher energy density end product. Due to the operating parameters involved in these processes, they are typically accomplished on larger and more centralized scales by skilled operators. Few technologies exist that utilize biomass in a sustainable manner under a distributed energy framework, which would allow energy consumers to use locally available resources and waste material to generate energy.

The alkaline thermal treatment of biomass has recently been proposed as a novel method for producing high purity H_2 with suppressed CO_x formation under moderate reaction conditions (i.e., 573 K and ambient pressure). Essentially, biomass, which in this study were the model compounds of glucose and cellulose, is reacted with an alkali metal hydroxide, such as NaOH, in such a molar proportion that all of the carbon and oxygen embodied in the reactants is fixed as an alkali metal carbonate, while all of the elemental hydrogen is released as pure H_2 gas. Thus, fuel

cell ready H_2 can be produced from biomass in a single reactor. This technology has great potential for sustainable bioenergy production since it can handle a wide range of feedstocks including biomass and biogenic wastes with high water content. In addition to having the potential to be a distributed energy generation technology, the alkaline thermal treatment of biomass could help meet increasing industrial demand for H_2 in a more sustainable manner, as 96% of current H_2 generation is derived from fossil fuels.

The alkaline thermal treatment technology is also relatively unexplored; thus, the effects of parameters such as feedstock type, reaction temperature, heating rate, NaOH:Biomass ratio, method of reactant mixing, flow of steam, and concentration of steam flow, on the gaseous and solid products formed are not fully understood. This study was undertaken to quantify the effects of these non-catalytic variables on the alkaline thermal treatment reaction and to elucidate potential reaction pathways in order to better evaluate the potential of the alkaline thermal treatment technology as a viable biomass conversion technology.

In the study of the alkaline thermal treatment of glucose, NaOH did play an important role in suppressing CO_x formation while facilitating H_2 production and promoting CH_4 formation. The non-catalytic alkaline thermal treatment of glucose in the absence of steam flow resulted in a maximum H_2 conversion of about 27% at 523 K with a stoichiometric mixture of NaOH and glucose. The solids analysis confirmed the presence of Na_2CO_3 in the solid product, indicating the inherent carbon management potential of the alkaline thermal treatment process. The addition of steam flow increased conversion to H_2 from 25% to 33%, while decreasing total CH_4 formation 5 fold.

After the investigation of the alkaline thermal treatment applied to glucose, cellulose was studied as a feedstock because it is the predominant component of lignocellulosic biomass, the

target feedstock source for second generation biofuels. Like in the glucose study, it was found that H_2 and hydrocarbon formation occurred with the addition of NaOH to cellulose under thermal treatment, while the further addition of steam enhanced H_2 production and suppressed hydrocarbon formation. Both the enhancement of H_2 conversion and the suppression of hydrocarbon formation with the addition of steam flow was found to be more significant for cellulose than it was for glucose, with in the cellulose case H_2 conversion doubling from 25% to 48%, and CH_4 formation falling 35 times from the no steam flow case. Also like the glucose study, much of the carbon and oxygen present in the reactants were converted to Na_2CO_3.

With the knowledge gained about the effects various reaction parameters had on the alkaline thermal treatment reaction, a study of the reaction pathways of the alkaline thermal treatment of cellulose reaction was undertaken. Compounds formed at intermediate temperatures were identified, tested for gaseous production when reacted with NaOH, and the gas product formation rate trends of these reactions were compared with those trends observed from the alkaline thermal treatment of cellulose reaction. The intermediates identified included sodium carboxylate salts, namely sodium formate, sodium glycolate, and sodium acetate, among others. The reactions of these compounds with NaOH were found to yield H_2 and CH_4, with the gaseous formation rate trends being similar to trends observed for the alkaline thermal treatment reaction for cellulose in certain temperature regions. Particular focus was placed on sodium glycolate, which was an intermediate found in high concentration and that reacted with NaOH to produce both H_2 and CH_4. The formation of Na_2CO_3 at intermediate temperatures was also studied, and the comparison of Na_2CO_3 conversion to H_2 conversion at intermediate temperatures revealed that H_2 and Na_2CO_3 formation do not always occur at the 2:1 H_2:Na_2CO_3 molar ratio implied by the proposed stoichiometry of the alkaline thermal treatment reaction for cellulose. The

aforementioned studies were conducted both in the presence and absence of steam flow to study its influence on the reaction.

Finally H_2 formation kinetic studies were performed on the alkaline thermal treatment of cellulose system as well as the H_2-producing sodium carboxylate salt reaction systems. Sodium formate and sodium oxalate were found to have better selectivity toward H_2 formation and their reactions were more kinetically favored than sodium glycolate with NaOH. A comparison of the isothermal H_2 kinetics between the cellulose and sodium glycolate systems at higher temperatures, however, revealed that H_2 conversion in the alkaline thermal treatment of cellulose appeared to be limited by the rate of conversion of sodium glycolate. From the results of these studies, recommendations are made for future research directions aimed at improving the alkaline thermal treatment of cellulose reaction.

TABLE OF CONTENTS

LIST OF FIGURES

LIST OF TABLES

ACKNOWLEDGMENTS

Any scientific endeavor, especially one that has been five years in the making, by its very nature will have numerous tacit contributors, and it is my intention to use this space to acknowledge those whose contributions were most impactful on me. First are those investigators and entities who appear in this dissertation, namely cited authors and technical suppliers. For the cited authors, thank you, your insights made my insights possible. For the technical suppliers, I would like to single out Vince Giarroco from Inficon, Mark Sinnott from Agilent Technologies, Robert Mellen from Mellen Company, Stuart Procter from Metrohm, and Noah from Tech Air. These individuals in particular fielded innumerable questions from a then-clueless graduate student with the utmost professionalism and kindness, and went way beyond to ensure that I was both satisfied and comfortable with their products. I am especially pleased to acknowledge Noah from Tech Air, who handled our lab's technical gas supplies throughout my tenure at Columbia, and shot the breeze with me about football weekly, both during the season and through the interminable offseason.

I would like to acknowledge my dissertation committee members for their input into this work: Dr. Alexander Orlov, Dr. Paul Duby, Dr. Klaus Lackner, and Dr. Robert Farrauto. In particular I would like to specially thank Dr. Lackner and Dr. Farrauto for their major contributions. I was challenged by them after my proposal defense to really own this work, and in doing so to take it in a new direction. With their support I was able to accomplish this, and I am forever grateful that they believed in me.

One of the most important lessons I learned in graduate school was to never be afraid to ask questions or to ask for help, and I was so fortunate to have so many incredibly intelligent colleagues who were also so kind and giving of their time. Thank you for teaching me about

chemical engineering and myself: Dr. Camille Petit, Dr. Youngjune Park, Dr. Andrew Lin, Dr. Kyle Fricker, Dr. Edward Swanson, Dr. Greeshma Gadikota, Dr. Huangjing Zhao, Mr. Xiaozhou Zhou, Mr. Maxim Stonor, Mr. William Li, Mr. Alexander McCurdy, Mr. Timothy Sharobem, and Dr. Federico Barrai.

To my family: my sister Kathy Ferguson, my mother Kathleen Ferguson, and my father Thomas Ferguson, and to my friends, I dedicate this dissertation. You weren't with me in the lab, but you were there to pick me up, to play tunes with me, to go to shows with me, to chat on the phone or on Skype with me, and to make hilarious jokes with me. I could not have been in the lab all these years had you not been in all those places at all those times with me.

Finally, to my advisor, Professor Ah-Hyung ("Alissa") Park. You have supported me from the beginning and encouraged me to become the scientist that I am today. Your unceasing energy and passion for high-quality and high-impact research were a source of inspiration for my own work. I still remember the look on your face when I told you I hadn't taken any chemistry courses in college during one of our first meetings after you decided to take me on. So thank you for taking a chance on an erstwhile physicist.

The pursuit of a Ph.D. affords one the opportunity to view the boundary of human knowledge, to then push against it, and to finally expand it. This dissertation is the culmination of that privilege that you have all afforded me and of which you have all been an integral part the last five years. With humility and gratitude, I present it to you.

To all those who tirelessly strive to express themselves

CHAPTER 1

INTRODUCTION

Since the dawn of the Industrial Revolution, fossil fuels have been the dominant energy resource fueling the global energy economy (Olah 2005). Fossil fuels are formed over geologic time scales from the decomposition of organic matter under different temperature and pressure conditions. This decomposition process forms fuels that are extremely energy dense, making fossil fuels excellent energy sources. Due to their favorable energetic properties and their relatively lost cost, fossil fuels will continue to remain the dominant energy resource for the foreseeable future, with the U.S. Energy Information Administration projecting that fossil fuels will supply 80% of global energy demand out to 2040. Global energy demand is also expected to rise during this period by 56% from its present value, with the majority of this predicted increase attributable to developing countries (EIA 2013).

Major negative impacts from sociopolitical and environmental sustainability perspectives, however, have been concomitant with the fossil fuel-driven energy economy. First, from a sociopolitical perspective, fossil fuel resources are not uniformly distributed throughout the world, which has lead to conflicts among nations for energy resources. Second, the emissions associated with fossil fuel utilization have been shown to be harmful to the environment and to human health. In particular, CO_2, a significant emission product from fossil fuel combustion, has been shown to be the most significant driver of climate change according to the latest Intergovernmental Panel on Climate Change Report (IPCC 2013).

Various strategies are being explored to ameliorate these deleterious impacts resulting from our current fossil fuel-driven energy economy. Strategies include improving the efficiencies of fossil fuel utilization processes, employing energy conservation measures, reducing and/or

capturing the emissions associated with fossil fuel utilization, and investigating alternative, non-fossil energy schemes. Due to the complexity of the global energy economy, a portfolio of technologies and strategies will need to be employed in order to move toward a more sustainable energy future.

This study focuses on a non-fossil approach to sustainable energy generation: the alkaline thermal treatment of biomass. As an energy feedstock, biomass is carbon neutral, renewable, spread throughout the world, and has been estimated to be able to provide nearly 7.5% of global energy demand (McKendry 2002a). However, one of the major disadvantages of biomass as an energy feedstock compared to fossil fuels is its low energy density. Figure 1.1 is a plot of volumetric energy density versus gravimetric energy density for a range of energy feedstocks and energy carriers, adapted from Demirel (Demirel 2012). Biomass, which on the figure is represented by Forest residues and Wood, is shown to be relatively low in energy density on both volumetric and gravimetric bases. The low energy density of biomass as a feedstock directly affects which feedstock conversion schemes can be employed; for example, transportation of the feedstock to utilization sites becomes constrained (Phanphanich and Mani 2011). Thus, many thermochemical and biological-based technologies have been developed in order to convert biomass into fuels and chemicals fungible with those currently utilized in the global energy economy. Many of these technologies are operated under higher temperatures and pressures and are thus best deployed at specialized facilities under the supervision of skilled operators. On the other hand, the alkaline thermal treatment technology conceivably can be operated as a distributed energy generation scheme. In brief, the alkaline thermal treatment technology converts biomass into high-purity H_2 with little to no CO_x co-generation under relatively mild reaction conditions (i.e. 573 K and atmospheric pressure). This allows for a scalable reactor

2

design, and the produced H_2 can be directly fed to a proton exchange membrane (PEM) fuel cell to produce electricity, without any of the fuel reforming steps that are usually required in biomass-to-H_2 processes in order to reduce CO concentrations below the 10 ppm threshold for PEM fuel cell utilization (Zhang and Datta 2002).

H_2 generation via the alkaline thermal treatment technology is accomplished for the model compounds of glucose and cellulose through the following global reactions:

$$C_6H_{12}O_6 + 12NaOH = 6Na_2CO_3 + 12H_2; \quad \Delta H^0 = -404 \text{ kJ/mol} \quad \text{(Rxn. 1.1)}$$

$$C_6H_{10}O_5 + 12NaOH + H_2O = 6Na_2CO_3 + 12 H_2 \quad \text{(Rxn. 1.2)}$$
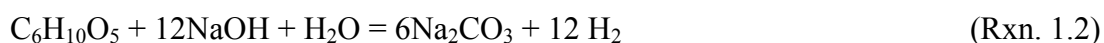
Thus the concept of the alkaline thermal treatment technology is to react the biomass feedstock with an alkali metal hydroxide, resulting in the fixation of all of the carbon and oxygen constituting the reactants in the form of an alkali metal carbonate, and releasing all of the hydrogen embodied in the reactants as H_2 gas. These reactions were previously investigated by Ishida et al., who studied non-catalytic H_2 formation from the alkaline thermal treatment reactions for several biomass feedstocks, as well as examined the effects of adding heterogeneous catalysis to the reactions (Ishida et al. 2005, Ishida et al. 2006).

Little literature aside from these studies exists on the alkaline thermal treatment technology, and thus the aim of this study is to explore the alkaline thermal treatment technology in greater detail, with emphases on the detailed characterization of reaction products, the effects of non-catalytic parameters on the reaction such as the NaOH:Biomass ratio and temperature, the identification of potential intermediate reaction pathways, and kinetic analyses of the identified intermediate reaction pathways and of the global alkaline thermal treatment reaction. The organization of this dissertation is as follows:

Chapter 2 provides more detailed background into the major biomass conversion technologies, with an emphasis on the thermochemical technologies, and reviews the alkaline thermal treatment technology and related work. The chapter will conclude with a statement of the Scientific Questions and Research Goals to be explored in this dissertation.

Chapter 3 explores the alkaline thermal treatment of glucose, the first model feedstock chosen for in-depth investigation. Glucose was chosen as a starting point because it is the monomer building block of the polymer cellulose, and cellulose makes up about half of lignocellulosic biomass feedstocks. Lignocellulosic feedstocks are the most abundant and cheapest of the biomass feedstocks, are non-edible, and are being targeted to produce second generation biofuels. In addition, as given by the reaction stoichiometry of Reaction 1.1, the alkaline thermal treatment of glucose does not stoichiometrically require steam as a reactant, providing a more simplified starting point for this relatively uninvestigated process compared to cellulose, which stoichiometrically does require steam as a reactant. The effects of reaction temperature and NaOH:Glucose ratio on gaseous and solid product formation are discussed, and greater detail into the gaseous and solid products is given than in previous studies.

Chapter 4 presents the results from the investigation of non-catalytic reaction parameters for the alkaline thermal treatment of cellulose. The chapter begins by bridging the glucose investigation detailed in Chapter 3 to the cellulose investigation through a comparison of the feedstocks in terms of the gaseous products formed under different reaction conditions. Subsequently, the investigation shifts to cellulose, and the effects of the NaOH:Cellulose ratio, the method of reactant mixing, and the presence and concentration of steam flow are revealed as they relate to the gaseous and solid products formed during the reaction. Finally, potential reaction pathways are proposed based upon the experimental results.

Chapter 5 builds upon the parametric study described in Chapter 4, going into much greater detail into the potential reaction pathways that may explain the observed gaseous products and formation trends observed from the alkaline thermal treatment of cellulose. Based upon a comprehensive literature review, sodium carboxylate salts were posited as intermediates of the alkaline thermal treatment reaction, which, after being formed through alkaline degradation, could then further react with NaOH to form gaseous compounds such as H_2 and CH_4, as well as Na_2CO_3. To test this hypothesis, the alkaline thermal treatment of cellulose reaction was studied at various intermediate temperatures up to 573 K and the solid products formed at these intermediate temperatures were characterized. Those solid intermediate products that were identified were subsequently tested for gaseous product formation through their reaction with NaOH under the same thermal conditions as were used for the cellulose system. The data from the intermediate systems and from the cellulose system were then compared in order to see if the formation and consumption of these intermediates could be linked to gaseous product formation in the alkaline thermal treatment of cellulose reaction. These studies were conducted both in the absence and presence of steam flow to elucidate its effect on the system.

Chapter 6 examines the sodium carboxylate salt intermediates that were identified to produce H_2 through their reaction with NaOH in more detail, focusing on the kinetics of the H_2 formation from these reactions. The H_2 formation kinetics of these sodium carboxylate salt intermediate reactions are also compared with the H_2 formation kinetics from the alkaline thermal treatment of cellulose. The conversion of sodium glycolate to H_2 appeared to be a rate-limiting step at higher temperature for the cellulose system, and its reaction with NaOH was explored in much greater detail, with a material balance proposed that was compared to the material balance proposed for the alkaline thermal treatment of cellulose. Results from the

kinetic studies are also related to the mechanistic study presented in Chapter 5. The chapter concludes with remarks about how to improve H_2 yield and lower the necessary reaction temperature for the alkaline thermal treatment of cellulose reaction based upon the kinetic results.

In order to evaluate the viability of the alkaline thermal treatment technology as well as to identify potential economic and sustainability barriers, economic and life cycle analyses must be carried out for potential applications of the technology. Chapter 7 presents economic and sustainability overview analyses for the case study of the alkaline thermal treatment of U.S. household waste.

Finally, Chapter 8 summarizes the key findings of this dissertation, giving the major conclusions as well as recommending future research directions based upon the findings.
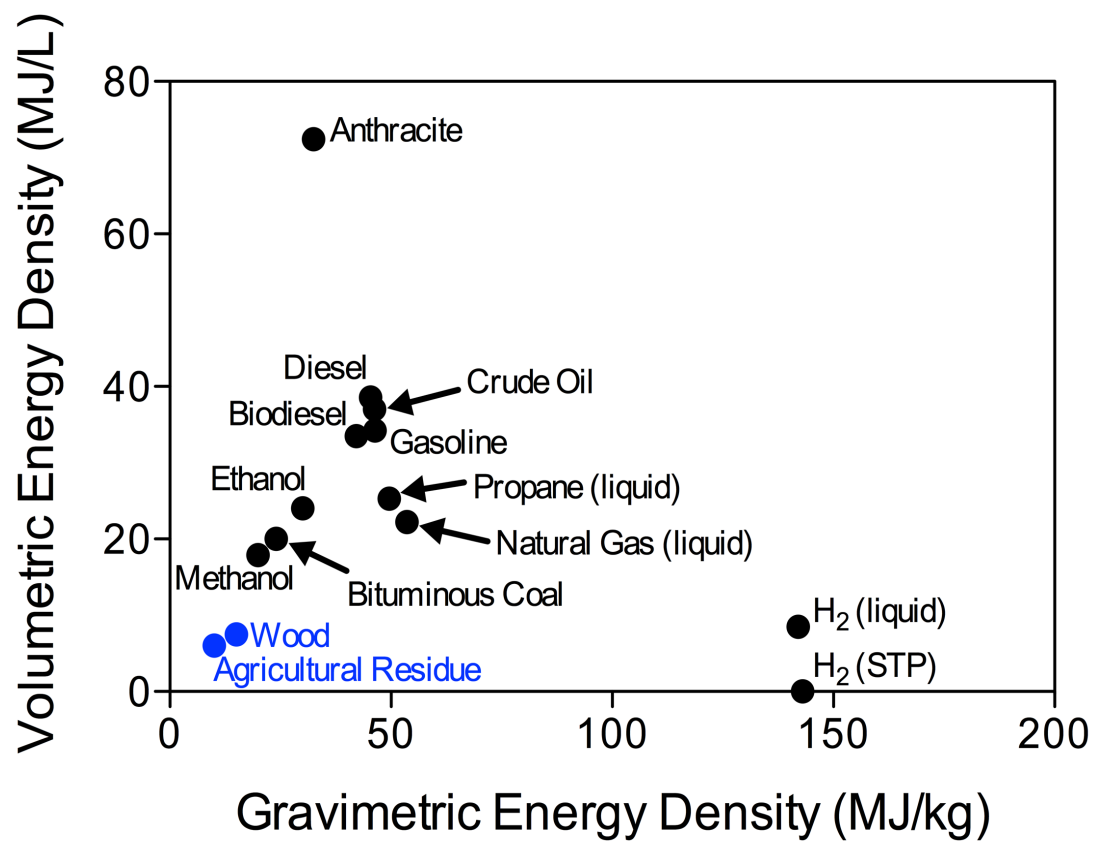
Figure 1.1 Volumetric and gravimetric energy densities for various energy carriers and fuels, with lignocellulosic biomass feedstocks highlighted in blue (Adapted from Demirel 2012).

CHAPTER 2

BACKGROUND

Biomass had been the dominant energy feedstock until fairly recently in human history, just prior to the beginning of the 20th century, which was when fossil fuels began to supply the majority of the world's energy (Smil 2005). Energy derived from biomass is expected to rise in the coming decades, increasing by 40% to 2030 from 2005 levels; however, when coupled to the projected increase in global energy demand, biomass is expected to continue to maintain its current 10% share of the total primary energy supply (TPES) out to 2030 (Cushion et al. 2010). Biomass energy is particularly important for the developing world, constituting over 30% of the TPES in South and East Asia and over 80% of the TPES in parts of the African continent (Smil 2005, Cushion et al 2010). Various biomass conversion technologies have been developed to convert the feedstock into a wide range of useful products, from heat to transportation fuels to commodity chemicals. These biomass conversion technologies generally fall under two broad categories: biological and thermochemical.

2.1 Biological Biomass Conversion Technologies

Biological biomass conversion processes utilize microorganisms and/or enzymes to convert biomass into fuels and chemicals. There are two main types of biological conversion processes: anaerobic digestion and enzymatic conversion. In anaerobic digestion, bacteria break biomass down, in the absence of O_2, into biogas, which is a mixture of CH_4 (60-70%) and CO_2 (20-40%). This biogas can be directly burned for heat or can be utilized in gas turbines to generate electricity (Srirangan et al. 2012, McKendry 2002b). On the other hand, in enzymatic conversion, biomass is first hydrolyzed into sugars by enzymes. The sugars are then converted

by yeast into ethanol through fermentation. In Brazil, the production of ethanol from sugarcane by fermentation is a major part of the country's energy economy, constituting 11% of the country's energy mix (Brazilian Energy Balance 2013). These biological conversion processes are advantageous in that they are highly selective, are operated at relatively low temperatures and ambient pressure, and can handle wet and dry feedstocks. However, these processes have poor kinetics relative to the thermochemical conversion processes and are more challenged in converting lignocellulosic feedstocks, the most inexpensive and prevalent biomass feedstock type (Huber et al. 2006, Brown 2011, McKendry 2002a, Srirangan et al. 2012).

2.2 Thermochemical Biomass Conversion Technologies

Thermochemical conversion processes, on the other hand, break the biomass down into useful products through the application of higher temperatures relative to the biological processes and, depending on the process, the application of other reaction parameters (e.g. pressure, catalysts). Although less selective than the biological processes, thermochemical biomass conversion is characterized by much better kinetics and the various thermochemical processes are able to convert a wider array of feedstocks. There are five main categories of thermochemical conversion technologies: combustion, gasification, pyrolysis, hydrothermal processing, and hydrolysis to sugars (Brown 2011).

Biomass combustion is the thermal reaction of biomass with O_2 to produce heat for energetic applications, and is the most well-established of the thermochemical routes. Combustion of biomass can take place at very small scales, such as in cooking or home heating, as well as at larger, industrial scales (100 – 3,000 MW). The main drawbacks of combustion include the production of heat as the only energetic product, the inability to handle high moisture

content feedstocks (i.e. >50%), and emission products that can foul the combustion process and that are harmful to human health (Brown 2011, McKendry 2002b, Srirangan et al. 2012).

Gasification is the partial oxidation of biomass to produce syngas, a mixture of CO and H_2. The produced syngas can be utilized in a number of ways, including direct use in a gas turbine, downstream processing of the syngas to produce high-purity H_2 suitable for fuel cells, and conversion of the syngas into other fuels and chemicals through Fisher-Tropsch synthesis (Kumar et al. 2009, Brown 2011, Srirangan et al. 2012, McKendry 2002b). In gasification, biomass is partially oxidized in a controlled atmosphere that can consist of air, steam, and/or O_2 at temperatures typically between 873 K – 1273 K. These conditions act to degrade the biomass into light gases such as those constituting syngas, as well as CH_4 and other light hydrocarbons. Also, depending on the reaction conditions, ash, char and tar can be co-produced, which can both foul the reactor as well as any catalysts present. The type of gasifier used, fixed-bed or fluidized, the biomass feedstock, the gasification temperature, the type of atmosphere in which gasification takes place, the Biomass:Oxidizing agent ratio, the process input flow rates, and the use of catalysts can all affect the products resulting from biomass gasification (Kumar et al. 2009). Due to the flexibility offered by gasification in terms of the resulting energetic products, it remains the subject of much investigation (Asadullah et al. 2002, Asadullah et al. 2003, Asadullah et al. 2004, Nishikawa et al. 2008, Hanaoka et al. 2005).

In biomass pyrolysis, biomass is thermally degraded under anoxic conditions to produce gases, liquids, and char in different proportions depending on the pyrolysis conditions (Brown 2011). The temperature at which pyrolysis takes place as well as the residence time significantly impact the products of pyrolysis. Pyrolysis temperatures can range from around 623 K – 1073 K (Srirangan et al. 2012) and residence times can range from less than a second to days. Low

temperature and long residence time favor the formation of char, high temperature and long residence time increases gas production, and intermediate temperature and short residence time favors liquid product formation (Bridgwater 2012). This later combination of intermediate temperature and short residence time is characteristic of fast pyrolysis, which is the pyrolysis technique that is receiving the most attention in the literature for its ability to produce easily storable and transportable bio-oil. Bio-oil can be used as boiler fuel, utilized in engines and turbines to generate electricity, or can be upgraded to transportation fuels and commodity chemicals (Bridgwater 2012). However, bio-oil must overcome the issues of poor thermal stability, corrosivity, and inconsistencies due to the heterogeneous nature of biomass (Srirangan et al. 2012, McKendry 2002b, Bridgwater 2012).

Combustion, gasification, and pyrolysis necessitate dry feedstocks for best performance. In the case where the biomass feedstock is high in moisture content (i.e. >35 wt%), hydrothermal treatment is the better-suited conversion technology to avoid the energy penalty associated with drying the feedstock (Navarro et al. 2007). Like with the other thermochemical conversion technologies, process conditions influence the types and predominant phase of the formed degradation products. Hydrothermal treatment of biomass in subcritical water (i.e. 553 K – 643 K and 10 – 25 MPa) produces mainly bio-oil, whereas reaction in supercritical water (i.e. > 647 K and > 22.1 MPa) favors the gasification products of H_2, CO, CO_2, and CH_4 (Toor et al. 2011). Due to the high pressures involved, hydrothermal treatment of biomass faces particular challenges in reactor and fuel-feeding system design (McKendry 2002b, Srirangan et al. 2012, Brown 2011).

Similar to enzymatic conversion of biomass via the biological pathway, hydrolysis to sugars describes thermochemical biomass conversion techniques where the biomass is

depolymerized into sugar monomers, which can then be converted to fuels. Acid hydrolysis, where a dilute acid such as H_2SO_4 or HCl breaks down lignocellulosic biomass into its constituent sugars, is one of the major hydrolysis techniques (Lenihan et al. 2010, Saeman 1945, Oefner et al. 1992). From the sugars, fermentation can be applied to produce ethanol, or catalysts can be employed to convert the sugars into fuels and platform chemicals, such as furans (Brown 2011). In particular, aqueous phase processing (APP) is a technique developed to convert biomass-derived sugars into alkanes, which are platform chemicals for synthesizing transportation fuel (Huber et al. 2005, Huber et al. 2006, Brown 2011). Sugars are reformed by APP at moderate temperature and pressure conditions (473 K – 533 K and 1 – 5 MPa) over heterogeneous catalysts. A schematic summary of the five major thermochemical biomass conversion processes is given in Figure 2.1.

As exemplified by the preceding discussion on thermochemical biomass conversion via hydrolysis to sugars, the use of additives in thermochemical processing can greatly alter the thermochemical degradation of biomass to favor a variety of desired products. One conversion product that can be selected for, and that has received considerable attention in the literature, is H_2. H_2 is a clean energy carrier, as its reaction with O_2 to produce energy only yields water as a byproduct. Industrially, around 50 million metric tons of H_2 are produced per year (Navarro et al. 2007, Balat and Balat 2009). This H_2 is utilized in a number of processes, including ammonia and methanol production, oil upgrading in refineries, and to lesser extents in energy production schemes, such as in fuel cells (Levin and Chahine 2010). Demand for H_2 is projected to grow in the near future, largely due to its use in refining crude oil that is increasingly becoming heavier and more sulfur-rich and the projected increase in the demand for ammonia. Demand could be even larger depending on the extent of the penetration of fuel cell technologies into the

transportation and energy generation markets in the near future (Levin and Chahine 2010). Currently, 96% of H_2 generation comes from fossil fuel resources (Balat and Balat 2009), and the generation methods are energy intensive; thus, the increased use of a renewable feedstock such as biomass could improve the sustainability of H_2 production (Mohan et al. 2008).

2.3   Thermochemical Biomass-to-H_2 Conversion in the Presence of Alkaline Additives

Considerable study has been done on the addition of alkaline additives to the aforementioned thermochemical conversion technologies to increase H_2 yields from biomass. Early studies reported H_2 gas as a byproduct when trying to thermally convert biomass in the presence of NaOH to products such as oxalic acid (Hsu and Hixson 1981, Othmer et al. 1942, Mahood and Cable 1919). More recently, Su et al. conducted a series of studies on the reactions of cellulose and lignin, components of lignocellulosic biomass, with a catalyst containing NaOH at ambient pressure under an inert atmosphere, and found that the dehydrogenation of cellulose to form H_2 was more favored at relatively low temperature, between 473 K and 623 K, with increasing NaOH concentration in the catalyst (Su et al. 2008, Su et al. 2010a, Su et al. 2010b). Another group conducted studies where feedstocks such as cellulose, polystyrene, and poly(vinyl alcohol), were first milled with different metal hydroxides, such as calcium and lithium, and then were thermally treated under an inert atmosphere at ambient pressure. They found that high-purity H_2 (>95%) was produced below 773 K, and that carbonate was a significant solid product (Zhang et al. 2009, Tongamp et al. 2010). Many groups have also examined the use of alkaline earth metal oxide sorbents to enhance H_2 production from the steam gasification of biomass. H_2 production is enhanced by the fixation of CO_2 produced during gasification by the sorbent as a carbonate, shifting the equilibrium of the water-gas shift reaction to favor greater H_2 production (Florin and Harris 2008, Ni et al. 2006, Lin et al. 2002, Lin et al. 2004, Hanaoka et al. 2005).

Many hydrothermal biomass conversion studies have also taken place in the presence of alkaline additives. The addition of alkali metal hydroxides, such as NaOH and KOH, was found to decrease tar yields and enhance H_2 production in subcritical water gasification, supercritical water gasification, and APP (Liu et al. 2010, Xu et al. 2006, Schmieder et al. 2000, Wantanabe et al. 2002). It was proposed that the alkali acts to suppress the dehydration and polymerization pathways of biomass thermal degradation while promoting the formation of smaller organic species, which can further degrade into CO. The CO is the converted to H_2 via the water-gas shift reaction, which is enhanced by removal of the CO_2 by the alkali additive (Onwudili and Williams 2009, Onwudili and Williams 2010, Yu and Savage 1998, Jin et al. 2008, Onsager et al. 1996).

2.4   The Alkaline Thermal Treatment of Biomass to Produce High-Purity H_2

The alkaline thermal treatment of biomass is yet another example of adding an alkaline material into a biomass thermochemical reaction to produce high-purity H_2 at relatively mild reaction conditions (i.e. 573 K and atmospheric pressure). As described in Chapter 1, the concept of the alkaline thermal treatment of biomass is to eliminate potential CO_x emissions during thermal treatment by capturing all of the carbon and oxygen embodied in the reactants as alkali metal carbonate, thereby releasing pure, fuel cell-ready H_2 gas. The reaction conditions and high H_2 purity allow for the potential design of a compact and scalable energy generation system that can be utilized by unskilled operators. This is in contrast to many of the more traditional thermochemical conversion processes, which because of the reaction conditions involved or the necessity for additional product reforming, require more complex reactors and the use of skilled operators. In addition to being able to generate H_2 from biomass and thus reduce dependence on fossil fuel-based H_2, the alkaline thermal treatment of biomass could have some especially

interesting niche applications, including energy generation from household waste, energy generation for farming applications from agricultural waste, and energy generation in the pulp and paper industry, as NaOH, a potential reactant in the alkaline thermal treatment technology, is a major chemical used in the paper industry.

The alkaline thermal treatment of biomass was first explored by Ishida et al. in two studies. The first study primarily examined the effects of feedstock and alkali metal hydroxide type on the formation of H_2 and CH_4. Regarding the effect of feedstock, cellulose, D-glucose, sucrose, and starch were reacted with NaOH under steam flow up to 873 K. Conversions of H_2 according to the stoichiometries of the alkaline thermal treatment reactions for each feedstock were 62%, 40%, 44%, and 42%, respectively, and the observed maximum H_2 formation rate for each feedstock occurred below 600 K. Regarding the effect of alkali metal hydroxide type, LiOH, NaOH, and KOH were each reacted with cellulose under steam flow up to 873 K. Conversions to H_2 according to Reaction 1.2 were 8%, 62%, and 72%, respectively. Minimal CH_4 was formed in the cellulose and LiOH reaction, whereas CH_4 formation became more significant than H_2 formation above 650 K for the NaOH system and above 700 K for the KOH system (Ishida et al. 2005).

In the subsequent study, catalysts were applied to the reaction of NaOH and cellulose under steam flow in an attempt to improve H_2 conversion. Several catalyst metals and different catalyst supports were studied and compared to the non-catalytic alkaline thermal treatment of cellulose system. In particular, Ni/Al_2O_3, Co/Al_2O_3, Ru/Al_2O_3, and Rh/Al_2O_3 increased H_2 conversion from 62% to nearly 100%, while suppressing CH_4 formation. Different supports were tested for the nickel catalyst (i.e. TiO_2, ZrO_2, SiO_2, Cr_2O_3, CeO_2) and all yielded about 100% H_2 conversion, as was also found in the Al_2O_3 case. These nickel catalysts on different supports

were recovered and tested for their durability in one or two repeated trials. The most significant deactivation was found for Ni/ZrO_2, followed by Ni/CeO_2, and then Ni/Al_2O_3. On the other hand, Ni/TiO_2 and Ni/Cr_2O_3 did not experience significant deactivation in repeated trials. Regarding the solid product remaining after the alkaline thermal treatment reaction, only that most of the product was Na_2CO_3 for the non-catalytic case was reported. In this study as well as in the previous study, no CO_x gases were detected (Ishida et al. 2006).

The alkaline thermal treatment of glucose has also been studied in the presence of electrospun nanocatalysts of iron on silica nanofibers. NaOH was the alkali metal hydroxide used and reaction temperatures up to 573 K were studied. Conversion of glucose according to Reaction 1.1 improved with the addition of the nanocatalysts, increasing from 41% to as high as 81%. Unlike what Ishida et al. observed for the cellulose system upon the addition of catalysts, the addition of the nanocatalysts did not completely suppress CH_4 formation from the alkaline thermal treatment of glucose; however, H_2 and CH_4 were found to form in distinct temperature regions, 393 K – 473 K for H_2 and 473 K – 573 K for CH_4, thus indicating that high-purity H_2 could be produced from the catalytic alkaline thermal treatment of glucose at low temperatures. Analysis of the solid product from the nanocatalyst study revealed that it was predominantly Na_2CO_3 (Hansen et al. 2011).

2.5 Research Objectives

2.5.1 Problem Statement

The alkaline thermal treatment technology has shown the potential to generate high-purity H_2 from model biomass feedstocks at relatively mild reaction conditions, opening the door for potential niche applications such as in distributed energy generation. However, few studies have been conducted on alkaline thermal treatment, and thus understanding of the full spectrum

of reaction products, the effects of varying different reaction parameters on the reaction, and of the potential reaction pathways, is lacking. Through an improved understanding of the effects of the non-catalytic reaction parameters on product formation from alkaline thermal treatment, as well as an improved understanding of the reaction pathways that lead to gaseous product formation, reactor and process design could be improved and smarter catalyst design would also become possible.

A process flow diagram for the alkaline thermal treatment process is given in Figure 2.2. Assuming complete conversion of the biomass via the alkaline thermal treatment process, two product streams result. The first is for H_2, which because it is not accompanied by any CO_x emissions, can be directly used in processes to synthesize chemicals and fuels, or be directly fed into a PEM fuel cell to produce electricity. The second is the metal carbonate, which for the case of Na_2CO_3 can be regenerated into NaOH through its reaction with $Ca(OH)_2$:

$$Na_2CO_3 + Ca(OH)_2 = 2NaOH + CaCO_3; \qquad \Delta H^0 = \ 57 \ kJ/mol \qquad \text{(Rxn. 2.1)}$$

This reaction is commonly employed in the Kraft Recovery Process in the paper industry. The $CaCO_3$ can then either be calcined to evolve pure CO_2 or be sequestered. The regenerated NaOH is fed back into the alkaline thermal treatment reactor to complete the process. Since the focus of this study was on the alkaline thermal treatment reaction, only the Alkaline Thermal Treatment Reactor, highlighted in the blue box in Figure 2.2, was considered in this study.

2.5.2 Scientific Questions and Research Goals

The key scientific questions underpinning this research are:

- How do non-catalytic reaction parameters such as temperature, NaOH:Biomass ratio, and steam flow effect the gaseous and solid products formed in the alkaline thermal treatment reaction for the model compounds of glucose and cellulose?

- What are the roles of NaOH and steam in the alkaline thermal treatment reaction?

- What are some of the major reaction pathways leading to the observed gaseous and solid product formation in the alkaline thermal treatment of cellulose?

- Are certain H_2-producing reaction pathways more favorable than others, in terms of having higher selectivity for H_2 generation and/or being more kinetically favorable at lower temperature?

The key goals of this research are as follows:

- To study the effects of reaction temperature on product formation in the alkaline thermal treatment of glucose and cellulose and identify temperature conditions where the best balance of H_2 formation kinetics and selectivity are achieved.

- To examine how the addition of NaOH and steam flow alter the thermal decomposition of glucose and cellulose and to identify the optimum concentrations of both to maximize H_2 production while minimizing side product formation.

- To identify the intermediates species of the alkaline thermal treatment of cellulose reaction, both in the presence and absence of steam flow, and to propose reaction pathways from these observed intermediates to explain the observed gaseous and solid product formation in the alkaline thermal treatment of cellulose.

- To subject these proposed reaction pathways involving the identified intermediates to the same thermal treatment conditions as in the alkaline thermal treatment of cellulose system in order to observe if correlations exist in gaseous formation rate trends.

- To compare H_2 and Na_2CO_3 conversions as a function of reaction temperature in order to ascertain if the $H_2:Na_2CO_3$ molar formation ratio is always 2:1 as given by the stoichiometries of Reaction 1.2 for cellulose, or if the overall $H_2:Na_2CO_3$ molar formation ratio changes as a function of temperature, indicating different reaction pathways.

- To probe the kinetics of H_2 formation from the alkaline thermal treatment of cellulose as well as of the H_2-producing intermediate reactions, and attempt to identify a rate-limiting step in H_2 conversion in the non-catalytic alkaline thermal treatment of cellulose.

- To apply the kinetic data obtained from the reaction of the intermediate species to make recommendations for future research directions aimed at improving H_2 generation from the alkaline thermal treatment of cellulose and the overall energetics of the process.
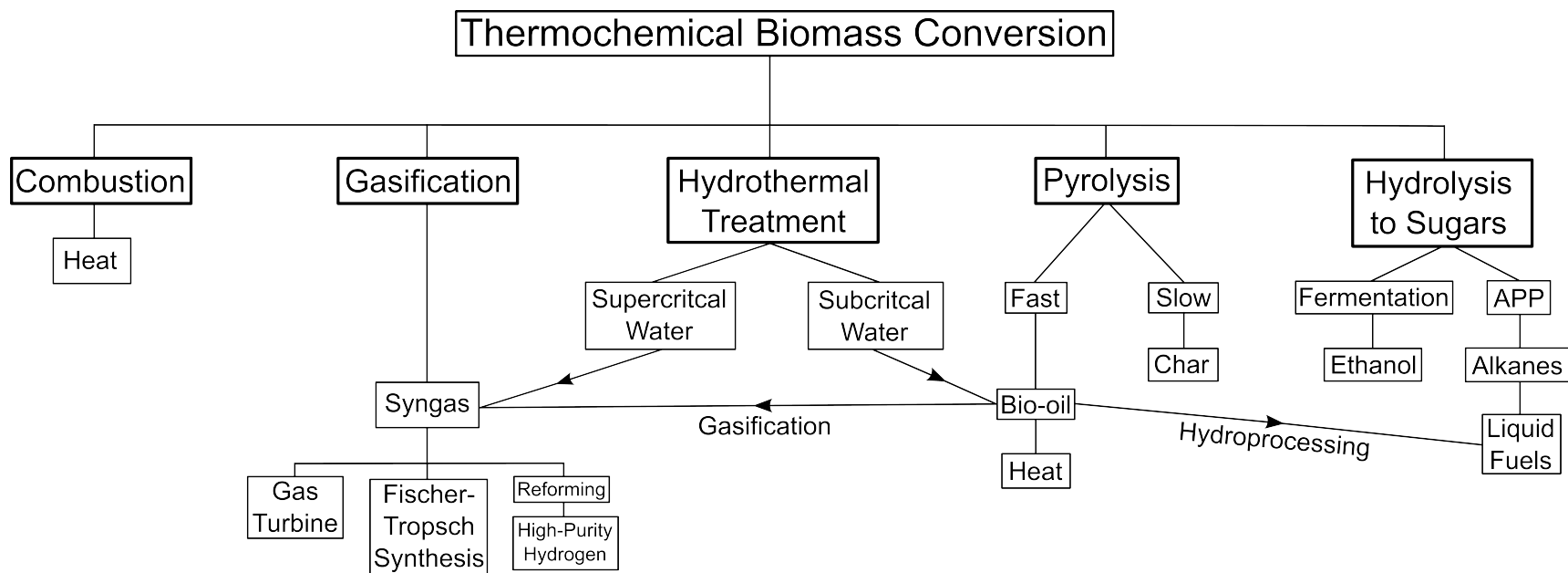
Figure 2.1 Process flow diagram for the conversion of biomass to high-purity H_2 via the alkaline thermal treatment technology.
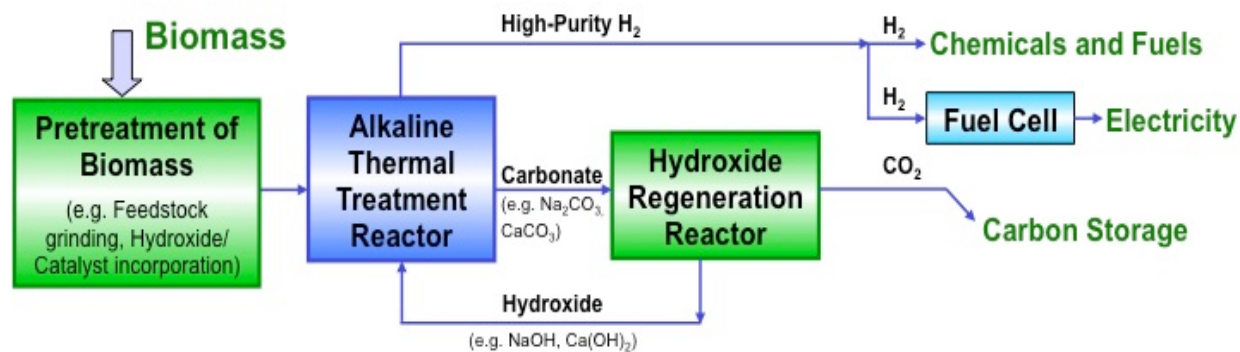
Figure 2.2 Schematic of the fundamental thermochemical biomass conversion techniques.

CHAPTER 3

A NOVEL APPROACH TO HYDROGEN PRODUCTION WITH SUPPRESSED CO$_X$ GENERATION FROM GLUCOSE

3.1 Introduction

In 2010, it was reported that fossil fuels accounted for $80 - 90\%$ of global energy consumption (Stambouli 2011), and they will continue to be the predominant source of energy for the foreseeable future, considering that they are still the most abundant and affordable source of energy. Rapid economic growth in developing countries such as China and India will further amplify the increasing demand for fossil fuels. Unfortunately, fossil fuel resources are not uniformly distributed in the world, and thus, many nations depend on importation for much of their fuel supply. The utilization of fossil fuels also results in the emission of many environmentally detrimental byproducts, including greenhouse gases. Therefore, the issues of energy security and imbalances in the global carbon cycle brought about by anthropogenic carbon emissions have prompted much investigation into new sustainable fuel and energy generation paradigms. Achieving a sustainable energy pathway requires both a multifaceted technological solution and the use of various energy sources. In particular, the development of efficient energy conversion schemes is desired for alternative feedstocks, rather than simply applying conventional fossil energy conversion technologies to them.

As an alternative energy resource, biomass is feedstock that is renewable, carbon neutral, diverse, and diffusely spread throughout the world. In the United States, the U.S. Energy

Information Administration (EIA) predicts that energy consumption from biomass will increase 2.9% annually from the period of 2009 to 2035, comprising 4.6% of U.S. energy consumption by 2035. For the developing world, which the EIA is projecting to have an 84% increase in energy demand versus a 14% increase for the developed world by 2035 (EIA 2011), biomass is a crucial energy resource. In 2001, nearly 50% of Africa's total primary energy supply was from biomass and waste (Amigun 2008). Biomass will therefore be an important energy feedstock for decades to come; however, it must be utilized in a sustainable and efficient manner.

As biomass is a very low energy density feedstock, thermochemical pathways have been developed to increase its energy density. One pathway is through the conversion of biomass to bio-crude via pyrolysis (Kalinci et al. 2009, Mohan et al. 2006, Bridgwater and Peacocke 2000, Meier and Faix 1999). Biomass feedstocks can also be converted into a synthesis gas (i.e., CO and H_2) through conventional or supercritical gasification processes, the latter being more well-suited to biomass feedstocks with greater than 35 wt% moisture content (Kalinci et al. 2009, Demirbas 2005, Navarro et al. 2007, Sutton et al. 2001). Fischer−Tropsch synthesis can then be employed to make hydrocarbon fuels from the synthesis gas. Most of these thermochemical processes can be made to be highly flexible, allowing for a range of fuels to be made from a wide variety of biomass feedstocks. However, there has been less investigation into processes where biomass can be utilized as a feedstock in a local, distributed generation scheme, one that does not require increasing the energy density of the feedstock through fuel conversion to make fuel transportation feasible. Distributed biomass conversion is particularly attractive for the developing world and rural communities, as many of these regions lack the infrastructure necessary for a large scale grid. The aforementioned thermochemical conversion technologies, such as gasification and pyrolysis, can also be scaled down into small units, but due to their high

operating temperatures and pressures the main difficulties of their distributed small scale deployment will lie in the need for skilled operators and the issue of safety. Therefore, the development of a biomass conversion scheme that can safely be operated at lower temperature and pressure is desired.

Several studies have been conducted to investigate one-step H_2 production methods from biomass primarily through the addition of alkaline and alkaline earth hydroxides, which transfer the carbon in the biomass to a stable, solid carbonate while producing H_2. Thus, unlike gasification and pyrolysis where both carbon and hydrogen remain in the fuel streams, this technology allows for inherent carbon management by fixing carbon in a solid carbonate matrix while maximizing H_2 production. Saxena proposed this concept in 2003, applying it to the reaction of carbon with NaOH and steam (Saxena 2003):

$$C + 2NaOH + H_2O = 2H_2 + Na_2CO_3; \qquad \Delta H^0 = -37 \text{ kJ/mol} \qquad \text{(Rxn. 3.1)}$$

Subsequently, alkaline thermal treatment of carbonaceous materials to produce H_2 has been applied to a number of biogenic feedstocks (Ishida et al. 2004, Zhang et al. 2009, Tongamp et al. 2010, Su et al. 2008, Su et al. 2010a, Su et al. 2010b, Saxena et al. 2008, Kumar et al. 2011, Hansen et al. 2011). With regard to biomass, Ishida et al. carried out a number of interesting studies on its alkaline thermal treatment using Ni-based catalyst to produce CO- and CO_2-free H_2 under relatively low temperature and atmospheric pressure conditions, while producing solid product, Na_2CO_3, which is an environmentally benign, potentially value-added product (Ishida et al. 2005, Ishida et al. 2006). The produced H_2 can be used to generate electricity using a number of energy conversion systems including fuel cells. The fuel cell technology offers a highly adaptable and efficient way to generate energy in a local, distributed framework. Specifically, the

polymer electrolyte membrane (PEM) fuel cell confers a number of benefits, which include low operating temperature, quick start up time, high energy density, and water vapor as the only source of emission (Heck et al. 2009). However, the catalyst in a PEM fuel cell can be irreversibly poisoned by CO with concentrations as low as $5 - 10$ ppm (Zhang and Datta 2002). Thus, the alkaline thermal treatment of biomass offers the potential to produce H_2 from biomass that can be directly fed into a PEM fuel cell without the need for reforming or gas cleanup processes to lower the CO concentration. Also, because the alkaline thermal reaction of biomass occurs at low temperature (thermodynamically and kinetically favorable at less than 573 K) and atmospheric pressure, a simplified and compact reactor design becomes possible. The overall reactions of glucose and cellulose with NaOH in the absence of oxygen can be written as:

$$C_6H_{12}O_6 + 12NaOH = 6Na_2CO_3 + 12H_2; \quad \Delta H^0 = \text{-404 kJ/mol} \quad \text{(Rxn. 3.2)}$$

$$C_6H_{10}O_5 + 12NaOH + H_2O = 6Na_2CO_3 + 12H_2 \quad \text{(Rxn. 3.3)}$$
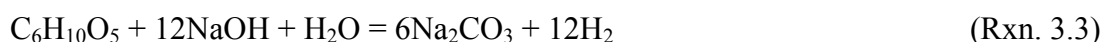
As shown in the above reactions, this scheme of bioconversion requires water for the systems using cellulosic biomass. Thus, alkaline thermal treatment can be readily used for a wide range of biomasses including the ones with high water content, whereas most of conventional thermal biomass conversion technologies such as gasification and pyrolysis prefer dry feedstocks.

With the addition of Ni-catalysts, Ishida et al. found cellulose conversions to H_2 close to 100% (Ishida 2006). Since this work, Su et al. have investigated H_2 conversion from cellulose using a novel $Al_2O_3 \cdot Na_2O \cdot xH_2O/NaOH/Al(OH)_3$ ionic catalyst containing the base. Their catalyst achieved as high as 60% H_2 conversion; however, with this approach CO concentration in the gaseous product stream was as high as 700 ppm under similar reaction conditions. It was reported that greater conversions to H_2 are observed as the sodium content in the catalyst was

increased (Su et al. 2008, Su et al. 2010a, Su et al. 2010b). None of the prior studies provided detailed analyses of gaseous and solid products during the alkaline thermal treatment of biomass, and thus, the reaction mechanisms are still poorly understood.

Therefore, this study focused on a systematic kinetic and mechanistic investigation of the non-catalytic alkaline thermal treatment of glucose, a surrogate for biomass. One of the important differences in this study to those conducted previously (Ishida et al. 2005, Ishida et al. 2006) was the use of solid NaOH powder mixed in with glucose as opposed to pretreated glucose using NaOH solution. The motivation for this was to avoid the energy penalty associated with the evaporation of the solvent, water, used in NaOH solution. The effects of the reaction temperature and the NaOH:Glucose reactant ratios on H_2 conversion, purity, and formation rates of gaseous products including CH_4, CO, and CO_2 were quantitatively investigated, while the compositions of solid products were determined to further probe the reaction pathways.

3.2   Materials and Methods

3.2.1   Experimental Setup and Procedure

The schematic of the experimental setup used in this study is shown in Figure 3.1. In order to maximize mass transfer during the reaction, NaOH (Acros) pellets were ground together with procured D-(+)-Glucose powder using a mortar and pestle. For the majority of experiments, 2.35 g of mixed sample was added to a 10 ml ceramic boat, which was placed inside a quartz tube reactor (2.54 cm O.D. × 91.44 cm length) operated at ambient pressure. In the case of experiments involving variation in reactant ratios, different total amounts of sample were used, whose amounts are given in section 2.2. The reactor was then sealed with ultra-torr fittings (Swagelok) and placed inside a three-zone horizontal split-tube furnace (Mellen Company, SC12R). Once the reactor was secured, N_2 carrier gas was introduced through the reactor via a

mass flow controller (Omega FMA5508) at a flow rate of 90 ml/min for 30 min prior to the experiments to purge the system. This carrier gas flow rate was also maintained throughout the experiments, with N_2 acting as a reference gas in gas chromatography (GC) measurements. Temperature in the reactor was raised at a constant ramping rate of 1 K/min from room temperature to the final reaction temperature, where the reactor temperature was held isothermally until the end of each experiment. Temperature inside the quartz tube reactor was monitored with a thermocouple situated above the ceramic boat.

The gaseous products exiting the reactor along with the carrier gas were sampled online throughout and analyzed by the GC (Agilent 7890A GC). First, a mass spectrometer (Agilent 5975C MS) attached to the GC was used to scan for all the gaseous species, and the major gaseous products were identified. For the subsequent gas analyses, a method was developed to quantify four important gaseous products: H_2, CO, CO_2, and CH_4, using the GC with two separate detectors, with an average sampling rate of 12 min per sample taken from the online gaseous product stream. A thermal conductivity detector (TCD) allowed for a detection limit for H_2 of 0.1%, while a flame ionization detector (FID) with an upstream nickel methanizer catalyst allowed for a 1 ppm detection limit for CO, CO_2, and CH_4. Chromatographic separation was done via a 60 m Agilent GS-GasPro column. All experiments were terminated once the concentration of H_2 in the gas stream fell below the detection limit of the TCD of 0.1%.

A Micro GC (Inficon 3000) was also used to analyze the gaseous products online. The Micro GC was equipped with two 10 m Molsieve columns for H_2, N_2, CH_4, and CO analyses, and an 8 m Plot U for CO_2 and C_2H_6 analyses. Its detection limit for CO was 10 ppm and the sampling rate was 4 min per sample, which was significantly faster than that of the Agilent GC. However, the Agilent GC's detection limits were significantly lower for carbonaceous

compounds. Thus, the Micro GC was used only for the fast kinetic studies discussed in section 3.3.3.

3.2.2 Investigations of Reaction Parameters

The effect of reaction temperatures on the alkaline thermal treatment of glucose was investigated in terms of the H_2 conversion and the formation rate of each gaseous product. A stoichiometric mixture of D-(+)-Glucose and NaOH was prepared based on Reaction 3.2 (total sample weight = 2.35 g). A wide range of reaction temperatures: 373 K, 423 K, 473 K, 523 K, and 573 K, were selected as the final reaction temperature, with the highest reaction temperature being limited by the melting temperature of NaOH (591 K). During each run, the reaction progress was monitored by sampling the gaseous product stream via the GC.

The molar ratios of the two solid reactants, D-(+)-Glucose and NaOH, were also varied to investigate the role of NaOH during the alkaline thermal treatment of glucose. The molar ratios of NaOH:Glucose were normalized based on the stoichiometric ratio of 12:1 given in Reaction 3.2. Both ratios lower and higher than the stoichiometric ratio were considered for the study: 0:1, 0.2:1, 1:1, 5:1, and 10:1, where 1:1 corresponds to the stoichiometric ratio of 12:1 NaOH:Glucose. The ratio of 0:1 represents the glucose pyrolysis case in the absence of NaOH. The total sample weights used were 0.64 g (0:1 case), 0.98 g (0.2:1 case), 2.35 g (1:1 case), 3.44 g (5:1 case), and 3.90 g (10:1 case), respectively. Based on our preliminary results performed using the different thickness of NaOH/glucose mixture layers, there was no significant mass transfer limitation observed for this type of batch experiment. The amount of glucose was kept above 0.14 g in order to maintain CO concentrations within the detectable range of the GC. The extent and kinetics of the reaction were determined based on the online GC measurements as described earlier.

3.2.3 Solid Product Characterization

At the end of each run, the remaining solids were collected and analyzed using Raman and ^{13}C Nuclear Magnetic Resonance (NMR) spectroscopies. Raman data were collected at room temperature using a LabRAM ARAMIS spectrometer (Horiba JobinYvon) equipped with a microscope and a 40 × objective, employing a 325 nm UV laser and 1200 grooves/mm grating. Measurements were performed on a glass slide with an exposure time of 20 seconds. Five scans were collected for each sample to improve the signal-to-noise ratio. The ^{13}C spectra of the solid products were also obtained using a 300 MHz NMR spectrometer (DPX 300, Bruker Bio Spin Co.). This was done to confirm and quantify the formation of Na_2CO_3 resulting from the reaction of D-(+)-Glucose and NaOH. A sample of pyrolyzed glucose and standards of Na_2CO_3 and unpyrolyzed D-(+)-Glucose were also analyzed via the same solid analyses methods for comparison. For the NMR measurements, products were dissolved in D_2O, with acetonitrile-d_3 added as an internal reference except in the cases of the D-(+)-Glucose and Na_2CO_3 standards. The diluted solid product was then added to 5 mm diameter NMR tubes (Wilmad®) and the analyses were performed overnight to enhance the signal-to-noise ratio.

3.3 Results and Discussion

Most of the prior work performed on alkaline thermal treatment reported high H_2 conversions and very low concentrations of CO_x while collecting very limited information on gaseous products other than H_2, CO, CO_2 and CH_4. Thus, an extensive gas analysis was performed to identify all the gaseous products using the Agilent 7890A GC/ 5975C MS based on the NIST MS Search 2.0 library. The total gaseous products were collected in a 40 L tedlar bag, manufactured by Grace, and at the end of the experiment the bag was well mixed prior to gas

sampling to obtain the average concentration of gaseous products. As shown in the MS spectrum given in the Supporting Information, there were peaks associated with gases other than those four reported by prior work. The identified gases include H_2, CH_4, C_2H_6, C_2H_4, CO, and other trace gases (possibly C_3 and C_4 hydrocarbons as well as benzene and toluene). Some of these gases were quantified to evaluate their impact on the purity of H_2 produced. It was found that although larger gaseous molecules such as C_2H_6 and C_2H_4 were formed during the alkaline thermal treatment of glucose, as shown in Table 3.1, which lists typical compositions of gaseous products, their amounts were significantly lower than that of both H_2 and CH_4. Therefore, for the kinetic experiments, the gas analysis was focused on the two major gaseous products, H_2 and CH_4, which accounted for > 98% of gaseous products, to increase the online gas sampling frequency. The formation of CO and CO_2 were also monitored throughout the experiments since CO is the primary poison to the catalyst in a PEM fuel cell and CO_2 is a greenhouse gas. As the Agilent 7890A GC method was designed to only measure these four gases in order to increase the online sampling frequency, spikes in concentration of other gaseous side products may have been undetected during data acquisition.

Figure 3.2 shows a typical output of the alkaline thermal treatment of glucose in terms of the formation rates of the four gaseous products: H_2, CO, CH_4, and CO_2. This particular result was obtained for a stoichiometric mixture of NaOH and glucose reacted at the final temperature of 573 K with a ramping rate of 1 K/min. The upper operating temperature was chosen to be 573 K for the temperature scan study since the melting temperature of NaOH is 591 K and the prior work has reported that the best kinetics for H_2 formation occur below 573 K (Ishida et al. 2005). The molar formation rates were obtained based on the concentrations measured by the GC and the given flow rate of the inert carrier gas, N_2. The detection limits of the GC for H_2 and

carbonaceous species were 3.7 μmol/min and 3.7×10^{-3} μmol/min, respectively. As shown in Figure 3.2, H_2 starts to form at around 390 K and its formation was sustained during the temperature ramping with a maximum formation rate around 537 K. As the reaction progressed isothermally, there was a slow decrease in the H_2 formation rate due to the depletion of reactants in the batch reactor. The experimental run was stopped as the H_2 concentration fell below the GC's detection limit, which is marked as a dotted line in Figure 3.2. The formation rate of CH_4 followed a similar trend as H_2, with a slight delay in the onset formation temperature, and achieved the maximum rate at around 550 K. Its formation rate was significantly lower than H_2 until 537 K. Thus, in order to maximize the H_2 formation rate in the product gas stream while minimizing carbonaceous gaseous side products, it is suggested to maintain the reaction temperature lower than 537 K. Despite the high CH_4 formation at this temperature, PEM fuel cells can operate with CH_4 concentrations as high as 30% (Seo et al. 2007, Giddey et al. 2005), which is higher than the concentration of CH_4 observed here. CO_2 was not detected throughout the temperature scan experiments from 298 K to 573 K for a stoichiometric ratio of NaOH and glucose, while there was small amount of CO formation between 480 K and 573 K. Even at their maximum formation rates, the CO generation rate was about three orders of magnitude below the H_2 production rate, illustrating suppressed CO_x generation during the alkaline thermal treatment of glucose. Similar trends in the gaseous product formation rates were observed for the rest of the study investigating the effects of the final reaction temperature and the reactant ratios; however, the actual temperature ranges associated with the formation of each gaseous species were slightly varied. Particularly, the onset temperature for the CO formation was not as reproducible as it was for H_2 since the CO concentrations were always very close to the GC's detection limit of 1 ppm and the kinetics of the reaction were complicated by mass and heat

31

transfer throughout the system. However, the integrated amount of gas production obtained by integrating the GC's online measurements was relatively consistent throughout the study. Therefore, most of the experimental results are discussed in terms of H_2 conversion and the total amounts of gaseous products formed, both obtained based on the integration of the GC data.

3.3.1 Effect of Final Reaction Temperature

The first parameter explored in the alkaline thermal treatment reaction of glucose was the reaction temperature. Based on the temperature scan experiment shown in Figure 3.2, it was suspected that the optimum reaction temperature would be around 540 K, where the maximum H_2 production occurred. In order to systematically analyze the effect of the reaction temperature, a series of experiments were performed setting the final isothermal reaction temperature as: 373 K, 423 K, 473 K, 523 K, and 573 K. To obtain the total molar production of gaseous products for each experiment, the molar formation rate versus time curves obtained using the GC, typified in Figure 3.2, were integrated via the Newman-Cotes method. The H_2 conversion was then calculated based on the stoichiometric ratio given in Reaction 3.2, where H_2 conversion of 100% was defined as 12 moles of H_2 produced for every mole of glucose present at the start of the experiment. Note that in all experimental results given in the study, error bars represent the range of values observed in repeated experiments.

As shown in Figure 3.3, from 373 K to 523 K the H_2 conversion steadily increased from 0.6% to 27.1% due to improved kinetics with increasing temperature. However, the H_2 conversion did not change significantly from 523 K to 573 K, with a slight increase from 27.1% to 29.5%. The maximum H_2 conversions achieved were comparable to those found in the literature. Ishida et al. reported about 40% H_2 conversion for the non-catalytic alkaline thermal treatment of glucose (Ishida et al. 2005). The difference between this data and their data was due

to their higher final reaction temperature of 773 K. They observed a small secondary peak of H_2 formation between 650 K and 773 K, which accounted for the remaining 10% of H_2 conversion not observed in this study (Ishida et al. 2005).

In addition to enhanced H_2 production, the development of the alkaline thermal treatment of biomass requires suppressed CO formation to minimize the subsequent gas cleanup steps. Thus, the total generation of CO, as well as CO_2 and CH_4, all gases that were not reported in the previous study of the non-catalytic alkaline thermal treatment of glucose (Ishida et al. 2005), were investigated at each reaction temperature and compared with H_2 production. As discussed in the experimental section, it was not possible to measure the concentrations of all the gaseous products during the kinetic studies due to the GC sampling time. Thus, instead of reporting the results in terms of concentrations, the molar ratios of each gaseous product to initial moles of glucose were reported to represent the extent of their formation during each experiment. As shown in Figure 3.4, the production of both H_2 and CH_4 increased with increasing temperature up to 523 K, and stayed roughly constant upon further temperature increase to 573 K. Based on the analysis of the total gaseous products, it was found that the selectivity towards H_2 increased at lower reaction temperatures. For the highest overall H_2 generation, which occurred at 573 K, the CH_4 concentration was about 1/4 of H_2, which is still under the range of the CH_4 limit of PEM fuel cells. In case of CO_x species, CO_2 was never detected throughout the experiments. Their data points are located at 10^{-5} mol-product/mol-glucose in Figure 3.4, which corresponds to the GC's detection limit for CO_x compounds. The zero formation of CO_2 suggests that one of the roles of NaOH in the alkaline thermal treatment of glucose may be CO_2 capture via a carbonation reaction.

CO showed a trend of increased production from negligible values to 4.4×10^{-4} mol/mol-glucose at 573 K. However, even at the maximum values at 523 K and 573 K, the molar ratio of CO was well over three orders of magnitude lower than those of H_2 and CH_4 for the same initial amount of glucose. The variability observed in the CO values was most likely due to operating near the GC's detection limit for CO of 1 ppm. It is important to report these values of CO since most of the prior work could not report low concentration values due to their GC's high detection limit of 30 ppm.

Considering both H_2 production and CO generation shown in Figures 3.3 and 3.4, 523 K was suggested to be the optimum reaction temperature for the alkaline thermal treatment reaction of glucose with suppressed CO_x generation. Therefore, the rest of the study was performed at 523 K.

3.3.2 Effect of Reactant Ratios

To further examine the role of NaOH in the alkaline thermal treatment of glucose, varying concentrations of NaOH with glucose were tested: the normalized NaOH:Glucose ratios of 0:1, 0.2:1, 1:1, 5:1, and 10:1, where 1:1 corresponds to the stoichiometric ratio of 12:1 NaOH:Glucose. The temperature ramping rate was kept at 1 K/min with a final isothermal reaction temperature of 523 K. The ratio of 0:1 represents the glucose pyrolysis case in the absence of NaOH.

As shown in Figure 3.5, NaOH-lean cases of 0:1 and 0.2:1 resulted in significantly less H_2 conversion; in fact, no H_2 was produced in the absence of NaOH, as also reported in many studies performed on glucose pyrolysis at low temperatures (Bassilakis et al. 2001, Shafizadeh and Bradbury 1979, Ponder and Richards 1993). The pyrolysis of glucose does produce H_2 but this generally occurs at much higher temperatures around $775 - 1025$ K (Demirbas 2002).

34

Considering the given reaction temperature of 523 K, this demonstrates the importance of NaOH in altering the decomposition reactions of glucose employed in this study. The maximum H_2 conversion of 27% was observed for the 1:1 case. For the NaOH-rich cases, the H_2 production slightly decreased from its maximum value. This may be due to heat and mass transfer issues within this complex reactive system. Since there are a number of potential parallel or competing reactions occurring (e.g., glucose decomposition with possible reaction with NaOH, CO_2 carbonation, pyrolysis), the excess NaOH may have played a different role in glucose conversion to H_2.

In addition to H_2 conversion, the normalized concentrations of other gaseous products as a function of the reactant ratio were investigated, with the results presented in Figure 3.6. The minimum value of the y-axis for H_2 was 10^{-2} mol-H_2/mol-glucose, whereas that for the carbonaceous species was 10^{-5} mol-product/mol-glucose due to their different GC detection limits. The most important finding from these experiments was the sharp increase in H_2 and CH_4 production, coupled with the sharp decrease in CO and CO_2 production, with increased NaOH concentration in the system from 0:1 to 1:1. The improvement in H_2 production and CO_x suppression was sustained but not improved as the amount of NaOH was further increased to the normalized NaOH:Glucose ratio of 10:1. Therefore, in terms of balancing high H_2 production with the minimization of CO and CO_2 formation, it was concluded that the optimum normalized ratio of NaOH to glucose for the alkaline thermal treatment system was 1:1, which corresponds to the stoichiometric ratio of NaOH and glucose given in Reaction 3.2. The CO production per mole of glucose had a slight increase of about four times from the 1:1 case to the 10:1 case; however, the increase was not significant as it was within the error range.

Since the effect of the reactant ratios was most predominant between the normalized NaOH:Glucose ratios of 0:1 and 1:1, those cases were further investigated in terms of the formation rates of gaseous products in order to gain further insight into the role of NaOH and the potential reactions that may be occurring in the alkaline thermal treatment system. The three cases selected for this part of the study were: two cases of alkaline thermal treatment (i.e., the normalized NaOH:Glucose ratios of 0.2:1 and 1:1), and glucose pyrolysis (i.e., the normalized NaOH:Glucose ratio of 0:1). As described in Figure 3.7, in all cases, the reactant(s) were first heated from room temperature to the final temperature of 523 K at a constant rate of 1 K/min, where the reaction was performed isothermally until the H_2 concentration fell below the GC's H_2 detection limit of 0.1%.

Several immediate differences were noted. First of all, as shown in Figure 3.7a, the H_2 production was a strong function of the amount of NaOH added. H_2 was not produced through glucose pyrolysis but significant amounts of H_2 were produced during the alkaline thermal treatment of glucose. For the 0.2:1 case, the formation rate peaked at 50 μmol/min just as the reactor temperature reached 523 K. In the 1:1 case, the peak H_2 formation rate occurred at the same temperature of 523 K, reaching 138 μmol/min; however, the onset temperature of H_2 formation was lower than that of 0.2:1 case. Comparing the 0.2:1 and 1:1 cases, both started by following very similar production trends. In the 1:1 case, though, the H_2 production was sustained for longer, resulting in greater overall production of H_2 for the same initial amount of glucose. This confirmed that NaOH played an important role in producing H_2 from solid materials containing C, H, and O such as glucose.

In case of the CH_4 formation, it was found that the maximum CH_4 formation rate was four orders of magnitude lower in glucose pyrolysis than in the 1:1 case of alkaline thermal

treatment (Figure 3.7b). In glucose pyrolysis, the onset of CH_4 formation was not seen until well after the reactor temperature had reached 523 K, and its production was short lived as well as minimal, reaching a maximum molar flow rate of 4.6×10^{-3} μmol/min. In fact, the temperatures associated with the onset production of gaseous products and the maximum formation rates did not vary significantly with the addition of NaOH, except for the case of CH_4. The formation of CH_4 was accelerated to lower temperatures as greater concentrations of NaOH were added to glucose. With the addition of NaOH in the 0.2:1 case, the onset temperature for CH_4 production was significantly lowered by nearly 100 K, and the overall CH_4 formation dramatically increased, reaching a maximum molar formation rate of 1.7 μmol/min at 523 K. Like in the case of H_2, further increase in NaOH content in the reactants to 1:1 caused a greater maximum CH_4 formation rate, reaching a maximum rate of 64 μmol/min at 523 K. Thus, it was quite clear that NaOH enhanced the production of CH_4 in the thermal conversion of glucose, pointing to an altered reaction mechanism from glucose pyrolysis, one that may be related to H_2.

Next, both CO and CO_2 formation rates were investigated for the same experimental sets. As shown in Figures 3.7c and d, in glucose pyrolysis (0:1 case), the significant gaseous products formed were CO and CO_2. The maximum CO formation rate was lowest for the 1:1 alkaline thermal treatment case, at 3.1×10^{-2} μmol/min, which was over a magnitude lower than that for the 0.2:1 case and nearly two orders of magnitude lower than that for the glucose pyrolysis case. In the 1:1 case, that of the highest NaOH content, CO formation was terminated before H_2 formation was completed; however, in the 0.2:1 case of lower NaOH content, CO formation continued even after the termination of H_2 formation.

In terms of the CO_2 formation, it was nonexistent for the 1:1 alkaline thermal treatment case, whereas lower or zero NaOH content in the reactant(s) resulted in significant formation of

CO_2 during the thermal conversion of glucose. The onset temperatures of the CO_2 formation were similar in the 0:1 and 0.2:1 cases; however, the peak CO_2 formation rate was about an order of magnitude higher in the case of glucose pyrolysis (3.7 µmol/min) than in the 0.2:1 case (0.28 µmol/min). Thus, it was concluded that NaOH suppresses the formation of CO_x compounds during the thermal conversion of glucose.

There have been significant efforts to identify the reaction mechanisms of the pyrolysis of biomass (e.g., cellulose and glucose), and due to the complexity of the reactions, many reaction pathways have been suggested. Although many of the pyrolysis studies in the literature were performed at significantly higher temperatures than those investigated this study (0:1 case), the formation of CO_x compounds and the absence of H_2 in the product gas at lower temperatures were analogous in many of the studies. In terms of H_2 production, fast pyrolysis processes performed at higher temperatures are more favorable (Ni et al. 2006). Regarding the gaseous products formed during low temperature pyrolysis, Bassilakis et al. performed interesting TG-FTIR tests on the pyrolysis products of biomasses, including glucose. They reported the trends of the formation rates as a function of the reaction temperature, which were very similar to those shown in Figure 3.7 (Bassilakis et al. 2001). Some have suggested that the predominance of CO and CO_2 in the product gas of glucose pyrolysis may be explained by pathways that lead to decarbonylization and decarboxylization, respectively (Shafizadeh and Bradbury 1979).

The chemistry of biomass undergoing pyrolytic heat treatment is already complex, and with the addition of additives such as NaOH, different reaction pathways become available. There are a number of possible reactions that could explain the observed trends of increased H_2 and CH_4 formation with decreased CO and CO_2 formation in the presence of NaOH. One of the potential sets of reaction pathways could involve the reaction between NaOH and the CO_x

compounds produced via glucose pyrolysis. As glucose pyrolysis occurs the generated CO and CO_2 could be consumed by NaOH through the Reactions 3.4 and 3.5 (Saxena et al. 2008):

$$CO_2 + 2NaOH = Na_2CO_3 + H_2O; \qquad \Delta H^0 = -127 \text{ kJ/mol} \qquad \text{(Rxn. 3.4)}$$

$$CO + 2NaOH = Na_2CO_3 + H_2; \qquad \Delta H^0 = -169 \text{ kJ/mol} \qquad \text{(Rxn. 3.5)}$$

These reaction schemes would account for the observed H_2 formation and decreased CO and CO_2 generation during the thermal conversion of glucose in the presence of NaOH. Considering the carbonation by NaOH is a fast reaction, it is expected that NaOH likely played an important role in the absence of CO_2 during the alkaline thermal treatment of glucose.

Two other possible reaction pathways that would enhance H_2 and CH_4 formations during the alkaline thermal treatment of glucose are the dehydrogenation of glucose as well as its decomposition into alkylated and hydroxylated carbonyl compounds in the presence of a strong base such as NaOH. Su et al. claimed dehydrogenation as the main reaction mechanism of cellulose decomposition over a combined gasification and water-gas shift reaction when the alkaline thermal treatment reaction was performed using their novel NaOH-containing ionic catalyst, since H_2 production is not favored at low temperatures (403-473 K) in the case of the endothermic gasification reaction (Su et al. 2010). Onwudili and Williams suggested glucose decomposition into alkylated and hydroxylated carbonyl compounds as a possibility after studying the effect of NaOH on the hydrothermal gasification of glucose, as opposed to the dehydration and polymerization pathway observed in glucose pyrolysis in the absence of NaOH. The H_2 production can be explained by the high concentration of water in their system, which may have led to water-gas shift reaction when the smaller carbonyl and hydroxylated carbonyl compounds reacted with water (Onwudili and Williams 2009). Another study also reported that

NaOH increased yields of carbonyl compounds and carboxylic acids during glucose pyrolysis at 548 K, while in the absence of NaOH the major pyrolysis products were furan and sugar derivatives (Ponder and Richards 1993). The subsequent decomposition pathways for the furan and sugar derivatives are likely different from those for the NaOH-induced alkylated and carboxylic acid compounds, which may also explain the composition of the gaseous products generated from the alkaline thermal treatment of glucose. Further investigation is desired to fully understand the reaction mechanisms that produce high purity H_2 via the catalytic alkaline thermal treatment of glucose.

3.3.3 Production Rate versus H_2 Purity

Since the alkaline thermal treatment of glucose produces H_2 with suppressed CO_x formation, the gaseous product could be a good candidate as a fuel for fuel cell applications such as in the PEM fuel cell. The fuel requirement for a PEM fuel cell primarily includes the CO concentration to be below 10 ppm. This should be achieved while producing H_2 at a sufficient formation rate. Thus, for the optimized reaction temperature of 523 K and the stoichiometric ratio of NaOH and glucose, a fast kinetic study was performed while monitoring online gas compositions and the formation rate of total gaseous products. For this particular online analysis, the Inficon 3000 Micro GC was used, as it extended the gas quantification out to C_2H_6 with minimal run times of 4 min. As this study included C_2H_6, the third most significant overall gas product at nearly 1% concentration, shown in Table 3.1, the Micro GC was able to quantify gases that made up over 99% of the overall gaseous product. Thus online concentrations can be reported more accurately; however, as in the other studies conducted with the Agilent 7890A GC, it is still possible that spikes of other larger hydrocarbons may have gone undetected,

making the reported concentrations here upper limits. Again, the experiment was terminated once the H_2 concentration fell below the detection limit of the Micro GC of 0.1%.

As shown in Figure 3.8a, low concentrations of CO ranging from 270 ppm to 578 ppm were detected at high temperature conditions close to the final reaction temperature of 523 K. These values corresponded very closely to the detection limit of the Micro GC of 10 ppm when considering the presence of the large amounts of the N_2 carrier gas in the product stream, which was not included in the concentration calculation. Although the actual concentrations of CO were above the 10 ppm threshold for a PEM fuel cell, these concentrations were still relatively low compared to that of other biomass conversion reactions such as gasification and pyrolysis. Without the additional processes, the fuel streams produced by these technologies contain significant amounts of carbon, which challenges their utilization in PEM fuel cell technologies. In order to further reduce the CO formation during the alkaline thermal treatment of glucose, faster ramping rates could be employed, since a preliminary study has shown that negligible CO formation was observed in the experiments described herein conducted at ramping rates of 10 K/min and 20 K/min instead of 1 K/min, while total H_2 formation remained constant among various ramping rates. The final reaction temperature could be lowered or water could also be added to perform in-situ water-gas shift reaction to further reduce the CO concentration in the product gas. Nevertheless, these measures should be applied only when the overall H_2 production rates can be maintained. For instance, the highest purity of H_2 was seen at lower reaction temperatures, however, the reaction kinetics limited the total formation rate of the gaseous products. Therefore, the optimization between the production rate and the H_2 purity would be an important factor for the optimization of the proposed alkaline thermal conversion of biomass.

As shown in Figure 3.8b, at higher reaction temperatures, the reaction kinetics allowed for much greater total gaseous product formation; however, side products began to significantly impact H_2 purity. The primary diluent for H_2 was CH_4, peaking at 42%, but fortunately occurring well after the reactor had reached 523 K. Although not a poison to the PEM fuel cell at lower concentrations (< 30%) (Zhang and Datta 2002, Seo et al. 2007), CH_4 may need to be reduced prior to the use of the product gas in a PEM fuel cell to achieve a higher H_2 concentration in the fuel stream. The reduction of CH_4 during the alkaline thermal treatment of biomass (e.g., glucose, cellulose) can be accomplished through Ni-based catalysis (Ishida et al. 2006). This will allow for the operation of the alkaline thermal treatment process at the kinetically favorable temperature of 523 K. Regarding C_2H_6, it peaked at nearly 8% concentration, again well after the reactor reached isothermal conditions. Its formation was not detected until after the reactor had been operated isothermally at 523 K for 24 min. This indicates that the formation of C_2H_6 may be related to reactions of the lighter gases with the charred solid products, rather than being directly related to the alkaline thermal treatment process. Thus, in a continuous reactor system where the gaseous and solid products can be continuously removed, the production of C_2H_6 could be significantly reduced or avoided.

3.3.4 Solid Product Characterization

Unfortunately, there have been only limited analyses done on the solid products of the alkaline thermal treatment of biomass. Some reported that when cellulose was prepared via a pretreatment using NaOH solution, the final solid products were mainly Na_2CO_3 (Ishida et al. 2006); however, this may not be true for the case of the mixing method employed in this study of pulverization of NaOH pellets with glucose. Thus, a series of experiments including Raman and

^{13}C NMR analyses were performed to characterize and identify the composition of the solid products.

The Raman spectrum of the solid product obtained from the optimal case, which was for a stoichiometric ratio of NaOH:Glucose mixture and reaction temperature of 523 K with ramping rate of 1 K/min, was compared with those of pyrolyzed glucose, pure Na_2CO_3, and pure D-(+)-glucose. As shown in Figure 3.9, the solid product from the alkaline thermal treatment experiment named '1:1 Sample' exhibited quite different peak patterns compared to D-(+)-glucose, indicating that glucose was definitely chemically converted. The formation of Na_2CO_3 in the alkaline thermal treatment sample was confirmed with the band at 1076 cm^{-1}. Although Na_2CO_3 should be the only product in the 1:1 sample based on Reaction 3.2, the formation of side-products was also evidenced by the presence of additional Raman bands at 1601 cm^{-1} and 1371 cm^{-1}. The exact assignment of those bands to specific vibrations is very challenging without the aid of other analytical techniques. It is likely that they are related to C-H, C-O-C, and C=C stretching from carbonaceous side-products (Socrates 2004).

To further confirm the presence of Na_2CO_3 and quantify its content in the solid product, ^{13}C NMR analysis was performed on three alkaline thermal treatment samples, each with a different normalized NaOH:Glucose ratio: 0.2:1, 1:1, and 5:1 cases, as well as pyrolyzed glucose, pure Na_2CO_3, and pure D-(+)-glucose. Figure 3.10 shows six spectra, with the top being that of Na_2CO_3, followed by unpyrolyzed D-(+)-Glucose, pyrolyzed glucose, the 0.2:1 sample, then the 1:1 sample, and finally the 5:1 sample. Like in the Raman results, the formation of Na_2CO_3 was confirmed for all alkaline thermal treatment samples by the presence of the carbonate peak, here at ~170 ppm. The carbonate peaks were integrated and compared against the area of the internal reference acetonitrile-d_3 peak at ~120 ppm in order to obtain the molar

quantity of Na_2CO_3 in the analyzed solid samples. The conversion in terms of the carbonate formation was then calculated by taking the ratio of Na_2CO_3 present in the sample to the theoretical moles of Na_2CO_3 given by the Reaction 3.2. Based on this method, the conversions were estimated to be 14.4%, 30.5% and 15.4% for the normalized NaOH:Glucose ratios of 0.2:1, 1:1 and 5:1, respectively, while the conversions calculated based on the H_2 formation (derived from the data presented in Figure 3.5) were 10.0%, 29.8% and 27.0%, respectively. Interestingly, the conversions estimated in terms of H_2 and Na_2CO_3 formations match well for the case of the stoichiometric mixture of reactants, while particularly the glucose-rich case of the 0.2:1 sample resulted in a greater conversion when it was estimated based on the Na_2CO_3 formation.

Regarding the lower conversion observed based on the Na_2CO_3 formation method compared with the H_2 formation method for the 5:1 case, the difference observed between two methods of estimating conversions may have been due to incomplete dissolution of the solid products in D_2O. Since a liquid-state NMR was used to quantify Na_2CO_3 content in solid samples, the accuracy of the measurement was highly dependent on the complete dissolution of the solid samples. Unfortunately, some of the solid byproducts of the alkaline thermal treatment of glucose were insoluble carbonaceous materials and those may have formed around the Na_2CO_3 particles, potentially locking in the carbonate and rendering it undetectable in the liquid sample by the ^{13}C NMR, thus leading to a lower estimate of conversion when compared to the H_2 formation method. The partial conversion of glucose to these insoluble carbonaceous materials may have also contributed to the incomplete conversion to H_2 in stoichiometric and NaOH-rich cases. Therefore, a solid-state NMR method has been suggested to be an alternative choice for the Na_2CO_3 quantification in solid samples and it is now a part of on-going effort.

In addition to the carbonate peak, additional peaks were observed in the spectrum of the 0.2:1 sample and to lesser extents in the 5:1 and 1:1 samples. These peaks were different from those observed for pure glucose and indicated the presence of other carbonaceous materials, which were most pronounced in the glucose-rich 0.2:1 case. The peaks below 50 ppm may have originated from the presence of carbon in alkane chains (C, CH_x) and alcohol/ether compounds (C-OH, C-O-C), while the peaks in the higher chemical shift range (170−190 ppm) may be related to the presence of carbonyl-containing (C=O) species (Pretsch et al. 2009). Again, the precise assignments of these peaks to specific compounds remain challenging given the complexity of the reactions. The pyrolyzed D-(+)-glucose sample was difficult to dissolve in D_2O and its spectrum did not show any peaks associated with carbonaceous compounds.

3.4   Conclusions

The alkaline thermal treatment of biomass is one of the novel biomass conversion technologies that has recently been proposed. Some have studied the effect of catalysts on the H_2 production; however, the reactions involved in the alkaline thermal treatment process are still poorly understood. In this study, the non-catalytic alkaline thermal treatment reaction for glucose was investigated to produce H_2 with suppressed CO_x formation. A series of experiments involving online gas analysis and solid characterization was conducted to provide insight into the reaction kinetics and mechanisms. In particular, the effects of reaction temperature and reactant ratios were studied in terms of H_2 conversion and formation rates of the major gaseous products. It was found that higher temperatures promoted increased H_2 production through better kinetics. The hydroxide, NaOH, was found to facilitate H_2 production, promote CH_4 formation, and suppress CO and CO_2 production. In fact, CO_2 was almost nonexistent in most of the gaseous products. The amount of NaOH also impacted the quality and the formation rates of H_2 in the

product stream. The 1:1 stoichiometric NaOH:Glucose ratio exhibited the best performance while both glucose-rich and NaOH-rich cases suffered from possible mass and heat transfer issues and possible undesirable side reactions. For glucose-rich cases, a significant degree of pyrolysis may have occurred resulting in increased CO_x formation. The solids analyses using Raman and ^{13}C NMR confirmed the formation of Na_2CO_3 during the alkaline thermal treatment of glucose, but more in-depth study on the solids is desired to fully understand the complex reaction mechanisms. Insight gained from this work will be applied to future studies with cellulose as well as to the incorporation of novel catalysts.

Table 3.1 Average concentration of each gaseous product from the alkaline thermal treatment of glucose (the final reaction temperature of 523 K, stoichiometric ratio of NaOH and glucose).

Gaseous Product	Concentration (%)
H_2	82.22
CH_4	16.00
CO	0.06
CO_2	0.00
C_2H_6	0.94
C_2H_4	0.23
Others*	0.58

*e.g. C_3, C_4 hydrocarbons, benzene, toluene
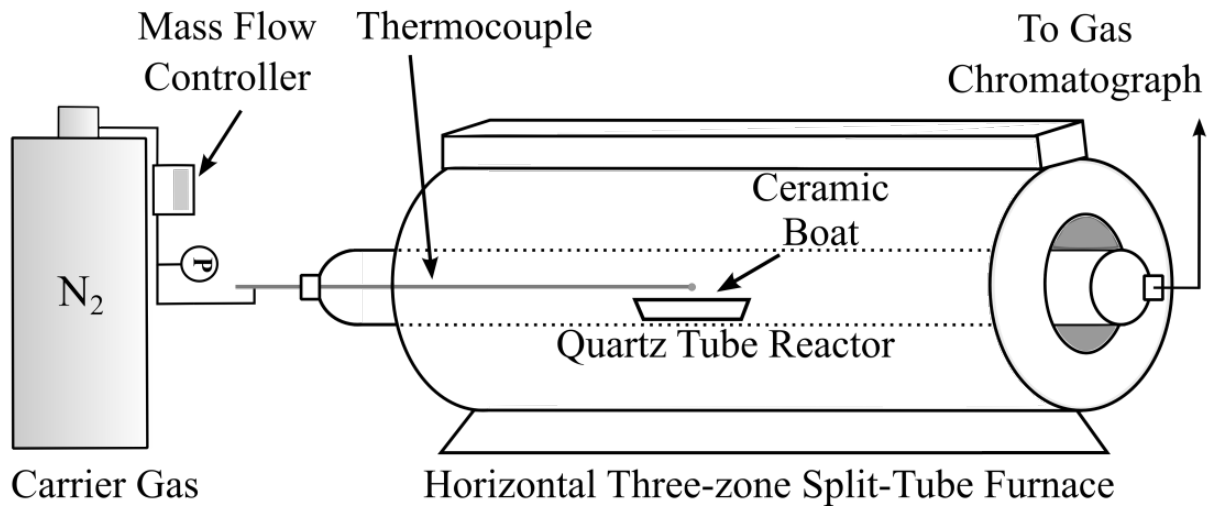
Figure 3.1 Schematic diagram of the experimental setup for batch experiments.
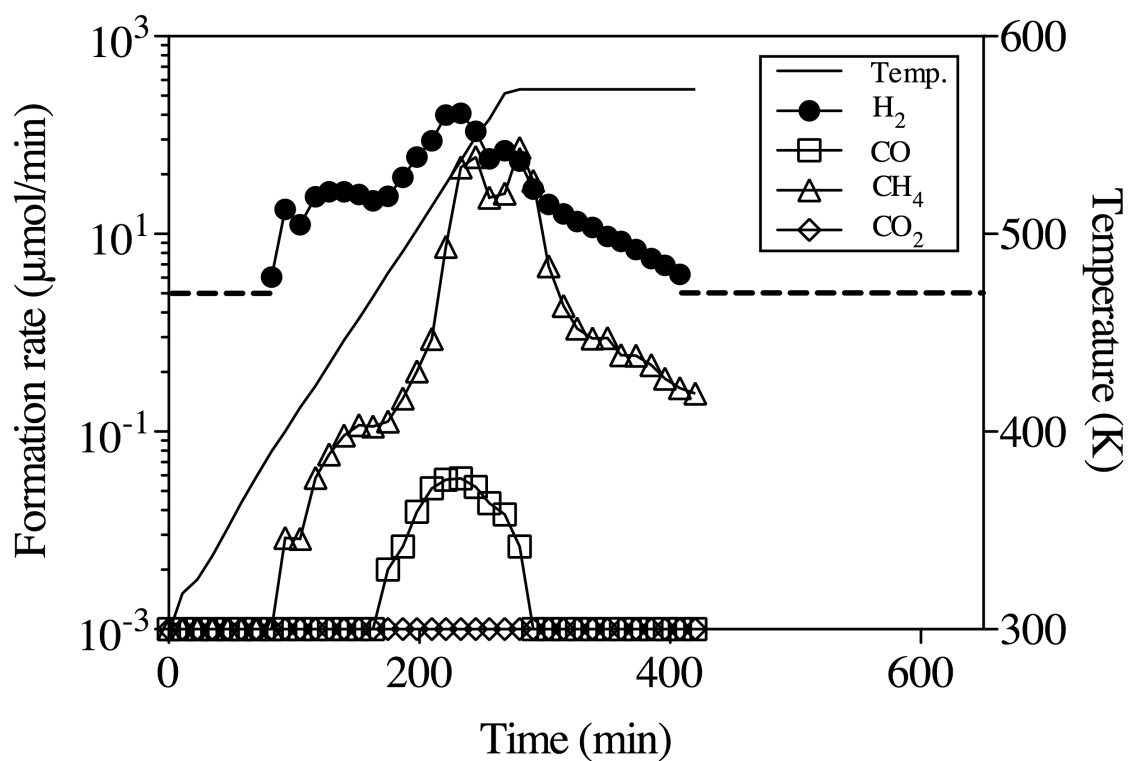
Figure 3.2 Molar formation rates of H_2, CO, CH_4, and CO_2 for a stoichiometric mixture of NaOH and glucose (12:1 NaOH to glucose on molar basis). Reaction temperature programming: 298 → 573 K at 1 K/min & isothermal at 573 K until [H_2] fell below the GC's H_2 detection limit of 0.1%.
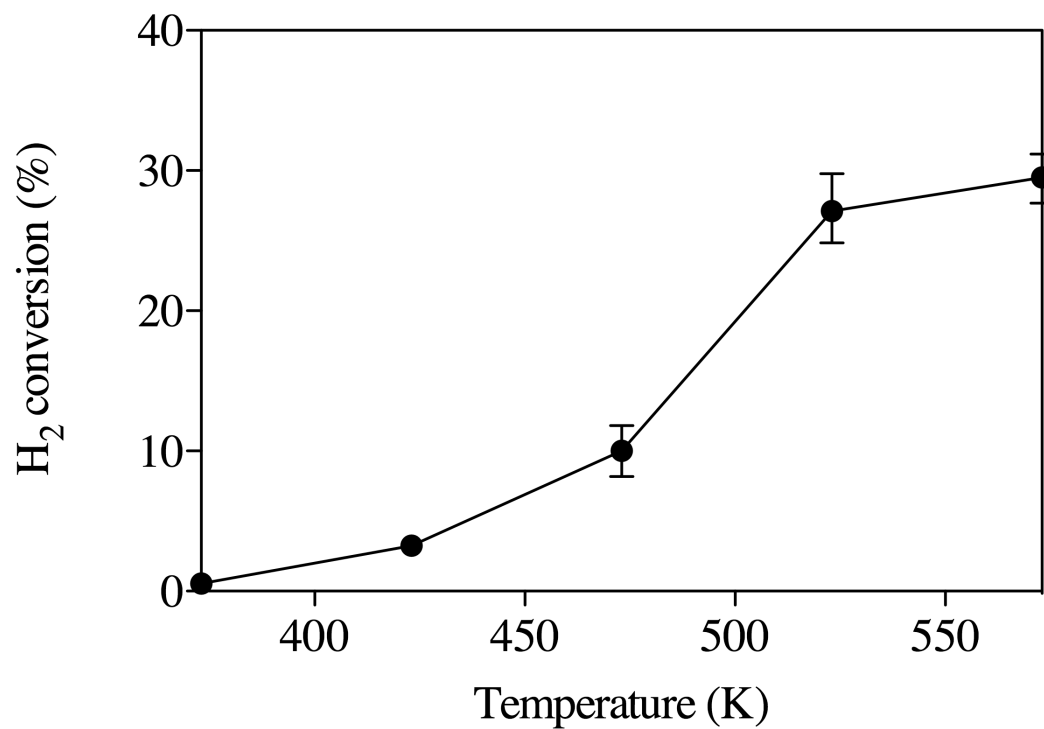
Figure 3.3 Conversion to H_2 for a stoichiometric mixture of NaOH and glucose (12:1 NaOH to glucose on molar basis) as a function of final reactor temperature. Reaction temperature programming: 298 K → given final temperature at 1 K/min & isothermal at final temperature until $[H_2]$ fell below the GC's H_2 detection limit of 0.1%.
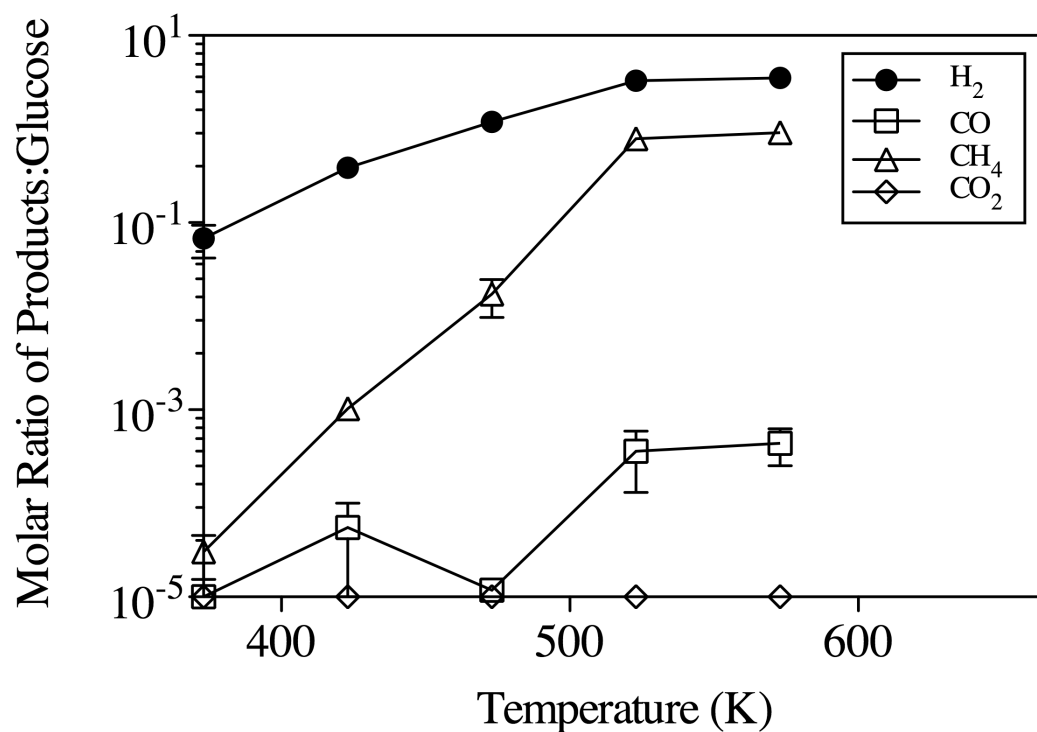
Figure 3.4 Comparison of the total amount of each gaseous product formed, per mole of glucose, for a stoichiometric mixture of NaOH and glucose (12:1 NaOH to glucose on molar basis) as a function of the final reactor temperature. Reaction temperature programming: 298 K → given final temperature at 1 K/min & isothermal at final temperature until [H_2] fell below the GC's H_2 detection limit of 0.1%.
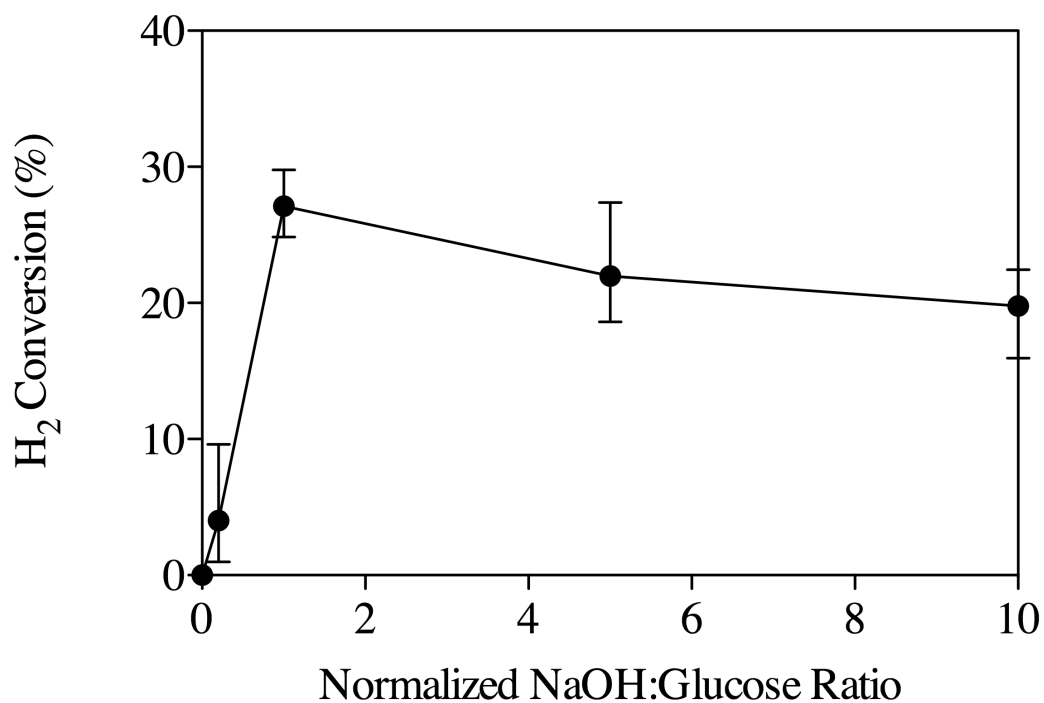
Figure 3.5 Conversion to H_2 for varying normalized NaOH:Glucose ratios (1:1 normalized NaOH:Glucose ratio corresponds to the stoichiometric ratio, which is 12:1 NaOH to glucose on molar basis). Reaction temperature programming: 298 → 523 K at 1 K/min & isothermal at 523 K until $[H_2]$ fell below the GC's H_2 detection limit of 0.1%. The NaOH:Glucose ratio of 0:1 represents glucose pyrolysis conditions.
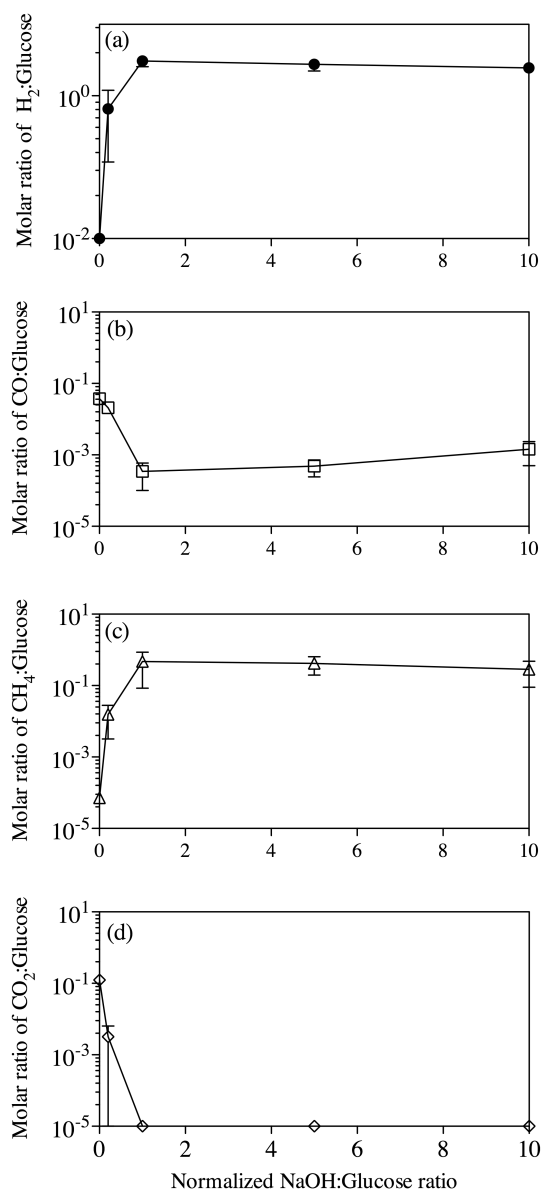
Figure 3.6 Comparison of the total amount of each gaseous product formed, per mole of glucose, as a function of the normalized NaOH:Glucose ratio (1:1 normalized NaOH:Glucose ratio corresponds to the stoichiometric ratio, which is 12:1 NaOH to glucose on molar basis). Reaction temperature programming: 298 → 523 K at 1 K/min & isothermal at 523 K until [H_2] fell below the GC's H_2 detection limit of 0.1%. The NaOH:Glucose ratio of 0:1 represents glucose pyrolysis.
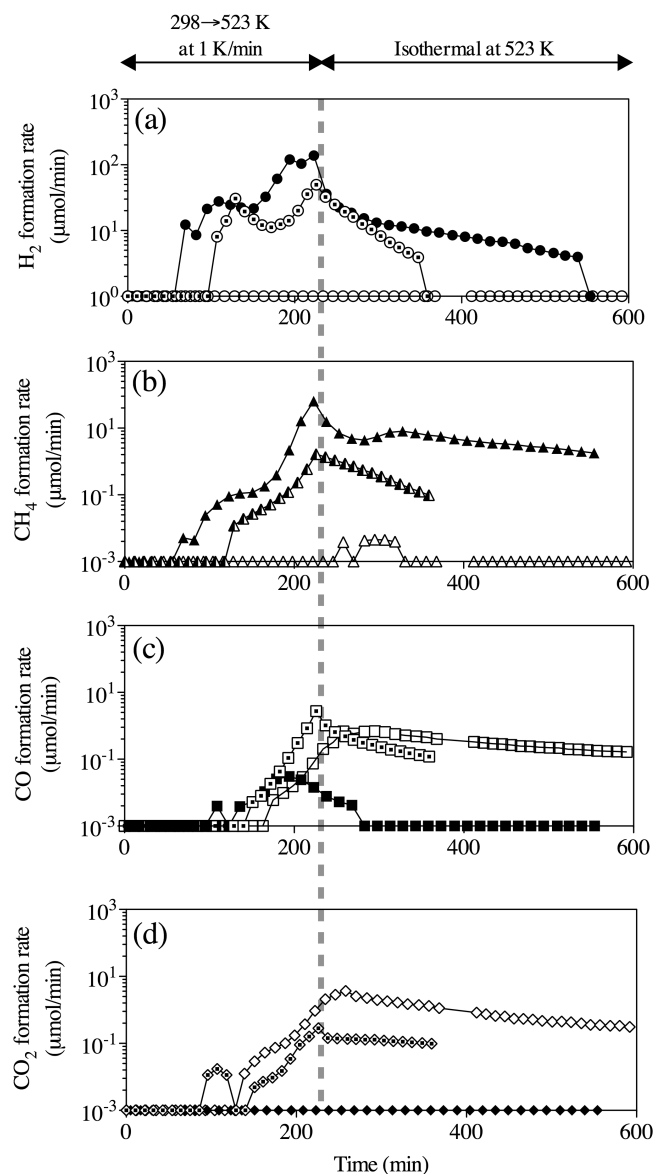
Figure 3.7 Comparison of formation rates of each gaseous product for varying normalized NaOH:Glucose ratios. The normalized NaOH:Glucose ratio of 0:1 represents glucose pyrolysis conditions (open symbols), and the normalized NaOH:Glucose ratios of 0.2:1 (dotted symbols, half shaded triangle for CH_4) and 1:1 (closed symbols) two cases of alkaline thermal treatment. Reaction temperature programming: 298 $\rightarrow$ 523 K at 1 K/min & isothermal at 523 K until [H_2] fell below the GC's H_2 detection limit of 0.1 %.
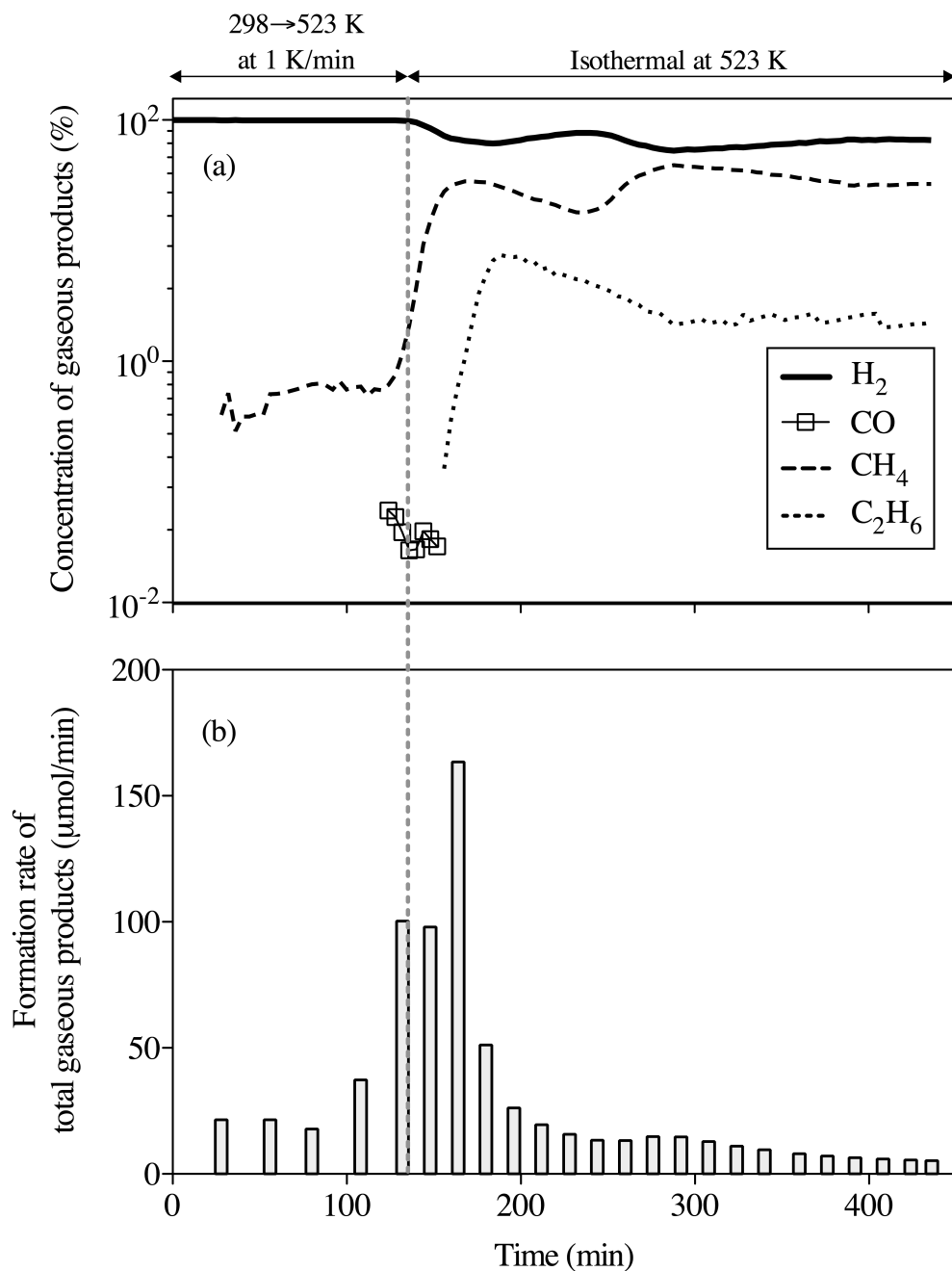
Figure 3.8 Concentrations of each gaseous product (a) and formation rates of total gaseous products (b) as a function of reaction time for a stoichiometric mixture of NaOH and glucose (12:1 NaOH to glucose on molar basis). Reaction temperature programming: 298 → 523 K at 1 K/min & isothermal at 523 K until [H_2] fell below the Micro GC's H_2 detection limit of 0.1%.
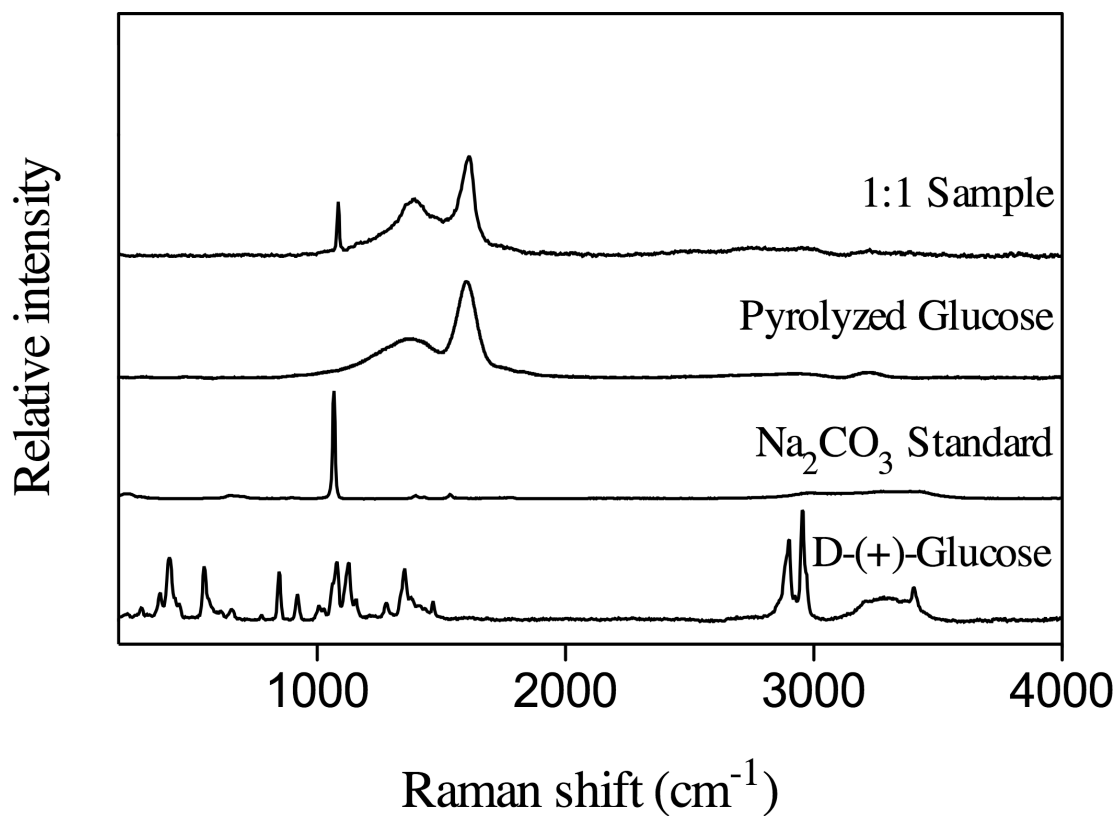
Figure 3.9 Raman spectra of solid products (Pyrolyzed Glucose for the normalized NaOH:Glucose ratio of 0:1 case, and 1:1 Sample for the stoichiometric ratio of 1:1 normalized NaOH:Glucose case) as well as Na_2CO_3 and D-(+)-Glucose standards, for comparison.
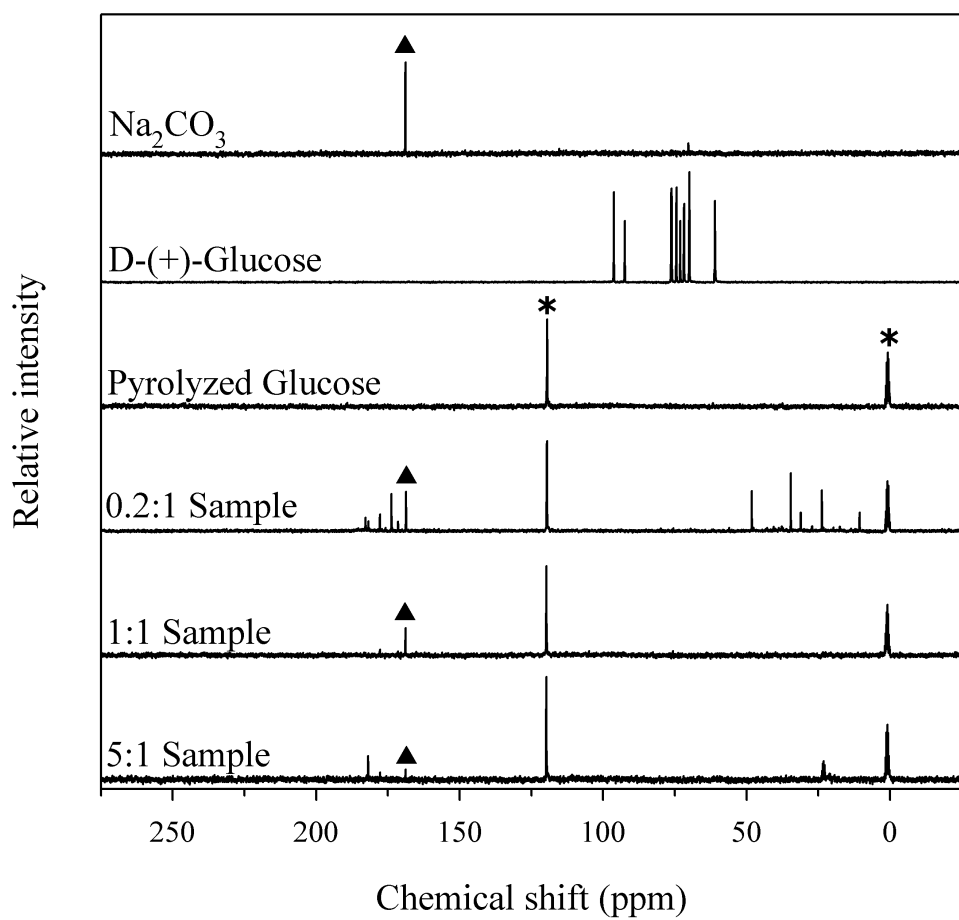
Figure 3.10 ^{13}C NMR spectra of Na_2CO_3 standard, D-(+)-Glucose, Pyrolyzed Glucose, and solid products of three alkaline thermal treatment cases for the normalized NaOH:Glucose ratios of 0.2:1, 1:1, and 5:1. (▲ - Na_2CO_3, * - acetonitrile).

3.5 Supporting Information
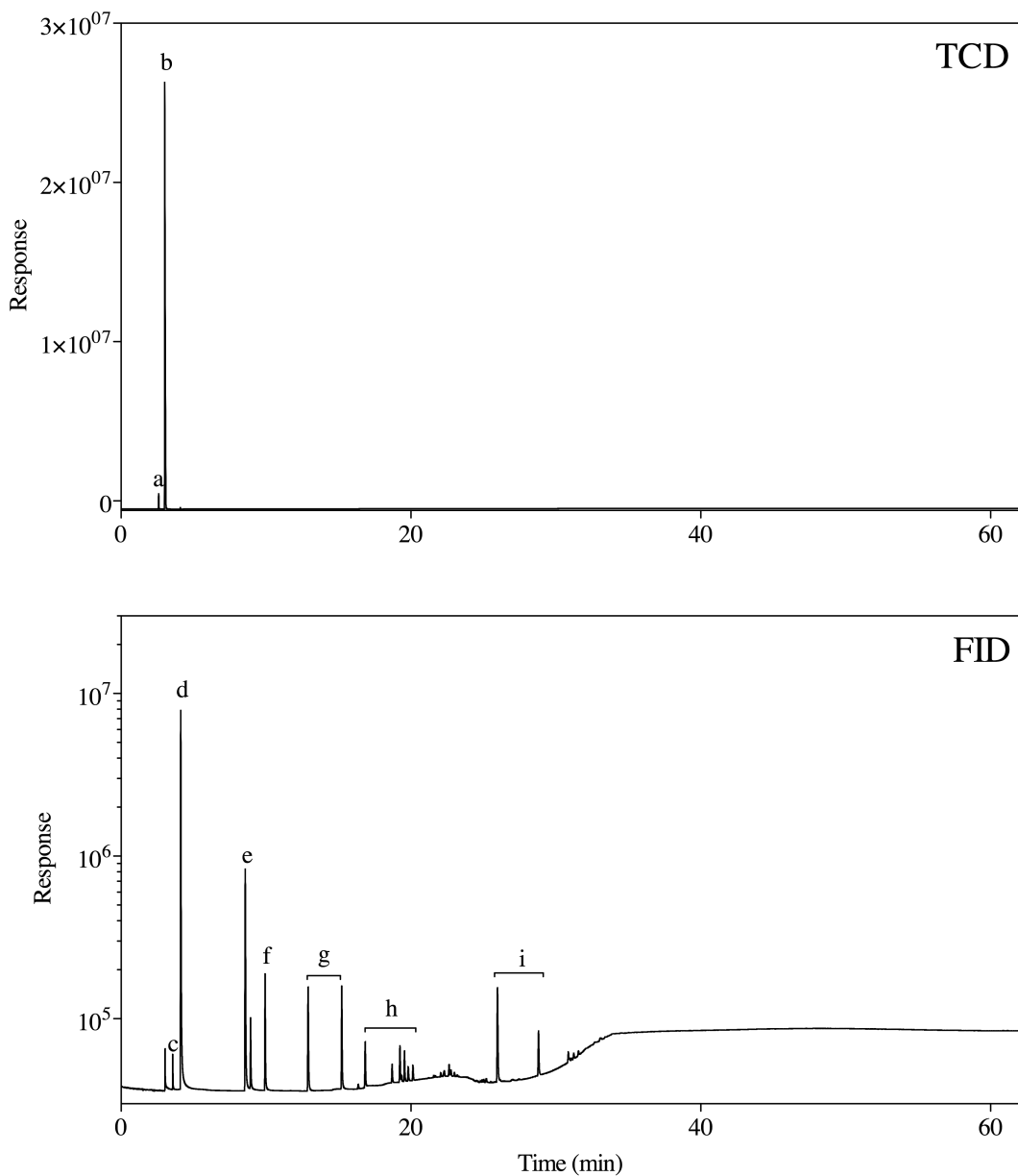
Figure 3.11 Full spectrum of the gaseous products formed from the alkaline thermal treatment of glucose detected by the GC equipped with a Thermal Conductivity Detector (TCD) for H_2 and N_2 and a Flame Ionization Detector (FID) for carbonaceous species. Separation was achieved with a 60 m GS-GasPro column. The GC oven temperature programming was as follows:

isothermal at 193 K for 3 min., ramp at 60 K/min to 253 K, ramp at 10 K/min to 533 K and hold

isothermally for 30 min. The compounds identified using the GC/MS and the NIST MS Search

Library 2.0 are as follows: (a) H_2, (b) N_2, (c) CO, (d) CH_4, (e) C_2H_6, (f) C_2H_4, (g)

Propane/Propene, (h) C_4 hydrocarbons, (i) Higher hydrocarbons (benzene and toluene,

respectively). Note the peaks before peak "c" and in between peaks "e" and "f" are the result of a

small amount of air that could not be eliminated in conducting the experiment. Integrating the

CO_2 peak, which is the peak between "e" and "f" gave a concentration of 5 ppm, or about 1% of

the concentration of CO_2 in the laboratory room air. Thus there is a 1% dilution associated with

these measurements.

CHAPTER 4

SYNTHESIS OF CO$_X$-FREE HYDROGEN FROM CELLULOSE VIA ALKALINE THERMAL TREATMENT (ATT)

The contents of this chapter are to be submitted to the International Journal of Hydrogen Energy as an Article entitled "Non-catalytic conversion of cellulose to high-purity hydrogen at mild reaction conditions via alkaline thermal treatment" (Ferguson and Park 2014).

4.1   Introduction

In its 2013 International Energy Outlook, the Energy Information Administration reported that fossil fuels accounted for 80% of world energy consumption, and they are projected to maintain this percentage in the global energy consumption mix through 2040 (EIA 2013). Due to the deleterious environmental and national security impacts of fossil fuel-based energy economies, research into and implementation of alternative energy schemes continues to proceed rapidly, with the renewable energy sector projected to grow at a rate of 2.5% per year through 2040 (EIA 2013). Energy from biomass is an important component in the renewable energy mix globally; for instance, biomass comprises half of the total energy mix for the African continent (Amigun et al. 2008) and nearly a quarter of the mix for Brazil (Huber et al. 2006). In the United States, increasing the share of renewable energy from biomass has become a priority, with the Renewable Fuels Standard setting the goal of increasing biofuels consumption by 200% by 2035 (Alonso et al. 2012).

One of the major limitations of biomass as an energy feedstock is its low energy density. Utilization of biomass as an energy feedstock thus becomes difficult due to the challenging economics of feedstock transport and storage (Phanphanich and Mani 2011). Consequently, many biomass conversion technologies have been developed to create more energy dense fuels

that are fungible with those derived from fossil fuels. These processes that convert biomass into energy, fuels, and chemicals can be broadly categorized under biological/biochemical and thermochemical technologies (McKendry 2002b). The main categories of biological conversion technologies are fermentation and anaerobic digestion. Although these processes can produce useful products such as ethanol, biogas, and H_2 (McKendry 2002b, Saxena et al. 2009) with high selectivities, the technologies are not as flexible in feedstock as are the thermochemical processes and they tend to have slower rates (Brown 2011).

Thermochemical conversion technologies, although less selective, have much faster rates and can handle a wide variety of feedstocks, including lignocellulosic biomass, which is the cheapest and most abundant biomass feedstock type (Huber et al. 2006). Thermochemical conversion technologies include: combustion, gasification, pyrolysis, hydrothermal treatment, and aqueous phase processing (APP) of sugars (Brown 2011). Combustion, although a very robust technology, produces heat as its only energetic product and is challenged by biomass feedstocks with high moisture content. Additionally, the combustion process produces harmful gaseous emissions as well as particulate emissions that can lead to ash fouling (McKendry 2002b, Brown 2011). Gasification partially oxidizes biomass at high temperature (1123 – 1373 K) into a syngas mixture that can be run in a gas turbine to generate energy or that can be converted into fuels and chemicals through Fischer-Tropsch synthesis (McKendry 2002b, Brown 2011, Asadullah et al. 2002, Asadullah et al. 2004). Pyrolysis occurs under a deoxygenated atmosphere typically at moderate temperatures (673 – 873 K). In particular, fast pyrolysis has been used to convert biomass into bio-oil by utilizing fast heating rates (1000 K/s) and low residence times (0.5 – 2 s) (Brown 2011, Rolin et al. 1983). This bio-oil can be used as a fuel; however, it has poor thermal stability and can be corrosive. Hydrothermal conversion schemes

have been developed to convert biomass with high moisture content (> 35 wt%) in a high-pressure aqueous environment to gaseous and liquid products (Brown 2011, Kruse 2009, Wantanabe et al. 2002, Yeh et al. 2012). Finally, APP is able to convert biomass-derived sugars into H_2 and platform molecules such as alkanes at relatively low temperature (473 – 533 K) and moderate pressure (1 – 5 MPa) (Huber et al. 2006, Brown 2011, Humber et al. 2012).

In general, the aforementioned thermochemical routes operate best at larger and more centralized scales. Less investigation has taken place into biomass-to-energy conversion methods that utilize biomass to generate energy or fuel on a distributed scale. Current thermochemical technologies are generally more difficult to implement at smaller scales due to the utilization of high temperature and/or pressure conditions, which require more complex reactor systems and skilled operators. A relatively new biomass conversion technology, alkaline thermal treatment, can produce high-purity H_2 at relatively low temperature, 573 K, and atmospheric pressure that can be directly fed into a proton exchange membrane (PEM) fuel cell. This high-purity H_2 is produced by reacting the biomass with a strong alkali metal hydroxide, and in the process the carbon and oxygen constituting the biomass and alkali metal hydroxide are fixated into a solid alkali metal carbonate matrix, and the embodied hydrogen in the reactants is released as H_2 gas. Because this process does not require additional purification steps to reduce CO levels below the 10 ppm limit required to run a PEM fuel cell (Zhang and Datta 2002), small-scale reactor design becomes possible. The alkaline thermal treatment technology could therefore allow for the generation of distributed energy from biomass and biogenic waste, allowing traditional energy consumers to become energy producers, as well as allowing for areas of the world not connected to a reliable electricity grid to produce energy.

The concept of using alkali metal hydroxides to produce H_2 from carbonaceous compounds was first proposed by Saxena for the reactions of CH_4 and carbon with NaOH (Saxena 2003). Subsequently, alkali metal hydroxide addition to carbonaceous feedstocks for H_2 production has been investigated in several studies (Tongamp et al. 2010, Zhang et al. 2009, Su et al. 2010a, Saxena et al. 2008, Ishida et al. 2004). Ishida et al. were the first to apply NaOH to model biomass feedstocks of glucose and cellulose to generate high-purity H_2 using the alkaline thermal treatment method. The reactions proposed by Ishida for glucose and cellulose, respectively, can be written as follows:

$$C_6H_{12}O_6 + 12NaOH = 6Na_2CO_3 + 12H_2; \qquad \Delta H^0 = 404 \text{ kJ/mol} \qquad \text{(Rxn. 4.1)}$$

$$C_6H_{10}O_5 + 12NaOH + H_2O = 6Na_2CO_3 + 12H_2 \qquad \text{(Rxn. 4.2)}$$
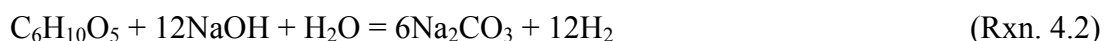
In their study, Ishida et al. were able to non-catalytically convert glucose and cellulose into H_2 with 40% and 62% efficiencies, respectively (Ishida et al. 2005). With the addition of heterogeneous catalysts, particularly Ni-, Co-, Ru-, and Rh-based catalysts, conversions of cellulose to H_2 approached 100% (Ishida et al. 2006). Hansen et al. also reported enhanced conversion for the alkaline thermal treatment of glucose reaction with NaOH to 81% after incorporating Fe-based nanocatalysts (Hansen et al. 2011).

This study focuses on the non-catalytic alkaline thermal treatment of cellulose. Cellulose is the majority component of lignocellulosic biomass, comprising 40-50% of lignocellulosic feedstocks. As steam is a necessary reactant in the alkaline thermal treatment of cellulose, shown in Reaction 4.2, this process may be well-suited to wet biomass feedstocks that normally are processed in high-pressure hydrothermal schemes. Previous studies on the alkaline thermal treatment of cellulose are lacking in data that show the effects of varying NaOH and steam

concentrations on the reaction. This study will examine the effects of NaOH concentration, method of reactant mixing, and presence and concentration of steam flow in the carrier gas stream, on the alkaline thermal treatment of cellulose. Based on the results of the gaseous and solid product analyses from these studies, potential reaction pathways are proposed.

4.2 Materials and Methods

4.2.1 Procedure for Alkaline Thermal Treatment Reactions

The experimental setup utilized in this study is shown in Figure 4.1. NaOH, either in the form of powder or solution, was mixed with either microcrystalline cellulose (Acros) or D-Glucose (Sigma) feedstocks. For experiments involving NaOH powder, the sample was prepared by grinding NaOH pellets (Acros; reagent ACS) with the feedstock using a mortar and pestle. For experiments involving NaOH solution, a 50 wt% NaOH solution (Acros) was mixed with the feedstock. Reactants were loaded into a quartz tube reactor (2.1 cm inner diameter, 26.5 cm length), centered, and held in place using plugs of quartz wool. For experiments involving NaOH solution in excess of the stoichiometric 12:1 NaOH:Biomass molar amount, reactants were loaded into a ceramic boat to hold the reactants, and the boat was then placed inside the quartz tube reactor. Once the sample was loaded inside the reactor, it was sealed using Ultra-Torr fittings (Swagelok), and placed inside a three-zone horizontal split-tube furnace (Mellen Co.). The reactor was then purged of air under a constant N_2 flow of 50 ml/min (STP) provided by a mass flow controller (Omega). This flow was maintained throughout the experiments and was also used as a reference for gas chromatography measurements. Once the reactor was purged of air, the furnace was heated to 373 K and the reactants were dried for 1 h. For experiments performed in the presence of steam flow, steam flow into the reactor was initiated after the 1 h drying phase. The experimental phase then began by heating the reactor at a rate of 2 K/min to

the desired final temperature, which for the majority of this study was 573 K. The temperature was then held isothermally until the online concentration of H_2 in the product gas stream fell below the analytical detection limit of the Micro gas chromatograph (Micro GC). Temperature inside the reactor was monitored with a thermocouple. The total gaseous products generated were also collected in a tedlar bag and analyzed by gas chromatography.

For experiments involving the flow of steam, the steam stream was generated by bubbling the 50 ml/min N_2 flow through a heated water column wrapped in insulation. The concentration of steam in the N_2 carrier stream was varied by changing the temperature of the water column. Prior to entering the reactor, the N_2/steam stream passed through a heated transfer line that was kept at a temperature at least 20 K higher than the water column to prevent condensation. Prior to entering the Micro GC, the gas product stream passed through a Liebig condenser (Sigma) cooled to 273 K using a 50/50 mixture of water and denatured alcohol to condense the steam. Circulation of the coolant through the Liebig condenser was provided by a refrigerated bath circulator (Jeio Tech RW-1025G).

4.2.2 Gaseous Analysis

To obtain the full spectrum of gases formed under the different reaction conditions of pyrolysis, alkaline thermal treatment in the absence of steam flow, and alkaline thermal treatment in the presence of steam flow, the total gaseous products generated during each experiment were collected in a tedlar bag and analyzed via GC/MS (Agilent 7890A GC/5975C MS). Prior to entering the MS detector, the gas from the tedlar bag was separated on a 60 m GS-GasPro column utilizing a GC oven temperature program of holding at 193 K for 3 min, ramping at 60 K/min to 253 K, ramping at 10 K/min to 533 K, and finally holding at 533 K for 20 min,

giving a total analysis time of 52 min per. Identification of gaseous compounds was achieved using the NIST MS Search 2.0 library.

For all experiments in this study, gaseous products were measured online throughout the experimental phase using a 3-Channel Micro GC (Inficon 3000). Two channels were equipped with 10 m Molsieve columns for H_2, N_2, CH_4, and CO separation, and the third with an 8 m Plot U column for separation of CO_2, C_2H_4, and C_2H_6. In each channel, gaseous detection was accomplished with a MEMS TCD, with detection limits for H_2 of 0.1% and 10 ppm for carbonaceous compounds. Online sample injections were made with a frequency of one sample every 5 min.

4.2.3   Solids Analysis

Upon termination of the experimental phase, the reactor was cooled and the solid products remaining removed from the quartz tube reactor for subsequent total inorganic carbon (TIC) analysis (UIC Inc. CM5130 Acidification Module). Samples were acidified to evolve forms of inorganic carbon present in the solids, which in the alkaline thermal treatment system would be Na_2CO_3. The inorganic carbon is evolved in the form of CO_2, which is swept by a carrier gas to a CO_2 coulometer for detection and quantitation.

4.3   Results and Discussion

4.3.1   Alkaline Thermal Treatment Comparison Between Glucose and Cellulose

The first objective of this study was to compare the alkaline thermal treatment of cellulose to the previously studied alkaline thermal treatment of glucose (Ferguson 2012). Because cellulose is made up of glucose monomers, similarities in the gaseous products formed were expected. Four NaOH:Biomass ratios were tested for both feedstocks: pyrolysis (0:1),

NaOH-lean (0.2:1 normalized to stoichiometric, 2.4:1 molar), stoichiometric (1:1 normalized to stoichiometric, 12:1 molar), and NaOH-rich (5:1 normalized to stoichiometric, 60:1 molar). The method of NaOH addition to both feedstocks was NaOH solution, and the reaction procedure detailed in Section 4.2.1 was followed, utilizing a final isothermal reactor temperature of 573 K.

Figure 4.2 shows H_2 conversion as a function of NaOH:Biomass ratio for both the glucose and cellulose feedstocks, with the NaOH:Biomass ratios normalized to the stoichiometric molar ratio of 12:1 given by Reactions 4.1 and 4.2 for glucose and cellulose, respectively. Both feedstocks exhibited remarkably similar H_2 conversions as a function of reactant ratios, indicating similar reaction pathways operating in both systems. For both feedstocks, no H_2 was produced under pyrolysis conditions. Small H_2 conversions were observed in the 0.2:1 NaOH-lean condition, with glucose yielding an average H_2 conversion of about 3% and for cellulose about 4%. A dramatic increase in conversion was observed at the stoichiometric condition, with an average H_2 conversion of 28% obtained for glucose and 27% conversion obtained for cellulose. In both systems, additional NaOH beyond the stoichiometric ratio caused slighter increases in average H_2 conversion, with glucose conversion being 32% and cellulose conversion being 34%.

Also shown on Figure 4.2 is the enhancement in H_2 conversion for the alkaline thermal treatment of cellulose upon the addition of steam flow. For these studies, the concentration of steam flow in the N_2 carrier stream was $P_{H2O} = 38.8$ kPa. As water is shown in Reaction 4.2 to be a reactant in the alkaline thermal treatment of cellulose, improvement in H_2 conversion was to be expected. The Normalized NaOH:Cellulose ratios tested here were: 1:1, 1.5:1, and 5:1. Improvement in H_2 conversion was significant, increasing over 78% upon the addition of steam flow for the stoichiometric ratio case. This significant increase in H_2 conversion upon the

addition of steam flow indicated the alteration of reaction pathways and motivated the further study of the effect of steam flow on the alkaline thermal treatment system.

The proposed stoichiometry of the alkaline thermal treatment of glucose does not require steam as a reactant whereas the stoichiometry of the cellulose reaction does; thus, it was expected that the addition of steam flow to the alkaline thermal treatment reaction for glucose would not lead to as great an increase in H_2 conversion as it did for cellulose. This result was confirmed in Figure 4.3, which shows the effect of steam flow on a stoichiometric NaOH:Biomass ratio for both the glucose and cellulose systems reacted to a final isothermal temperature of 573 K. Like in the cellulose system, the inclusion of steam flow boosted H_2 formation in the glucose system; however, the increase in formation was not as significant as it was for the cellulose system. The addition of steam flow to the glucose system caused an increase in conversion from 25% to 33%, a 32% increase.

In both the glucose and cellulose systems, hydrocarbon formation significantly decreased with the addition of steam flow. The total CH_4 formation decreased by about 5 times with the addition of steam flow to the glucose system. The addition of steam flow caused a much more dramatic reduction in the total CH_4 formation for the cellulose system, decreasing by over 35 times from the no steam flow case. For both feedstocks, the addition of steam flow suppressed CO, C_2H_6, and C_2H_4 formation such that they were undetected in the final gaseous product. Thus it is clear that the addition of steam flow has a positive impact on H_2 generation and selectivity, and the effect was much more pronounced for the cellulose system than it was for the glucose system. With parallels having been drawn between the glucose and cellulose cases of the alkaline thermal treatment reaction, showing that cellulose has the greater potential for non-catalytic H_2 conversion, the rest of this study will explore the effects of NaOH concentration, method of

reactant mixing, and steam flow on the alkaline thermal treatment reaction of cellulose in greater detail.

4.3.2   Alkaline Thermal Treatment of Cellulose and Detailed Gaseous Analysis

To begin the more detailed study of the non-catalytic alkaline thermal treatment of cellulose, it was important to first establish a base case comparison to the literature, as this reaction had only been studied by one group prior (Ishida et al. 2006). For this base case, a stoichiometric 12:1 molar mixture of NaOH solution and cellulose was heated after a 1 h drying phase at 373 K to 773 K at a rate of 2 K/min. Steam was introduced into the reactor at P_{H2O} = 19.2 kPa, the same concentration as used in the previous study by Ishida et al., following the drying phase and the flow was maintained throughout the experiment. The gaseous products formed were measured online via Micro GC with a sampling frequency of one sample every 5 min, and these online results are shown in Figure 4.4. Several similarities were observed between the results of this base case and that previously published by Ishida et al. First, online trends for H_2 and CH_4 were very similar in both studies. For H_2, both experiments show detectable formation starting around 473 K and the formation rate then increased to its maximum rate, which in this experiment was around 530 K and in the Ishida case was about 523 K. Given the sampling frequency limitations of the gas chromatography method, these are closely corresponding temperatures. A second broader H_2 formation rate peak was subsequently observed in both this study and the Ishida study. In this study, the magnitude of the maximum formation rate observed in this peak was approximately 3 times lower than the maximum formation rate from the first peak at 530 K. The temperature at which this secondary maximum occurred was 580 K in this study and 588 K in the Ishida study. Both studies also saw a third, much smaller peak at higher temperatures, achieving a maximum H_2 formation rate at 710 K for

this study and 721 K for the Ishida study. The different H_2 peaks observed in both studies indicated different H_2 formation mechanisms. For CH_4, both studies showed the CH_4 formation rate peaking at much higher temperatures than the maximum H_2 formation rate. The maximum CH_4 formation rate occurred at 666 K in this study and 675 K in the Ishida study.

Unlike the Ishida study, Figure 4.4 shows the formation of other carbonaceous gas products aside from CH_4, namely CO, CO_2, C_2H_4, and C_2H_6, above 623 K. The formation rate trends for both C_2H_4 and C_2H_6 roughly corresponded. Both gases achieved maximum formation rates after that of CH_4, with both occurring at 710 K; however, the maximum C_2H_6 formation rate was roughly an order of magnitude greater than that of C_2H_4, and the maximum CH_4 formation rate was over 30 times greater than maximum C_2H_6 formation rate. Ishida et al. reported a CO_x-free product gas stream throughout their experiment; however, their detection limit was 30 ppm whereas in this study the detection limit for these and other carbonaceous species was 10 ppm. Both CO and CO_2 were detected in this base case study, with formation for CO beginning at 623 K and maintaining at levels either just below or at the detection limit of the Micro GC for the duration of the experiment. For CO_2, its formation began at 645 K, rose slightly until 710 K, and then fell to the Micro GC's detection limit by the end of the experiment at 773 K.

In some repeated trials of the alkaline thermal treatment of cellulose to 773 K, once surpassing 573 K in temperature, the online concentration of CO in the product gas stream was nearly 200 ppm, which is more than 20 times the recommended level for fuel cell-ready H_2. The likely explanation for these variations among repeated trails is the batch nature of this study, which meant that mixing was not perfectly repeatable and thus side reactions that lead to carbonaceous gas products such as CO would exhibit different formation rate trends as a result.

Below 573 K, however, H_2 purity was consistently above 95% with no CO formation detected in any of the repeated trials. Also, nearly 75% of the total H_2 production occurring from the non-catalytic alkaline thermal treatment of cellulose was observed to have occurred upon reaching 573 K. For these reasons, it was decided that the subsequent studies of reactant mixing, NaOH concentration, and steam flow concentration would be conducted with a temperature limit of 573 K.

Regarding H_2 conversion, based on the stoichiometry of Reaction 4.2, this study found approximately 49% conversion, whereas Ishida et al. reported 62% conversion. The discrepancy in conversion may be due to the method of conversion calculation. When calculating conversion based on integrating the online H_2 formation rate curve, as was done in the Ishida study, significant variability was found among repeated trials in this study, likely due to too low of a GC sampling frequency. Some trials were found to match the 62% conversion found in the Ishida study whereas some cases were lower. However, when calculating conversion based upon the total gaseous product collected in the tedlar bag, good agreement was found among repeated trials in this study. Thus the total gaseous product collected in the tedlar bag was used for reporting overall conversion as well as obtaining the overall gaseous product composition in this study.

Figure 4.5 shows the total range of gaseous products for the studies of: a) cellulose pyrolysis, b) NaOH and cellulose at the stoichiometric ratio given by Reaction 4.2 (12:1), and c) stoichiometric NaOH and cellulose mixture in the presence of steam flow ($P_{H2O} = 38.8$ kPa). For all three experiments, the reactants were dried for 1 h at 373 K and then heated to 573 K at 2 K/min, with steam being introduced after drying phase for the steam flow case. Upon reaching 573 K, the reactor was immediately quenched. The product gases generated throughout the

experiment were collected in a tedlar bag and were sampled by GC/MS in order to measure the full range of gaseous products formed in each case. Identification of these compounds was accomplished using the NIST MS Search 2.0 library.

For cellulose pyrolysis, shown in Figure 4.5a, the main gaseous products were CO and CO_2 as well as several oxygenated hydrocarbons typically found during the pyrolysis of cellulose, such as furans and furfural. The immediate shift in degradation pathways was seen with the addition of NaOH to cellulose, shown in Figure 4.5b. CO, CO_2, and oxygenated hydrocarbons were suppressed and C_1 through C_4 alkanes and alkenes were the predominant gaseous products. H_2, although produced under these conditions as will be shown subsequently, is not shown in the GC/MS chromatogram because it was undetectable in this particular GC/MS setup. With the further addition of steam flow to the NaOH and cellulose system, shown in Figure 4.5c, the same C_1 through C_4 alkanes and alkenes were formed; however, their concentrations were greatly suppressed. Not shown here is the increase in H_2 production with the addition of steam flow. Thus it appeared that the major role of NaOH was to suppress the usual dehydration and polymerization pathways of cellulose pyrolysis while favoring pathways that break cellulose down into H_2 and light hydrocarbons. A similar mechanism was also posited in the previous study on the alkaline thermal treatment of glucose (Ferguson et al. 2012). The role of steam flow in the alkaline thermal treatment of cellulose system was one of enhancing H_2 production while suppressing hydrocarbon side product formation. With the major effects of the non-catalytic variables identified, each variable will now be explored in greater detail.

4.3.3   Effects of Reactant Mixing Method and NaOH Concentration

The first two parameters that were explored were the method of reactant mixing and the NaOH:Cellulose ratio. As described in the experimental methods section, NaOH and cellulose

were either mixed by crushing NaOH pellets with cellulose with a mortar and pestle ("Pulverized") or by mixing cellulose with a 50 wt% NaOH solution ("Pretreatment"). Three molar ratios of NaOH:Cellulose, normalized to stoichiometric, were investigated for both Pulverized and Pretreatment methods: 0.2:1 (NaOH-lean), 1:1 (stoichiometric ratio), and 5:1 (NaOH-rich). In addition, these ratio studies were compared to the case of cellulose pyrolysis. After a 1 h drying phase at 373 K, the reactants were heated to 573 K at a rate of 2 K/min. The reactor was held isothermally at 573 K until the online H_2 concentration in the product gas stream fell below the Micro GC detection limit of 0.1%. In addition to online measurements, the total gas product formed in each experiment was collected in a tedlar bag and measured via Micro GC. These total gas products are reported in Figure 4.6 for both Pulverized and Pretreatment methods for all NaOH:Cellulose ratios tested. The vertical bars represent the mean values for each gas, and error bars represent the range of values found from repeated trials.

For the case of cellulose pyrolysis, the only gas products detected via Micro GC were CO and CO_2, correlating with the results shown in the GC/MS chromatogram in Figure 4.5a. The addition of NaOH at the 0.2:1 ratio caused immediate changes in the gaseous composition for both the Pulverized and Pretreatment methods, with H_2, CH_4, C_2H_6, and C_2H_4 observed in both mixing methods. Overall, the trends observed with increasing NaOH concentration were similar between the Pulverized and Pretreatment cases. For H_2, the amount formed per mole of starting cellulose in the experiment was similar at each ratio for each mixing method. For CO_2, at the stoichiometric ratio and beyond, it was not detected in either mixing method. However, regarding CO for the Pulverized cases, its detection was observed in at least one repeated trial at all NaOH concentrations. It was also at a significantly high concentration, with the mean at the stoichiometric ratio of 1.8×10^{-2} mol CO/mol cellulose being only about 3.5 times less than the

pyrolysis case, 6.2×10^{-2} mol CO/mol cellulose. Finally, in general, concentrations of hydrocarbons were much larger for the Pretreatment cases than the Pulverized cases. These results combined with the CO results indicated that alkaline thermal treatment was better promoted in the Pretreatment mixing method than in the Pulverized method, likely due to the improved mixing between the cellulose and the NaOH. In addition, results from the Pulverized cases were found to be less repeatable than the Pretreatment cases, again likely due to the difficulty in replicating mixing conditions in the Pulverized method. It was for the reason of improved mixing that the forthcoming discussion of the effect of NaOH concentration on the alkaline thermal treatment reaction will take place only in the context of the Pretreatment method.

Interestingly, the total CO formed per mole of cellulose at the 0.2:1 normalized ratio, 0.2 mol CO/mol cellulose, was about 3 times higher than that from cellulose pyrolysis, 6.2×10^{-2} mol CO/mol cellulose. This indicated that NaOH may play a role in enhancing decarbonylation of cellulose, which at higher NaOH concentrations was not observed perhaps due to its reaction with NaOH to form H_2:

$$CO + 2NaOH = H_2 + Na_2CO_3; \qquad \Delta H^0 = \text{-169 kJ/mol} \qquad \text{(Rxn. 4.3)}$$
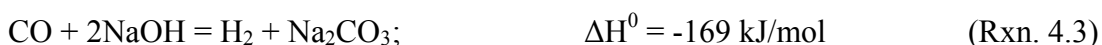
This reaction has been documented in the literature (Saxena et al. 2008, Rowell and Dickson 1918), and has been shown to initiate around 548 K. However, the total amount of H_2 this amount of CO could produce is 0.2 mol H_2/mol cellulose, which is about 6% of the total H_2 produced per mole of cellulose in the next highest NaOH:Cellulose ratio of 12:1. Additionally, the kinetics for Reaction 4.3 below 573 K have been shown to be slow (Saxena et al. 2008), and the majority of H_2 production in the alkaline thermal treatment reaction occurs prior to 573 K. If

the reaction of CO with NaOH were a significant source of H_2, the online gas formation rate trends should show the presence of CO below 548 K, as Reaction 4.3 was shown not to occur below this temperature. Beyond the 0.2:1 ratio, no CO was detected at any point in these experiments. Thus, although a possible source of H_2, Reaction 4.3 was not considered to be a significant source of H_2 for the alkaline thermal treatment reaction.

Upon reaching the stoichiometric ratio, both CO and CO_2 were not detected, and levels of H_2, CH_4, C_2H_4, and C_2H_6 all increased significantly. The H_2 average increased by over 6 times from 0.5 to 3.2 moles H_2/mol cellulose, CH_4 by over 70 times from 1.5×10^{-2} to 1.1 mol CH_4/mol cellulose, C_2H_4 by over 40 times from 1.5×10^{-4} to 6.1×10^{-3} mol C_2H_4/mol cellulose, and C_2H_6 by over 3 orders of magnitude from 2.6×10^{-5} to 5.6×10^{-2} mol C_2H_6/mol cellulose. Further addition of NaOH to the system that was 5 times that of stoichiometric (5:1) did not have a significant effect on the reaction compared to the stoichiometric case. The H_2 average increased by 27% from 3.2 to 4.0 mol H_2/mol cellulose, CH_4 decreased by 29% from 1.1 to 0.8 mol CH_4/mol cellulose, C_2H_4 decreased by 13% from 6.1×10^{-3} to 5.4×10^{-3} mol C_2H_4/mol cellulose, and C_2H_6 increased by 23% from 5.6×10^{-2} to 6.9×10^{-2} mol C_2H_6/mol cellulose. For all of the hydrocarbon gases, however, the difference between the 1:1 and 5:1 normalized cases were within the experimental error.

The results from Figure 4.6 show that NaOH significantly alters the thermal degradation of cellulose, allowing for H_2 and hydrocarbon formation while suppressing CO_x formation, and that these H_2-producing reactions can occur to some extent without water, despite its inclusion in the stoichiometry of Reaction 4.2.

4.3.4   Effect of Steam Flow Concentration

The influence of steam flow on the alkaline thermal treatment of cellulose was subsequently studied. Three partial pressures of steam in the 50 ml/min N_2 carrier stream were studied and compared to the no steam flow case: 4.3 kPa, 12.4 kPa, and 38.8 kPa. In the literature, the partial pressure of steam flow in the carrier gas stream was 19.2 kPa; thus, the range in this study examined higher and lower concentrations of steam flow in the carrier gas stream than previously reported. The experiments were conducted using the Pretreatment mixing method, the same thermal profile in the reactor that was used in the NaOH:Cellulose ratio experiments, and the stoichiometric ratio of reactants. Steam flow was introduced into the reactor after the 1 h drying phase. The results reported from these studies are from the total gaseous product collected in the tedlar bag, and error bars represent the range of values from repeated trials. The total gaseous product formation out to C_2 hydrocarbons is shown in Figure 4.7. The overall observed trend was an increase in H_2 formation per mole of cellulose with a decrease in hydrocarbon formation with increasing steam concentration. For H_2, this increase was most significant upon the introduction of steam flow. Going from the 0 kPa to the 4.3 kPa case, H_2 increased by 64%, from 3.18 to 5.23 mol H_2/mol cellulose. Further increasing the steam flow concentration to 12.4 kPa had no effect on H_2 formation, and H_2 formation at the highest steam loading of 38.8 kPa was only 8% higher than that of the 4.3 kPa case.

Steam flow was found to have a more dramatic effect on hydrocarbon formation as its concentration in the carrier gas stream was increased. CH_4 was reduced by over an order of magnitude with the introduction of steam flow at 4.3 kPa, from 1.1 to 0.1 mol CH_4/mol cellulose, fell by an additional 20% from 0.1 to 9.2×10^{-2} mol CH_4/mol cellulose at a steam loading of 12.4 kPa, and then was more than halved going from the 12.4 kPa to the 38.8 kPa steam loading, decreasing to 4.1×10^{-2} mol CH_4/mol cellulose. Similarly for C_2H_4, its total formation decreased

by over an order of magnitude from 6.1×10^{-3} to 3.5×10^{-4} mol C_2H_4/mol cellulose from the 0 kPa to the 4.3 kPa case, and at higher steam concentrations was undetected. C_2H6 decreased by well over 600 times from 5.6×10^{-2} to 8.7×10^{-5} mol C_2H_6/mol cellulose from the 0 kPa to the 4.3 kPa case, and, like C_2H_4, was undetected at higher steam flow concentrations.

Regarding CO_x compounds, only a small amount of CO was detected in one case, that being the 4.3 kPa steam loading. CO was detected in repeated trials at this loading; however, its detection occurred for 20 min of the 180 min duration of these trials, and the online concentration was at the limit of detection of the Micro GC throughout this time. Therefore, although there may be some decarbonylation at this water loading, it can be considered negligible. CO_2 was undetected for all experimental trials.

Table 4.1 summarizes the concentrations of the total gaseous product for H_2 and hydrocarbons for the alkaline thermal treatment of cellulose, comparing the no steam loading case (0 kPa) with the highest steam loading case (38.8 kPa). Steam was shown to significantly impact the H_2 purity of the product stream, increasing from 73% to 98+% in this non-catalytic system. Conversely, hydrocarbon side products experienced a significant decrease in concentration in the presence of steam flow, decreasing from 27% of the gaseous concentration to below 2%. Thus steam flow was able to improve the selectivity of the alkaline thermal breakdown of cellulose into H_2.

The possibility of steam flow causing greater selectivity for H_2 formation over hydrocarbon formation can be further examined by comparing the total gaseous products between the no steam flow and steam flow cases. For example, with the addition of steam at the loading level of 4.3 kPa, an additional 2.1 mol H_2/mol cellulose was produced compared to the 0 kPa case, while the decreases in total hydrocarbon formation were as follows for each gas: 1.0

mol CH_4/mol cellulose, 5.7×10^{-3} mol C_2H_4/mol cellulose, and 5.6×10^{-2} mol C_2H_6/mol cellulose. If it is assumed that all of the H_2 contained in the reduction of the hydrocarbon gases went to form the additional H_2 gas (e.g. 2 moles of H_2 can be obtained from 1 mole of CH_4, 2 moles of H_2 can be obtained from 1 mole of C_2H_4, 3 moles of H_2 can be obtained from 1 mole of C_2H_6), this would translate to approximately 2.1 moles of additional H_2, which accounts for the increase in H_2 formation observed in the 4.3 kPa steam loading case. Similar analyses for the 12.4 kPa and 38.8 kPa cases accounted for 106% and 91%, respectively, of the increase in H_2 production. These close H_2 balances also point to the selectivity effect steam flow has on H_2-producing reactions in the alkaline thermal treatment of cellulose system.

Figure 4.8 gives the H_2 data obtained in the steam flow study in terms of overall conversion based on the stoichiometry of Reaction 4.2. As previously discussed, steam flow made an immediate impact on H_2 formation and thus conversion, but additional steam flow produced very marginal benefits. Conversion without steam flow was 27%, and this value significantly increased to 44% with the addition of steam flow at the 4.3 kPa loading. Nearly tripling the partial pressure of steam flow to 12.4 kPa caused no change in conversion. Tripling the partial pressure of steam flow yet again only showed an improvement to 47% conversion, an 8% difference from the 4.3 kPa case. Thus the reaction is not limited by steam flow beyond a partial pressure of 4.3 kPa.

4.3.5   Reaction Kinetics and Potential Reaction Pathways

In order to begin to postulate reaction pathways, an analysis of the online gaseous formation rate data is necessary. Shown in Figure 4.9 are the online gaseous formation rates as a function of temperature for two cases of the alkaline thermal treatment of cellulose, one in the absence of steam flow (0 kPa) and the other in the presence of steam flow (4.3 kPa). Only H_2 and

CH_4 are shown in these cases, as the steam flow cases showed zero to negligible formation of other gaseous products. In the presence of steam flow, there appeared to be a very slight delay in the onset temperature for H_2 formation, which occurred at 471 K versus 461 K in the no steam flow case. Both exhibited similar increases in the H_2 formation rate as a function of temperature up until their respective maximum H_2 formation rates, which occurred at 517 K in the steam flow case and 511 K in the no steam flow case. Here it should be noted that the temperature where the maximum H_2 formation rate occurred of 517 K was lower than the temperature of maximum H_2 formation in the base case alkaline thermal treatment study shown in Figure 4.4 of 530 K. Further comparison of the H_2 formation rate curves between Figures 4.4 and 4.9 show that both have very similar trends with two peaks of H_2 formation; however, the curve is essentially shifted by about 10 K lower for the data presented in Figure 4.9 compared to the data presented in Figure 4.4. Other repeated trials also exhibited slight variations within a ~10 K window, the cause of which could be heat and mass transfer issues in this batch system.

Both maximum H_2 formation rates for the no steam flow case and the steam flow case shown in Figure 4.9 were extremely similar, being about 0.4 mol H_2/mol cellulose-min. Thus the conclusion that steam flow enhanced the initial H_2 formation rates cannot be made. The second region of H_2 formation, however, demonstrated significant differences in online H_2 formation rates. In the no steam flow case, following the maximum H_2 formation rate, the H_2 formation rate essentially continually decreased until reaching the detection limit of the Micro GC. However, in the steam flow case, a second smaller, but broader, peak of H_2 formation was observed, peaking at around 560 K. The maximum formation rate at 560 K was over 4 times higher than the maximum formation rate in this secondary temperature region for the no steam flow case, which in the no steam flow case occurred upon the reactor reaching 573 K.

In the presence of steam flow, CH_4 reached a peak online formation rate at the same temperature as the maximum formation rate of H_2, 517 K. This shows that significant degradation of cellulose leading to several gaseous release events occurred around this temperature. After this peak event, the CH_4 formation rate then slowly increased with increasing temperature, peaking in the same temperature window as the second H_2 formation peak region, and then very slowly tapered off. The differences in peak formation rates between H_2 and CH_4 in this secondary formation window were significant, with the H_2 formation rates being 50 times greater than the CH_4 formation rates. These trends contrast greatly with the no steam flow case, where the highest CH_4 formation rate occurred at 573 K, well after the maximum H_2 formation rate at 511 K. In fact, the CH_4 formation rate around 573 K was nearly equivalent to the H_2 formation rate observed at this temperature. Thus it appears in this secondary temperature region from around 547 K to 573 K, steam flow is able to selectively drive the reaction to produce more H_2 while suppressing the CH_4 that would normally be released in the absence of steam flow.

Much work has been done on the thermal degradation of polysaccharides in acidic and alkaline environments in order to understand how thermal breakdown is affected by the system pH. For acidic environments, cellulose can undergo hydrolysis, breaking down into glucose monomers, which then further breaks down into products such as furfural, which can undergo dehydration to form tars and char (Saeman 1945, Oefner et al. 1992). In alkaline environments, the cellulose molecule begins to degrade at the reducing end, proceeding through the chain and eliminating glucose units. The degradation through the chain is terminated when the stopping reaction is reached. This occurs either when the reducing end group is converted to an alkali-stable structure, an *m*-saccharinic acid endgroup, or a crystalline region of the cellulose is reached that is not accessible to the alkali (Haas et al. 1967). The glucose units that have been

eliminated from the chain are also chemically converted by the alkali into isosaccharinic acid and smaller molecules such as formic, acetic, and lactic acids, the proportions of which are dependent on cellulose feedstock, metal hydroxide type, and processing conditions (Van Loon and Glaus 1997, Richards and Sephton 1957). Release of gaseous products, including H_2, concomitant with the formation of the aforementioned derivatives has also been reported (Othmer et al. 1942). Thus an explanation for the two peaks of H_2 production observed in Figure 4.9 for the steam flow case could be two types of H_2-producing events, the first being primarily from the degradation of cellulose into intermediate products and the second primarily from reactions of the intermediate products. It was observed that under steam flow, the alkaline thermal treatment of cellulose system became a melt around the temperature where the peak H_2 formation rate occurred, whereas in the absence of steam flow, little to no observable melting occurred. Thus the role of steam flow could be to both facilitate the mixing of the system, allowing for reduced mass transfer limitations between the NaOH and the cellulose, and to promote the formation of intermediate products derived from cellulose degradation that can undergo reactions that form H_2 while suppressing those that lead to CH_4 and other hydrocarbon gas formation. A study of the intermediate products formed during the alkaline thermal treatment of cellulose and their potential reactions to form gaseous products will be reported in the subsequent chapter.

As Na_2CO_3 is the expected solid product of the alkaline thermal treatment of cellulose reaction according to Reaction 4.2, total inorganic carbon analysis was conducted on the experimental samples to determine the extent of carbonation. Figure 4.10 shows the results of these analyses for the samples produced in the NaOH concentration study conducted in the absence of steam flow (Fig. 4.10a) as well as the steam concentration study (Fig. 4.10b), which

was conducted with a stoichiometric mixture of NaOH:Cellulose, with H_2 conversion also included for comparison. Conversions are based on the stoichiometry of Reaction 4.2, with 100% conversion implying that all of the cellulose was converted to Na_2CO_3 and H_2. With increasing NaOH concentration, shown in Figure 4.10a, both H_2 and Na_2CO_3 conversions increased greatly from the 0.2:1 to the 1:1 normalized ratio and then experienced relatively little change going from the 1:1 to the 5:1 normalized ratio. However, Na_2CO_3 conversion was consistently greater than H_2 conversion, being 3 times greater in the 0.2:1 case, about 2.3 times greater in the 1:1 case, and about 1.7 times greater in the 5:1 case. This implies that other reactions were occurring other than the overall alkaline thermal treatment reaction given in Reaction 4.2. Perhaps the greater hydrocarbon formation observed in the absence of steam flow had concomitant Na_2CO_3 formation; this and other possibilities are currently being investigated.

Contrasting the no steam flow results with the samples prepared under steam flow, shown in Figure 4.10b, it is immediately observable that H_2 and Na_2CO_3 conversions were nearly identical in all steam flow cases. For 4.3 kPa, Na_2CO_3 conversion was about 8% higher than H_2 conversion, was negligibly different in the 12.4 kPa case, and was almost 10% higher than H_2 conversion in the 38.8 kPa case. In the 0 kPa case, Na_2CO_3 conversion was nearly 2 times higher than H_2 conversion. These results again showed a change in reaction pathways facilitated by steam. The close correspondence of H_2 and Na_2CO3 conversions in the steam flow cases implied that steam flow was selecting for the overall alkaline thermal treatment reaction given by Reaction 4.2.

4.4   Conclusions

The non-catalytic alkaline thermal treatment technology, a promising distributed energy generation technology for biomass, has been examined for cellulose, the majority component of

lignocellulosic biomass. Gaseous formation rate trends out to 773 K confirmed findings in the literature, and effects of the parameters of method of reactant mixing, NaOH concentration, and steam concentration, on the reaction products as well as on potential reaction pathways were elucidated. Specifically, it was found that NaOH promoted the formation of H_2 and hydrocarbon gases from the thermal degradation of cellulose while suppressing CO_x compounds. The further addition of steam flow was found to both create a melt in the system, improving mass transfer, as well as to select for H_2-producing pathways while suppressing hydrocarbon-producing pathways. Na_2CO_3 content was found to be greater than expected based on H_2 conversion for the no steam flow cases, pointing to mechanism(s) by which water selects for the overall reaction given by Reaction 4.2. H_2 purity was found to be over 98% with no detectable CO formation for a stoichiometric ratio of NaOH:Cellulose reacted to 573 K with a steam concentration of P_{H2O} = 38.8 kPa, making this H_2 gas stream suitable for PEM fuel cell utilization. The addition of NaOH and steam beyond the required stoichiometric amounts did not significantly enhance the alkaline thermal treatment reaction, with the maximum H_2 conversion observed in these trials being approximately 47%. A better understanding of how NaOH and steam flow break down cellulose under thermal treatment to produce H_2 will aid in optimization of the alkaline thermal treatment process, including in the design and incorporation of catalysis, and this investigation is currently underway.
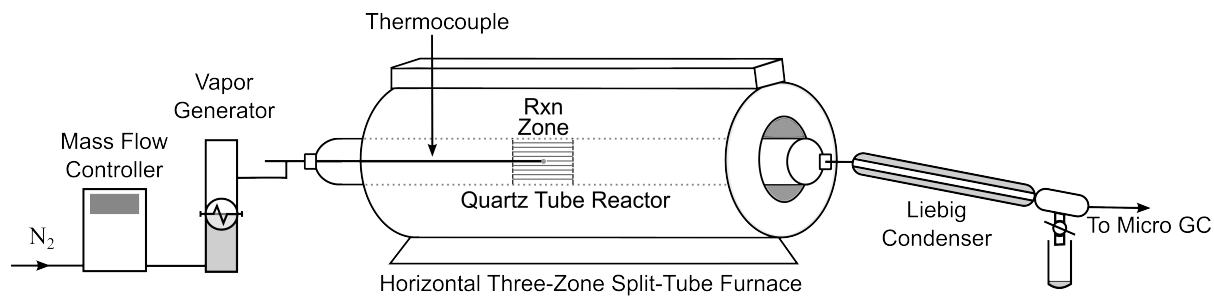
Figure 4.1 Experimental setup used in the study of the alkaline thermal treatment of glucose and cellulose.
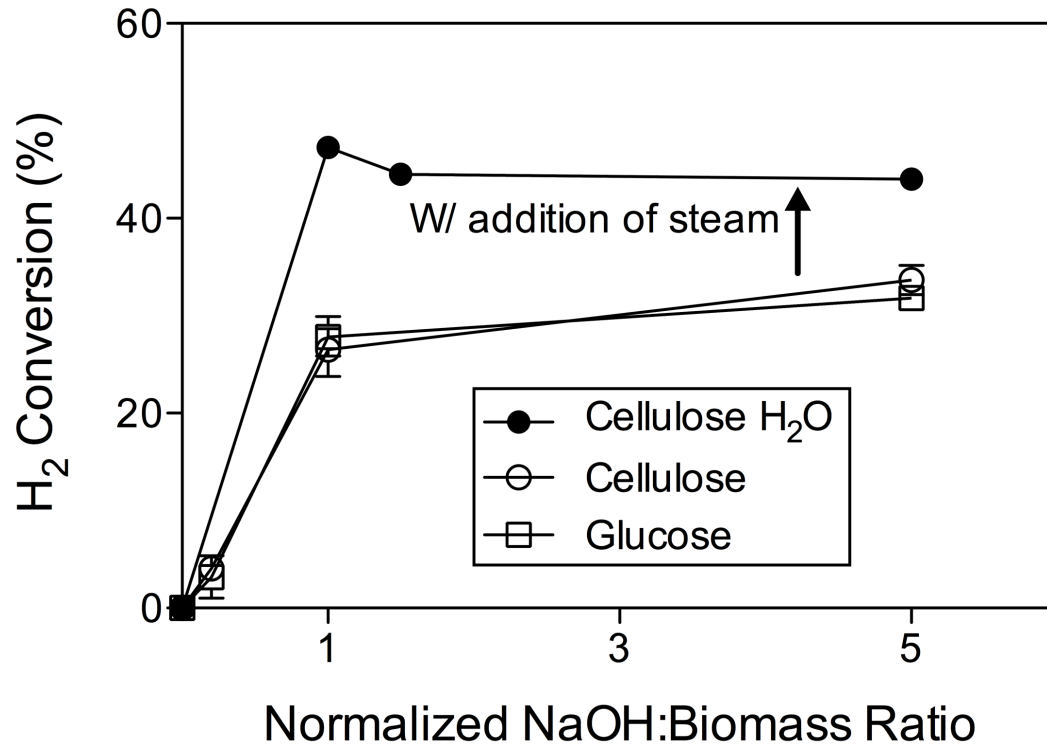
Figure 4.2 Comparison of conversions of glucose and cellulose to H_2, according to Reactions 4.1 and 4.2, respectively, as a function of NaOH:Biomass ratio. Reactor temperature programming: reactants dried for 1 h at 373 K, 373 K → 573 K at 2 K/min held isothermally at 573 K until $[H_2]$ fell below GC's H_2 detection limit of 0.1%. A Normalized NaOH:Biomass ratio of 1 is equivalent to the stoichiometric molar ratio of 12:1 NaOH:Biomass. For the Cellulose H_2O case, steam flow initiated at 373 K with $P_{H2O} = 38.8$ kPa.
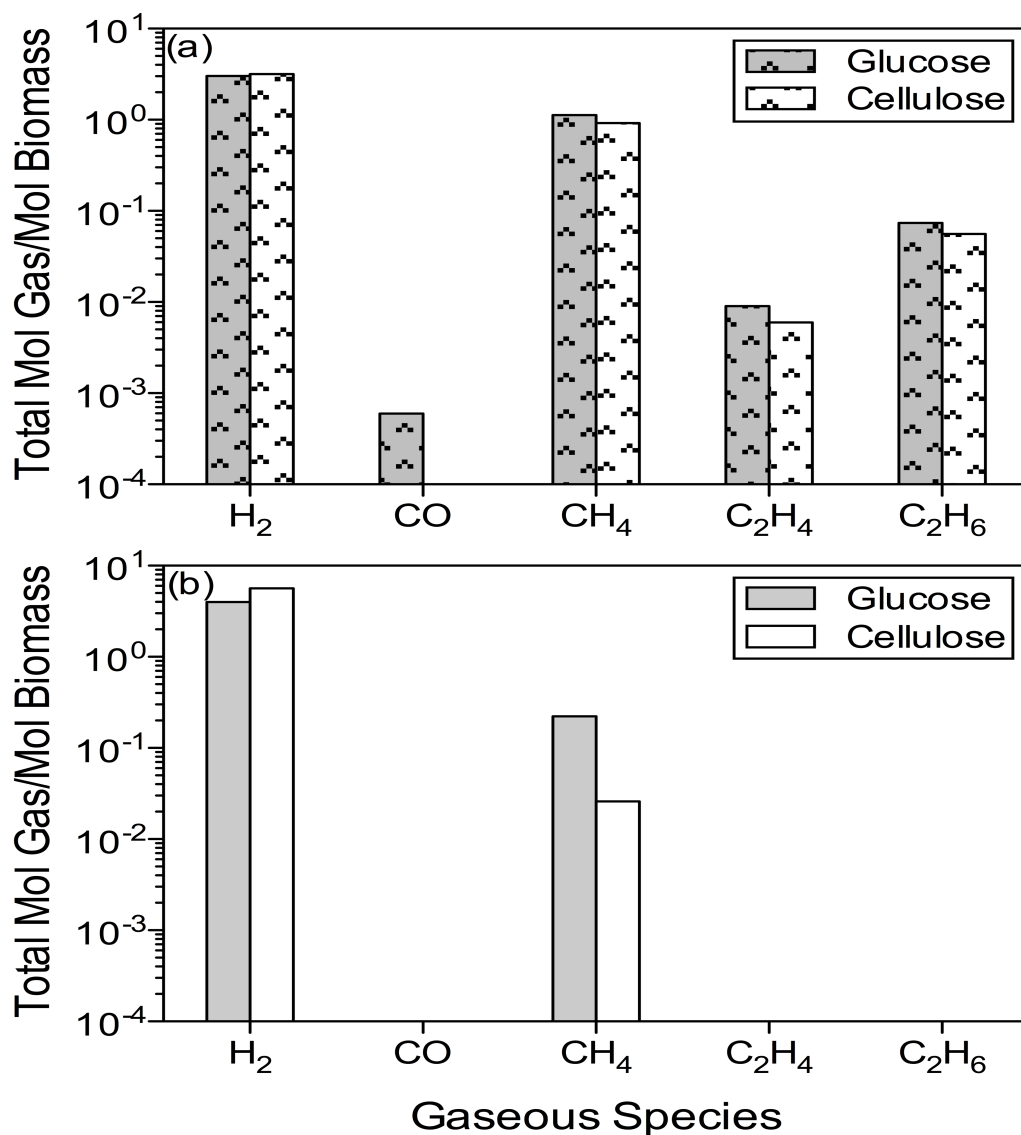
Figure 4.3 Concentrations of each gaseous product from the total collected gaseous product of the alkaline thermal treatment of glucose and cellulose, both in a) the absence and b) the presence of steam flow (P_{H2O} = 38.8 kPa). For both the cellulose and glucose systems, the reactants (12:1 NaOH:Biomass molar ratio) were mixed using the Pretreatment method. Reactor temperature programming: reactants dried for 1 h at 373 K, 373 K $\rightarrow$ 573 K at 2 K/min held isothermally at 573 K until [H_2] fell below GC's H_2 detection limit.
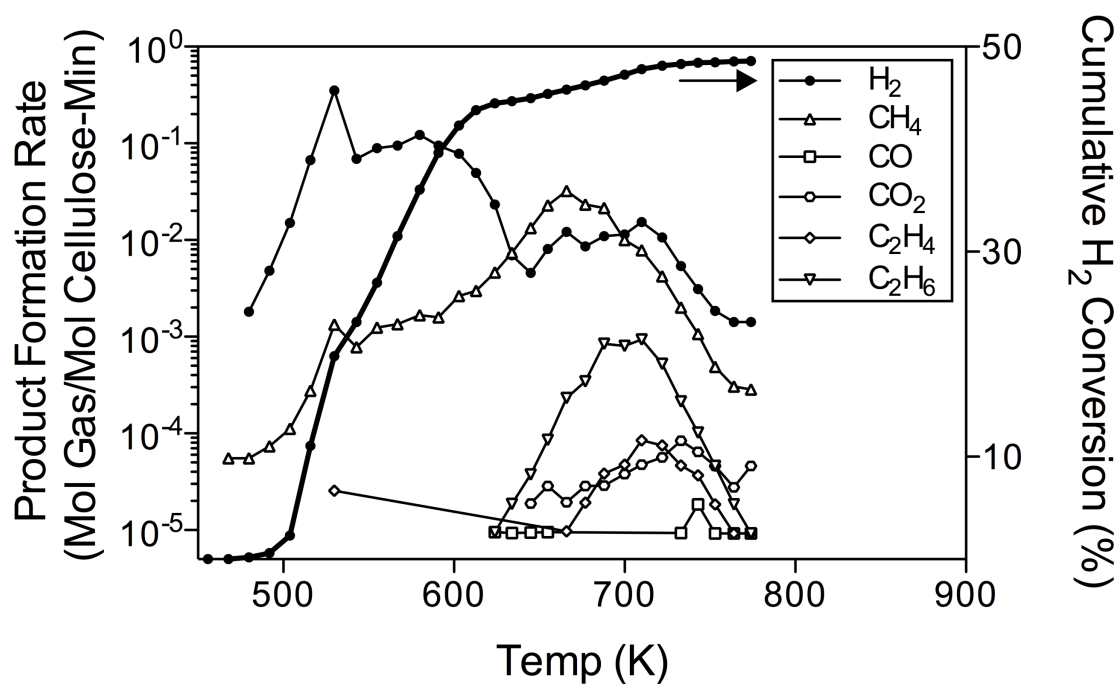
Figure 4.4 Online gaseous product formation rates as a function of temperature, per mole of cellulose, for the alkaline thermal treatment of cellulose. A stoichiometric mixture of NaOH:Cellulose (12:1 molar) was prepared and dried for 1 h at 373 K under N_2 flow. Steam at P_{H2O} = 19.2 kPa was then introduced into the N_2 flow. The reactor was then heated to 773 K with a heating rate of 2 K/min, with the formed gas products sampled online once every 5 min via Micro GC.
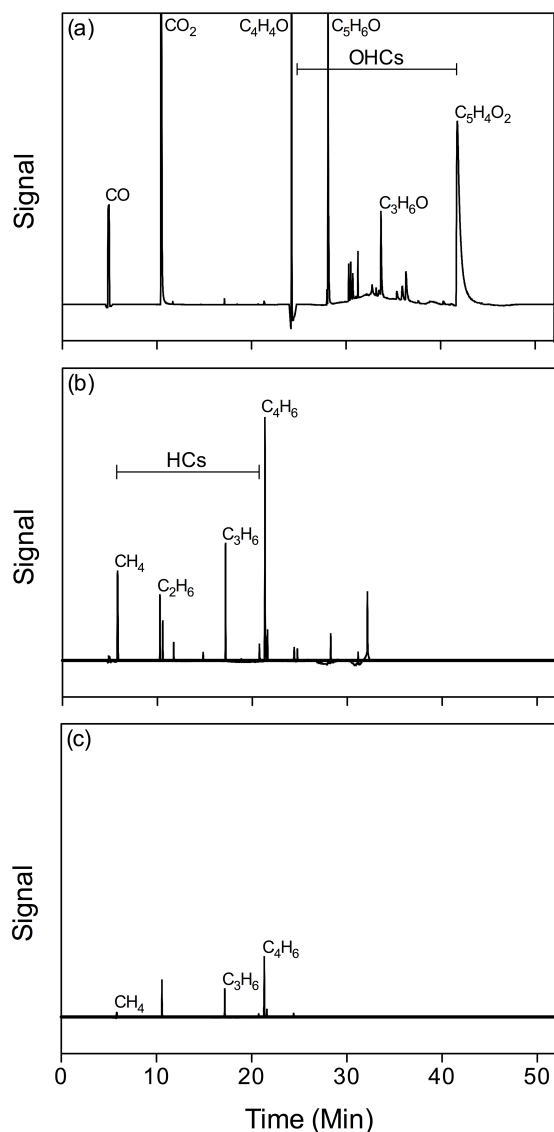
Figure 4.5 GC/MS chromatograms of the total gaseous product formed for a) cellulose pyrolysis, b) stoichiometric (12:1 molar) mixture of NaOH and cellulose without steam flow, and c) stoichiometric mixture of NaOH and cellulose with steam flow (P_{H2O} = 38.8 kPa). Reactor temperature programming: reactants dried for 1 h at 373 K, 373 K → 573 K at 2 K/min. For the steam flow case, introduction occurred after the drying phase. Upon reaching 573 K, the reactor was immediately quenched. Formed gaseous products were collected in a tedlar bag, which was then sampled by the GC/MS.

88
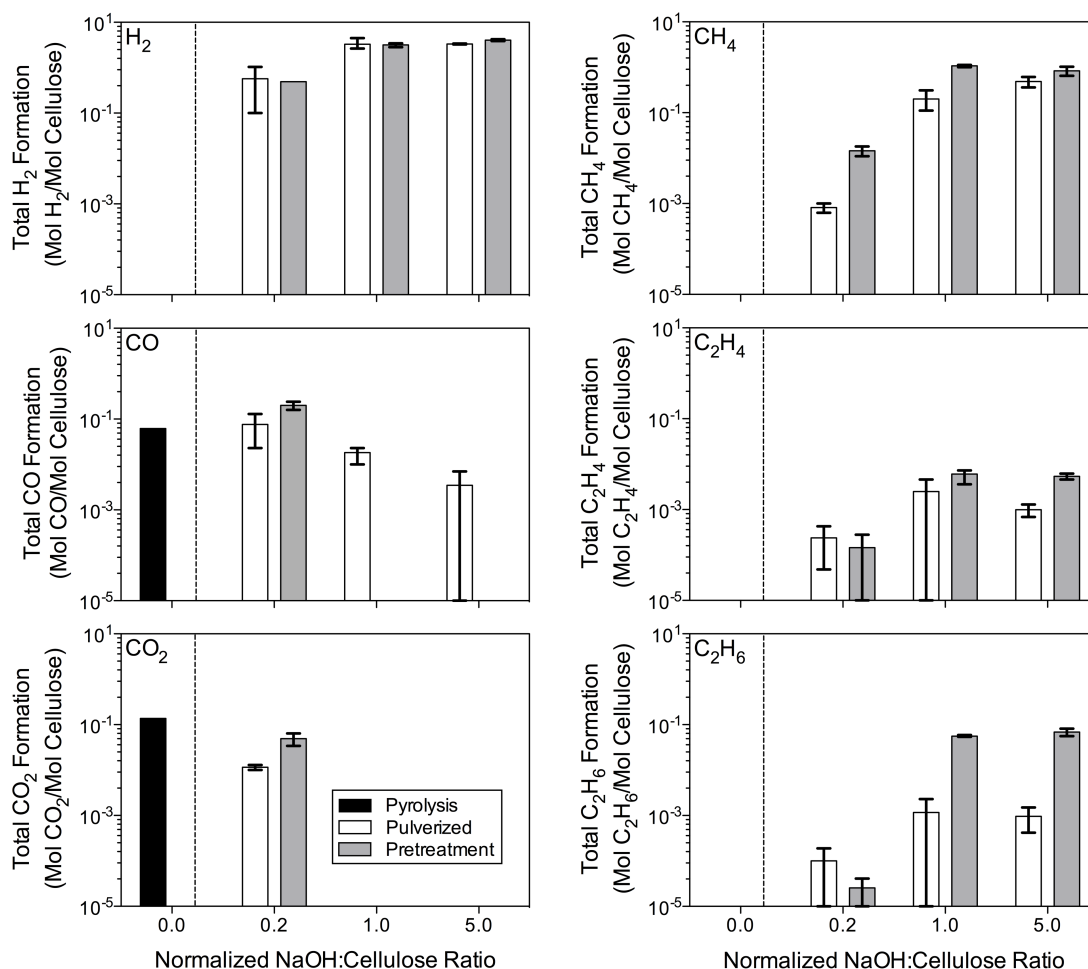
Figure 4.6 Total gaseous production per mole of cellulose as a function of varying the NaOH:Cellulose ratio and method of cellulose treatment with NaOH, in the absence of steam flow. NaOH was added either as powder derived from crushing NaOH pellets with cellulose using a mortar and pestle ("Pulverized") or was added to cellulose in the form of a 50 wt% NaOH/water solution ("Pretreatment"). Reactor temperature programming: reactants dried for 1 h at 373 K, 373 K → 573 K at 2 K/min and held isothermally at 573 K until [H_2] fell below GC's H_2 detection limit of 0.1%. Black bars represent the case of cellulose pyrolysis in the absence of NaOH.
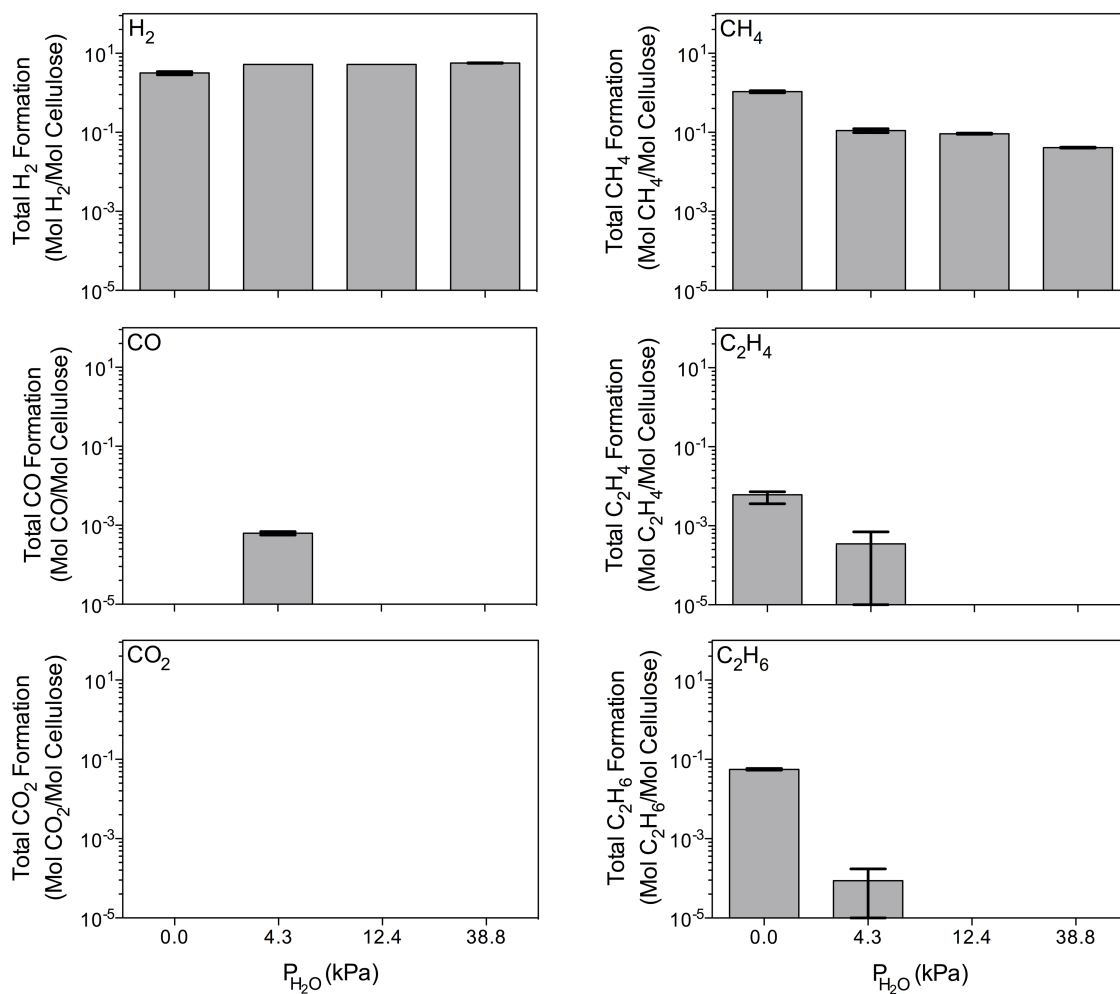
Figure 4.7 Total gaseous product yields per mole of cellulose as a function of varying steam concentration. A stoichiometric, 12:1, molar ratio of NaOH:Cellulose was employed, and the method of NaOH mixing was the Pretreatment method. Reactor temperature programming: reactants dried for 1 h at 373 K, 373 K → 573 K at 2 K/min and held isothermally at 573 K until [H_2] fell below GC's H_2 detection limit of 0.1%.

Table 4.1 Concentrations of each gaseous product from the total collected product gas of the alkaline thermal treatment (ATT) of cellulose, comparing cellulose ATT in the absence and presence of steam flow (P_{H2O} = 38.8 kPa). A stoichiometric, 12:1, molar ratio of NaOH:Cellulose was employed, and the method of NaOH mixing was the Pretreatment method. Reactor temperature programming: reactants dried for 1 h at 373 K, 373 K → 573 K at 2 K/min and held isothermally at 573 K until [H_2] fell below GC's H_2 detection limit of 0.1%. The product gases were collected in a tedlar bar and analyzed by Micro GC and GC/MS. The concentration listed for C_3 and C_4 hydrocarbons are estimations based on relative peak areas from GC/MS data.

Gaseous Product	Concentration (%)	
	Cellulose ATT No Steam	Cellulose ATT Steam
H_2	73.0	98.2
CH_4	24.8	1.5
C_2H_6	1.3	0.0
C_2H_4	0.1	0.0
C_3, C_4 hydrocarbons	0.8	0.3
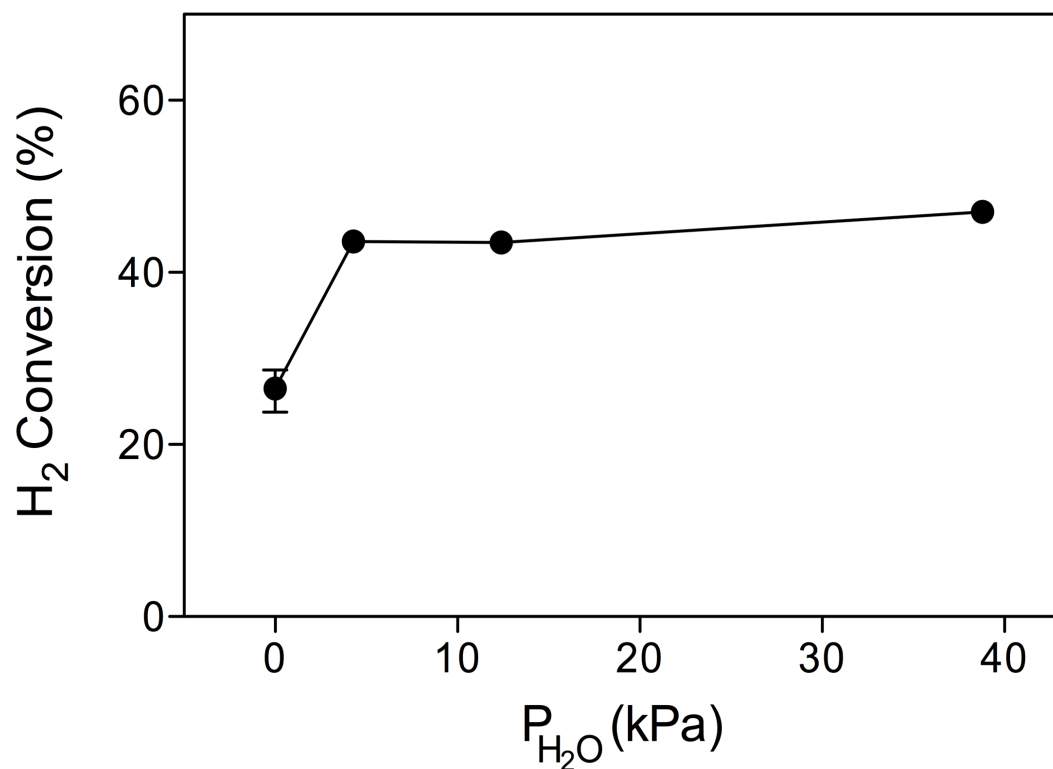
Figure 4.8 Conversion of cellulose into H_2, according to Reaction 4.2, as a function of steam flow concentration. Reactor temperature programming: reactants dried for 1 h at 373 K, 373 K → 573 K at 2 K/min and held isothermally at 573 K until $[H_2]$ fell below GC's H_2 detection limit of 0.1%. Steam flow was introduced into the reactor upon reaching 373 K. A stoichiometric 12:1 NaOH:Cellulose molar mixture prepared under the Pretreatment method was used in all experiments.
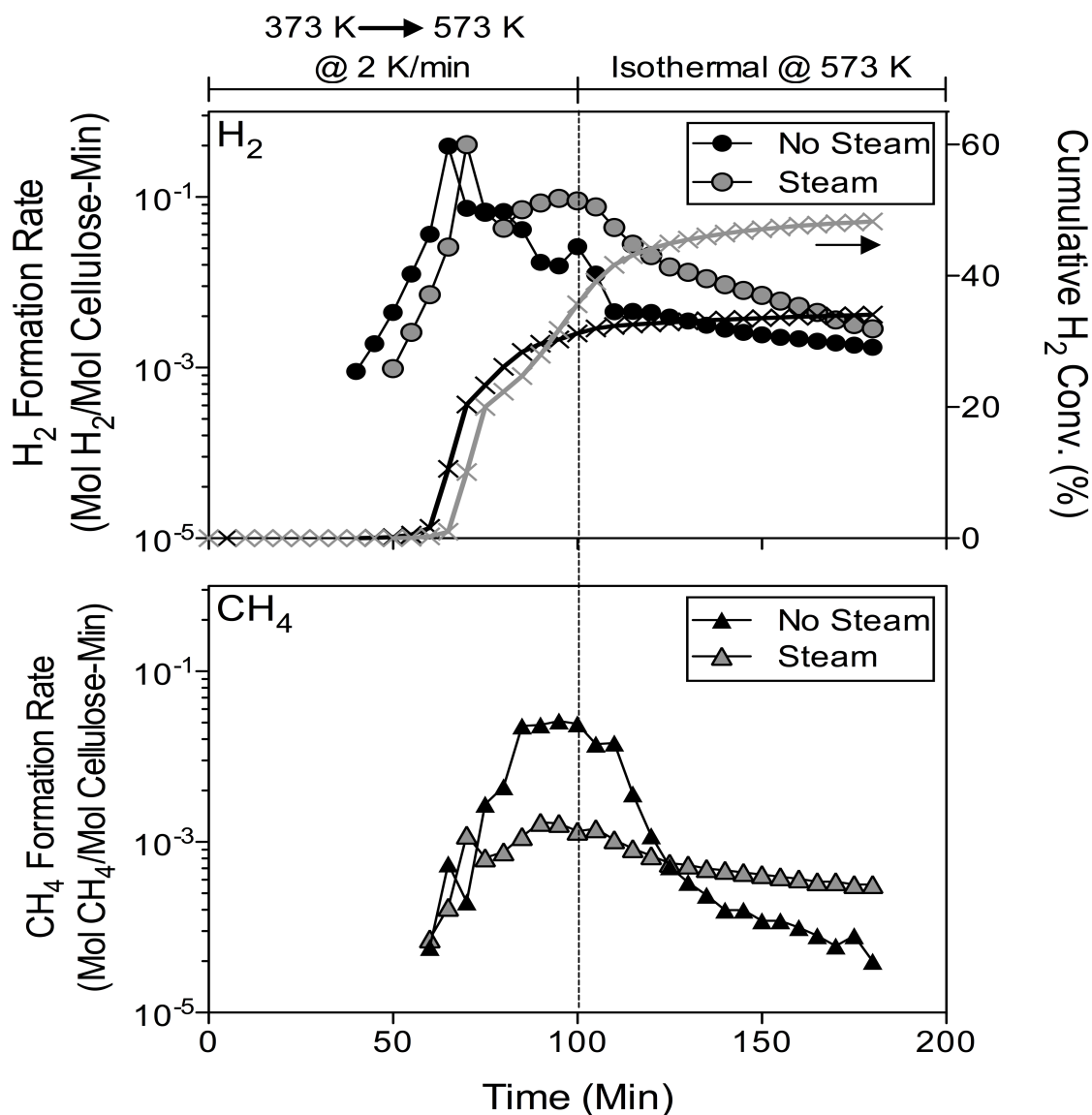
Figure 4.9 Online gaseous product formation for H_2 and CH_4 comparing no steam flow and steam flow (P_{H2O} = 38.8 kPa) cases. Reactor temperature programming: reactants dried for 1 h at 373 K, 373 K → 573 K at 2 K/min and held isothermally at 573 K until [H_2] fell below GC's H_2 detection limit of 0.1%. An NaOH:Cellulose stoichiometric molar mixture prepared under the Pretreatment method was used in both experiments.
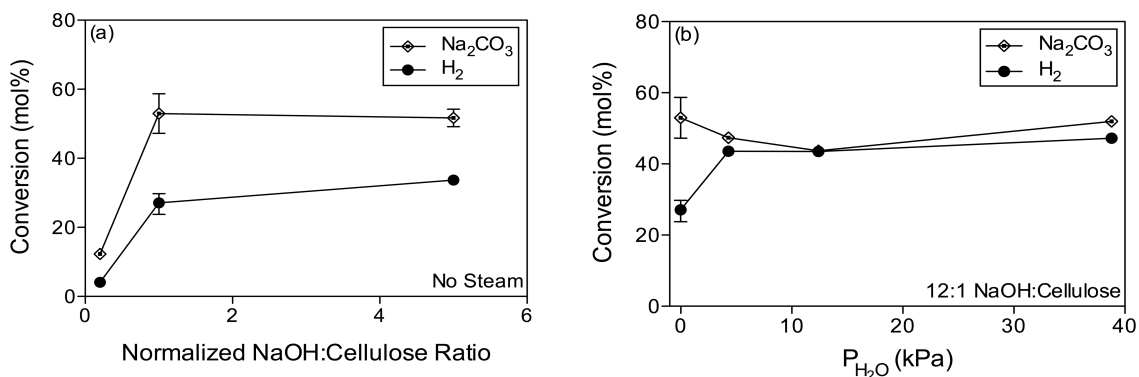
Figure 4.10 Comparison of Na_2CO_3 to H_2 conversion for a) varying NaOH:Cellulose ratio under no steam flow conditions and b) varying steam concentration under a stoichiometric (12:1) NaOH:Cellulose ratio. Reactants were prepared under the Pretreatment method. Reactor temperature programming: reactants dried for 1 h at 373 K, 373 K $\rightarrow$ 573 K at 2 K/min and held isothermally at 573 K until $[H_2]$ fell below GC's H_2 detection limit of 0.1%.

CHAPTER 5

MECHANISTIC STUDY OF ATT OF CELLULOSE BASED ON INTERMEDIATE FORMATION AND CONVERSION

The contents of this chapter are to be submitted to the Energy and Environmental Science as an Article entitled "Production of high-purity hydrogen from cellulose through a carboxylate intermediate pathway via alkaline thermal treatment" (Ferguson and Park 2014).

5.1   Introduction

With global energy consumption expected to increase by 56% between 2010 and 2040, and fossil fuels expected to supply 80% of global energy demand during this period, sustainable alternative energy feedstocks and schemes are needed to counter the deleterious environmental and energy security impacts concomitant with fossil fuel-based energy economies (EIA 2013). Biomass is a sustainable energy feedstock that is carbon neutral, spread throughout the world, and has the potential to supply nearly 7.5% of current global energy demand (McKendry 2002a). The most established thermochemical biomass-to-energy conversion technologies broadly fall under the following categories: combustion, pyrolysis, gasification, hydrothermal treatment, and aqueous phase processing of sugars (Brown 2011). These technologies are able to convert a wide array of biomass feedstocks into fuels and chemicals fungible with those derived from fossil fuels. Due to the temperatures and pressures involved, and the fact that many of these processes require multiple steps to obtain the required product purity, these processes are typically conducted by skilled operators at larger scales at centralized generation facilities.

One biomass-to-energy scheme that can operate on a local scale in a distributed energy generation framework is the alkaline thermal treatment technology. Relatively less investigated, the alkaline thermal treatment technology is able to produce high-purity, fuel cell-ready H_2 in

relatively mild temperature and pressure conditions (573 K and atmospheric pressure). This allows for the design of a distributed energy generation system that can be utilized by unskilled operators, allowing for energy consumers to become energy producers.

First proposed for biomass by Ishida et al. in 2005, in the alkaline thermal treatment reaction, biomass is reacted with an alkali metal hydroxide to produce H_2 gas and alkali metal carbonate as the only products (Ishida et al. 2005). Thus, the action of the alkali metal hydroxide is to fix all of the carbon and oxygen embodied in the reactants as an alkali metal carbonate, releasing all of the hydrogen embodied in the reactants as H_2 gas. The alkaline thermal treatment reactions for cellulose with NaOH and steam can be represented as follows:

$$C_6H_{10}O_5 + 12NaOH + H_2O = 6Na_2CO_3 + 12H_2 \qquad \text{(Rxn. 5.1)}$$
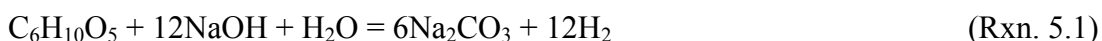
The addition of metal catalysts to the alkaline thermal treatment reaction has also been explored, with conversions to H_2 increasing from 62% in the absence of catalyst to nearly 100% with Ni-, Co-, Rh-, and Ru-based catalysts (Ishida et al. 2006). Subsequently, investigation into the non-catalytic parameters of the reaction has taken place for both the glucose and cellulose feedstocks. NaOH was found to suppress the usual decarbonylation and decarboxylation pathways of pyrolysis for both glucose and cellulose while enabling H_2 and hydrocarbon gas formation, and the further addition of steam flow was found to enhance H_2 production and suppress hydrocarbon formation (Ferguson 2012). General reaction pathways were suggested in these and other studies (Su et al. 2010, Hsu and Hixson 1981, Zhang et al. 2009); however, the pathways for the formation of H_2 and other gaseous products from the alkaline thermal treatment reaction are still poorly understood. A better understanding of how the alkali metal hydroxide

96

and steam break down cellulose under thermal treatment to produce the high-purity H_2 could result in improvements in reactor, process, and catalyst design.

The alkaline degradation of polysaccharides has been well studied, with areas of study including: the obtainment of structural information about polysaccharides[11] the production various chemicals (Hsu and Hixson 1981, Whistler and BeMiller 1958, Othmer et al. 1942, Niemela and Sjostrom 1986, Krochta et al. 1987, Cross et al. 1892), additives for pyrolysis (Shafizadeh and Lai 1972, Philpot 1971, Radlein et al. 1991, Ponder and Richards 1993, Patwardhan et al. 2010), and the decomposition of cellulosic materials found in radioactive waste (Van Loon and Glaus 1997, Knill and Kennedy 2003). The decomposition of polysaccharides, such as cellulose, in the presence of alkali metal or alkaline earth metal hydroxides is influenced by a number of factors, such as the type of metal hydroxide, the concentration of metal hydroxide relative to biomass, the temperature at which degradation is performed, the duration of the degradation, and the reaction medium under which degradation takes place.

One particular method of H_2 production from biomass involving alkaline degradation that has parallels to the alkaline thermal treatment of cellulose is alkaline hydrothermal gasification. Utilizing an NaOH concentration of 1.67 M and hydrothermal gasification conditions of 723 K and 34 MPa, Onwudili and Williams obtained a gaseous product of about 80% H_2 and about 10% CH_4 concentration from cellulose, bearing some similarity to concentrations of H_2 and CH_4 found in the alkaline thermal treatment of cellulose reaction. Onwudili and Williams argued that the pathway for H_2 formation proceeded first through degradation of the biomass into sodium formate, releasing H_2 in the process, then through degradation of the sodium formate into CO, and finally the reaction of CO with H_2O to form more H_2 through the water-gas shift reaction. To test if H_2 formation proceeded through a sodium formate intermediate pathway, hydrothermal

gasification tests were conducted on the sodium formate to see if it would produce H_2 at analogous temperature and pressure conditions to that of the parent biomass case. The results confirmed this pathway as well a similar pathway in which CH_4 formation could be explained by a hydrothermal decomposition of sodium acetate (Yu and Savage 1998, Onwudili and Williams 2009, Onwudili and Williams 2010).

Based on the alkaline hydrothermal gasification studies as well as the other studies on the alkaline degradation of cellulose, it was hypothesized that the production of H_2 and other hydrocarbon gases observed in the alkaline thermal treatment of cellulose may be attributed to two types of reactions, the first being gaseous release resulting from the degradation of the cellulose into intermediates, with those intermediate compounds being primarily the sodium salts of carboxylic acids. The second type of H_2 release event would then be from the reactions of the sodium carboxylate salt intermediates with NaOH, which would also produce Na_2CO_3. For example, assuming a sodium formate driven pathway, the formation of H_2 may proceed as follows:

$$C_6H_{10}O_5 + 12NaOH + H_2O = 6NaCOOH + 6NaOH + 6H_2 \qquad \text{(Rxn. 5.2)}$$

$$6NaCOOH + 6NaOH = 6Na_2CO_3 + 6H_2; \quad \Delta H^0 = \text{-39 kJ/mol} \qquad \text{(Rxn. 5.3)}$$
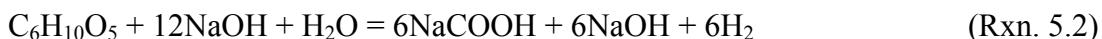
An analogous reaction involving sodium acetate could account for observed CH_4:

$$NaCH_2COOH + NaOH = Na_2CO_3 + CH_4; \quad \Delta H^0 = \text{-71 kJ/mol} \qquad \text{(Rxn. 5.4)}$$
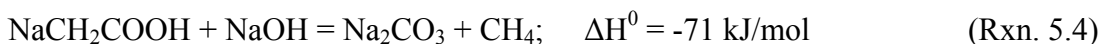
The reactions of sodium formate and sodium acetate with NaOH to produce H_2 and CH_4, respectively, have been demonstrated (Roswell and Dickson 1918); however, detailed study on these reactions is not found in the literature.

This study examines the potential reaction pathways of the alkaline thermal treatment reaction for cellulose to elucidate those pathways relevant to H_2 and hydrocarbon gas formation. First, the degradation products of the alkaline thermal treatment of cellulose at intermediate temperature conditions were identified, both in the presence and absence of steam flow. Subsequently, those intermediates identified as potential sources of H_2 and hydrocarbon gases were reacted in the presence and absence of both steam flow and NaOH using the same thermal treatment conditions as employed in the alkaline thermal treatment of cellulose reaction. Analyses of Na_2CO_3 formation in the solid products resulting from the alkaline thermal treatment reactions of cellulose at intermediate temperatures, as well as in the solid products resulting from the reactions of the intermediate species with NaOH, were also conducted. From these results, potential reaction pathways for the alkaline thermal treatment of cellulose reaction are proposed.

5.2   Materials and Methods

5.2.1   Alkaline Thermal Treatment of Cellulose Study

Figure 5.1 shows the reactor setup used in this study of the alkaline thermal treatment of cellulose. It is a semi-batch system that has been used in alkaline thermal treatment studies described previously (Ferguson 2012). Essentially, microcrystalline cellulose (Acros) was mixed with a 50 wt% NaOH solution (Acros) in a stoichiometric ratio according to Reaction 5.1 (12:1 NaOH:Cellulose molar) and loaded into a quartz tube reactor, which was placed inside a three-zone horizontal split-tube furnace (Mellen Co.). The reactor was purged of air under constant N_2 flow of 50 ml/min (STP), heated to 373 K and the reactants dried for 1 h. The experimental phase was then initiated, with the reactants heated at 2 K/min to the final temperature. In the cases where steam was flowed into the reactor, introduction of the wet N_2 carrier gas stream into the reactor (P_{H2O} = 38.8 kPa) began after the 1 h drying phase. Upon reaching the final

temperature, the reactor was removed from the furnace and immediately quenched by flowing air over the reactor, ending the experimental phase. The following temperatures were investigated: 473 K, 498 K, 513 K, 523 K, 548 K, and 573 K. The temperatures were chosen based on the results for H_2 formation rates as a function of temperature from an earlier investigation of the alkaline thermal treatment of cellulose. Gaseous formation was also measured online via Micro GC (Inficon), and the configuration of this instrument is describe elsewhere (Ferguson 2012).

5.2.2 Reactions of Intermediate Species Study

The following identified intermediate species were investigated for gaseous formation when reacted with NaOH: sodium formate (Sigma Aldrich), sodium acetate (Fisher Scientific), sodium glycolate (Acros), sodium propionate (Sigma Aldrich), sodium succinate (Acros), and sodium oxalate (Fisher Scientific). As in the alkaline thermal treatment of cellulose studies, reactions were performed in the semi-batch setup in Figure 5.1 and studied both in the absence and presence of steam flow (38.8 kPa). The intermediate species were also thermally treated both in the presence and absence of NaOH. The same heating rate of 2 K/min up to 573 K was used in order to compare to the formation rate trends to those observed in the alkaline thermal treatment of cellulose. After the reactor cooled, the solids remaining in the reactor after the experiment were removed and analyzed by ion chromatography and for total inorganic carbon content.

5.2.3 Solid Product Characterization Techniques

Ion chromatography analysis

As the intermediates of the alkaline thermal treatment of cellulose were expected to consist mainly of the sodium salts of carboxylic acids, ion exclusion chromatography was employed for sample analysis. A Metrohm 861 Advanced Compact IC was used equipped with a

Metrosep Organic Acids 250/7.8 column for component separation. The eluent used was 0.5 mM H_2SO_4 and the suppressor used was 20 mM LiCl.

Samples were prepared for analysis in the following manner. First, the solid product generated from the alkaline thermal treatment of cellulose reaction was ground to a fine powder with a mortar and pestle. Next, 40 mg of the crushed solids were added to 15 ml of deionized water, and this solution was well mixed. The mixed solution was then passed through a 0.45 μm filter to remove any potential undissolved fine particles prior to introduction to the instrument.

In addition to this Organic Acids 250/7.8 column, which utilizes ion exclusion, separation was also done by a Metrosep A Supp 5-250/4.0 ion exchange column for identification of those compounds more challenging to separate by the ion exclusion technique. This qualitative analysis was done by Metrohm for samples representative of all of the peaks that could not be positively identified by the ion exclusion technique alone.

Total inorganic carbon analysis

Assuming complete conversion of the cellulose and NaOH to H_2 given by the stoichiometry of Reaction 5.1, the only solid product of the reaction should be Na_2CO_3. Thus total inorganic carbon (TIC) analysis gives additional insight into the extent of reaction according to Reaction 5.1. TIC analysis (UIC Inc. CM5130 Acidification Module) was performed for all experimental samples and compared to H_2 conversion as measured by the Micro GC. TIC was quantified through the acidification of the solid product to evolve forms of inorganic carbon present, which for the alkaline thermal treatment system would be Na_2CO_3, as CO_2. The evolved CO_2 was then swept by a carrier gas into a CO_2 coulometer for quantitation.

5.3   Results and Discussion

5.3.1 The Alkaline Thermal Treatment of Cellulose and Identification of Intermediates

Formation of Gaseous Products

A base case for the conversion of cellulose to gaseous products via alkaline thermal treatment, both in the presence and absence of steam flow, is given in Figure 5.2. Both the no steam flow (Fig. 5.2a) and steam flow (Fig. 5.2b) cases were run utilizing a stoichiometric molar ratio of 12:1 NaOH:Cellulose, given by 5.1. The reactants were dried for 1 h at 373 K under a constant 50 ml/min (STP) of N_2 flow. Upon completion of the drying phase, steam flow was introduced (P_{H2O} = 38.8 kPa), carried by the N_2 flow, for the experiment testing steam flow as a reactant. The reactor was then heated at a rate of 2 K/min to 573 K, and held isothermally at this temperature until the online concentration of H_2 in the gaseous product stream fell below the Micro GC's detection limit of 0.1%. The choice of 573 K as the final isothermal temperature was based on previous study of the alkaline thermal treatment of cellulose system reacted to 773 K, where it was found that up to 573 K, the highest H_2 formation rates and best selectivity toward H_2 formation were observed.

Regarding H_2 formation, the initial formation rate trends were similar for both the no steam flow and steam flow cases. The no steam flow case did start to exhibit H_2 formation at lower temperatures, starting around 460 K compared to around 473 K for the steam flow case. However, both the no steam and steam flow cases had nearly identical maximum H_2 formation rates, around 0.4 mol H_2/mol cellulose-min, and the temperature at which these peak formation rates occurred was similar for both cases, 511 K for the no steam flow case and 517 K for the steam flow case. These similarities in H_2 formation between the no steam flow and steam flow cases indicated that steam flow did not significantly affect H_2 formation in the alkaline thermal treatment of cellulose at lower temperatures.

Significant differences in H_2 formation between the no steam flow and steam flow cases arose after the maximum H_2 formation rates were observed. A second peak of H_2 formation, much broader than the first, was seen in the steam flow case but was absent in the no steam flow case. This formation rate trend in the steam flow case started around 550 K, peaked just before reaching 573 K, and fell shortly after reaching the isothermal phase. This contrasted with the no steam flow case, which after the maximum H_2 formation rate observed at 511 K did not show any significant secondary increases aside from a small spike at 573 K. The maximum H_2 formation rate in this secondary region was about 4 times greater in the steam flow case, 9.6×10^{-2} mol H_2/mol cellulose-min, than the no steam flow case, 2.6×10^{-2} mol H_2/mol cellulose-min. The differences in H_2 formation in this secondary, higher temperature region showed that steam was now clearly influencing the H_2 formation pathways of the alkaline thermal treatment of cellulose, indicating that different reaction pathways were likely leading to H_2 formation than were observed in the first H_2 formation region. In terms of overall conversion to H_2, based on the stoichiometry of Reaction 5.1, 34% conversion was achieved in the no steam flow case whereas 48% conversion was achieved in the steam flow case.

Hydrocarbon gas product formation, on the other hand, was much more significant in the no steam flow case than the steam flow case. The onset of CH_4 formation occurred around 500 K for both the no steam flow and steam flow cases and had similar magnitudes of formation rates, 5.8×10^{-5} mol CH_4/mol cellulose-min for the no steam flow case and 7.3×10^{-5} mol CH_4/mol cellulose-min for the steam flow case. Both cases then experienced an increase in the CH_4 formation rate with increasing temperature; however, the increase in formation rate for the no steam flow case was much more significant. A large peak of CH_4 formation was observed from around 550 K to 573 K in the no steam flow case, with a maximum formation rate of about $2.6 \times$

10^{-2} mol CH_4/mol cellulose-min. This was over an order of magnitude greater than the peak CH_4 formation rate observed in the steam flow case from 550 K to 573 K. It was within this temperature region that formation of C_2 hydrocarbons, C_2H_6 and C_2H_4, was also observed in the no steam flow case, whereas these compounds were undetected in the steam flow case. Thus it appeared that when steam flow was present in the alkaline thermal treatment reaction, it was able to select toward H_2 formation pathways and away from hydrocarbon gas formation pathways in this secondary, higher temperature region.

Formation of Sodium Carboxylate Salt Intermediates

Similar trends for gaseous product formation from the alkaline thermal treatment of cellulose system as a function of temperature have been reported elsewhere for the steam flow case (Ishida et al. 2006); however, the reaction pathways have not been elucidated. In order to establish the formation of sodium carboxylate salts as potential reactive intermediates in the alkaline thermal treatment of cellulose reaction, the formation of the sodium carboxylate salts must first be confirmed and their identities obtained. The potential formation of sodium carboxylate salts was studied by conducting alkaline thermal treatment of cellulose reactions to intermediate temperatures up to and including 573 K, and then analyzing the remaining solid products via IC. Upon dissolving the solids in DI water in preparation for IC analysis, it was found that all of the samples except for the no steam flow and steam flow cases reacted to 473 K were highly soluble. The likely explanation for this observation was that at such a low temperature, the majority of the cellulose had not reacted with the NaOH, and thus the cellulose remained a significant insoluble product in solution. However, at higher temperatures, the cellulose and NaOH undergo more reaction, creating water-soluble intermediate species.

The chromatograms from the IC analyses are shown in Figure 5.3, and are normalized on a per mole of starting cellulose basis. Those anions that were identified by the ion exclusion technique were: glycolate, formate, acetate, propionate, and carbonate. Small amounts of dicarboxylate anions, which are better detected by ion exchange, were also identified: succinate and oxalate. Thus it was found that the alkaline thermal treatment of cellulose does produce the sodium salts of carboxylic acids, including sodium formate and sodium acetate, which were identified as relevant intermediates to produce H_2 and CH_4, respectively, in the alkaline hydrothermal gasification of biomass (Onwudili and Williams 2010). The formation of predominantly C_1-C_3 sodium carboxylate salts during the alkaline thermal treatment of cellulose was consistent with observations and proposed pathways in the literature (Niemela and Sjostrom 1986, Krochta et al. 1987, Niemela 1990, Krochta and Hudson 1985). Alkali metal hydroxides have been found to favor fragmentation of the cellulosic degradation products into C_1-C_3 organic acids, whereas alkaline earth metal hydroxides favor rearrangement pathways that lead to the formation of isosaccharinic acid (Machell and Richards 1960, Richards and Sephton 1957).

Qualitatively examining the chromatograms, it was first observed that at 473 K, little carboxylate formation occurred in both the no steam flow (Fig. 5.3a) and steam flow cases (Fig. 5.3b). As the temperature was increased, both the no steam flow and steam flow systems showed much more significant carboxylate formation. Overall, more sodium formate was observed in the steam flow cases than the no steam flow cases. Sodium acetate concentration peaked at 548 K and then decreased to 573 K in the no steam flow case, whereas it continually increased up to 573 K in the steam flow case, indicating that steam flow was suppressing its consumption. Sodium glycolate was observed at the highest concentrations in both the no steam flow and steam flow cases. Beyond 523 K, both cases exhibited very different behavior with regards to

sodium glycolate, with it being undetected in the no steam flow case and its concentration slowly decreasing in the steam flow case. Interestingly in the no steam flow case, at 548 K, where sodium glycolate was no longer detected, two unknown peaks became prominent that were not observed in the steam flow case; perhaps these unknowns were formed from the consumption of sodium glycolate in the no steam flow case.

Qualitative observations of the solid products

At the conclusion of each alkaline thermal treatment of cellulose intermediate temperature experiment, the solid products inside the reactor were photographed. The physical evolution of the solids in the alkaline thermal treatment of cellulose as a function of temperature is displayed in Figure 5.4 for both the no steam flow (Fig. 5.4a) and steam flow cases (Fig 5.4b). In the alkaline thermal treatment of cellulose in the absence of steam flow, as the cellulose and NaOH mixture was heated, the mixture darkened in color from yellow/orange at the start of the experiment to an orange/tan at 473 K, and darkened thereafter to brown by 523 K, and finally to a black by 573 K. Little evidence of melting or expansion of the reaction products was observed. This contrasts sharply with what was observed upon the addition of steam flow to the system. The products did start out similarly to the no steam flow case up to 473 K, with no melting occurring and the color of the mixture being tan, although it was a lighter tan than the no steam flow case. However, once the first large peak in the H_2 formation rate was observed at around 517 K for the steam flow case, shown in Figure 5.2, significant bubbling and melting of the products was observed, and the color of the mixture was an off-white, as can be seen in the 523 K picture in Figure 5.4b. As the temperature was further increased, unlike in the no steam flow case, the color did not change but remained off-white, and bubbling could still be observed.

These qualitative observations gave further evidence for the breakdown of cellulose by strong alkali metal hydroxides into sodium carboxylate salts. The sodium carboxylate salts are all highly soluble in water; therefore it is reasonable that once steam flow is added to the system, a melt should be produced. Thus, steam flow may not only favor the breakdown of cellulose into those sodium carboxylate compounds more favorable for H_2 production while suppressing CH_4 formation, it may also be acting to better mix the system through the formation of a melt, enhancing the alkaline thermal treatment reaction.

5.3.2   Conversion of Sodium Carboxylate Salt Intermediates

In order to determine how the observed sodium carboxylate salts may be further transformed in the alkaline thermal treatment reaction, these compounds were reacted at the same conditions as the cellulose was reacted with NaOH. Thermal treatment studies were conducted on the sodium carboxylate salts alone, in the presence of NaOH, and in the presence of NaOH and steam flow (P_{H2O} = 38.8 kPa) to elucidate the role of each variable. Shown in Figure 5.5 are the results of these studies for sodium formate, sodium acetate, and sodium glycolate. The top plots in Figure 5.5 show the concentrations of each sodium carboxylate salt in the solid alkaline thermal treatment product as a function of temperature, and the middle and bottom plots show the H_2 and CH_4 formation rates, respectively, as a function of temperature for the reactions of the sodium carboxylate salts with NaOH. The results for each sodium carboxylate salt will now be discussed.

Sodium Formate

In the absence of NaOH, sodium formate did not form H_2 or CH_4 during the thermal treatment. This addition of NaOH at a 1:1 molar ratio, as given by the stoichiometry of Reaction 5.3, caused H_2 formation, initiating at 503 K for the no steam flow case. The H_2 formation rate

steadily increased with increasing temperature, essentially reaching a steady value between the temperatures of 533 K and 559 K of about 4.0×10^{-2} mol H_2/mol sodium formate-min, and beyond this temperature decreased. The amount of H_2 generated was 0.96 mol H_2/mol sodium formate, which according to the stoichiometry of Reaction 5.3 meant that H_2 conversion was nearly 100%. This was also confirmed by TIC analysis, which showed the remaining solid sample to have been nearly completely converted to Na_2CO_3. The reaction of sodium formate with NaOH in the presence of steam flow is shown in Figure 5.5b, and the similarities in trends and H_2 formation rate magnitudes between the steam and no steam flow cases demonstrated that steam does not significantly affect the sodium formate and NaOH reaction. Like the no steam flow case, conversions to H_2 and Na_2CO_3 were nearly 100%.

In comparing the formation of sodium formate in the intermediates, however, in general more sodium formate was found in the steam flow cases than the no steam flow cases. Sodium formate concentration at 473 K was nearly equivalent to the no steam flow case, and at 498 K it was about half of the value observed in the no steam flow case, 0.1 mol sodium formate/mol cellulose versus 0.2 mol sodium formate/mol cellulose. However, after 498 K, the concentrations of sodium formate found in the steam flow cases were much greater than the no steam flow cases. Sodium formate concentration in the steam flow cases peaked at 0.3 mol sodium formate/mol cellulose at 513 K, nearly 3 times larger than the value observed in the no steam flow case at that temperature. Unlike the no steam flow cases, detectable levels of sodium formate were observed throughout the studied temperature range in the steam flow cases.

Sodium Acetate

As in the sodium formate case, sodium acetate was thermally treated alone and no gaseous production was observed; however, the addition of NaOH at the stoichiometric ratio of

108

1:1, according to Reaction 5.4, was found to cause CH_4 formation, but not H_2 formation. In both the no steam flow and steam flow cases, up to 573 K, relatively little reaction occurred between the sodium acetate and NaOH, and any reaction that did occur was near the final 573 K temperature. The formation of CH_4 from the reaction was more significant, though, in the no steam flow case, with formation rates being about 50 times larger than those observed in the steam flow case. The decrease observed in sodium acetate concentration in the intermediates going from 548 K to 573 K in the no steam flow case could not be explained by the sodium acetate and NaOH reaction to for CH_4 alone, as little CH_4 was shown to form. Thus in the no steam flow case, sodium acetate is likely being consumed in other chemical reactions or degradations. TIC analyses in both the no steam flow and steam flow cases of the sodium acetate and NaOH reaction also confirmed that very little reaction according to Reaction 5.4 had occurred, as little carbonation was observed.

Sodium Glycolate

The results of the reaction of sodium glycolate and NaOH, both with and without steam flow, are also shown in Figure 5.5. Sodium glycolate was the dominant carboxylate product observed in the alkaline thermal treatment of cellulose. A similar result was also found by Krochta et al., who found in their study that in a 20 N solution of NaOH, conversion of cellulose to glycolate was by far the dominant pathway at reaction temperatures of 513 K and 533 K (Krochta et al. 1988). Unlike sodium formate or sodium acetate, no literature exists on the thermochemical reaction of sodium glycolate with NaOH. If all of the sodium glycolate were to be converted to H_2 and Na_2CO_3, similar to the alkaline thermal treatment of cellulose stoichiometry given by Reaction 5.1, 3 moles of NaOH would need to be reacted with every mole of sodium glycolate:

109

$$NaC_2H_3O_3 + 3NaOH = 3H_2 + 2Na_2CO_3; \qquad \Delta H^0 = -161 \text{ kJ/mol} \qquad \text{(Rxn. 5.5)}$$

Thus a 3:1 NaOH:Sodium glycolate mixture was studied in the same manner as the aforementioned sodium carboxylate salt reactions with NaOH for gas production.

Interestingly, both the no steam and steam flow sodium glycolate and NaOH reactions produced significant amounts of H_2 and CH_4. The initial formation rate trends for both gases were very similar in the no steam flow and steam flow cases, with H_2 initiating at 516 K and CH_4 at 534 K. However, from 561 K to 571 K, a large spike in both the H_2 and CH_4 formation rates was observed in the no steam flow cases, whereas in the steam flow cases the formation rates of both gases experienced slight increases. Finally at 573 K, the formation rates for both H_2 and CH_4 decreased in the no steam case, whereas they continued to increase in the steam flow case. Thus, although the maximum H_2 formation rate was about 2.5 times larger in the no steam flow case than the steam flow case, including the 20 min isothermal period at 573 K, nearly twice as much total H_2 was produced in the steam flow case, 1 mol H_2/mol sodium glycolate, compared to the no steam flow case, 0.6 mol H_2/mol sodium glycolate. Total CH_4 formation was 15 times lower in the steam flow case, 1.4×10^{-2} mol CH_4/mol sodium glycolate, than the no steam flow case, 0.2 mol CH_4/mol sodium glycolate.

In both the no steam flow and steam flow cases, the concentration of sodium glycolate in the intermediate products of the alkaline thermal treatment of cellulose reaction peaked just as gaseous products began to be observed from the sodium glycolate and NaOH reaction. Similar behavior was also observed for sodium formate and NaOH reaction with and without steam flow, and the sodium acetate and NaOH reaction without steam flow. This indicated that the decrease in concentration of the sodium carboxylate salts in the intermediates may be due to their

reactions with NaOH at higher temperatures to form the observed gaseous products. The peak concentration in the steam flow case of 1.3 mol sodium glycolate/mol cellulose at 523 K was similar in magnitude to the peak concentration of 1.2 mol sodium glycolate/mol cellulose in the no steam flow case at 513 K. However, after the peak concentration events for the no steam flow and steam flow cases, each case exhibited very different trends in sodium glycolate concentration at higher temperatures. In the no steam flow case, concentration of sodium glycolate in the solids declined such that by 548 K, sodium glycolate was no longer detected in the sample. In the steam flow case, however, sodium glycolate concentration decreased but was still present in the products up to 573 K, with about 1.1 mol sodium glycolate/mol cellulose remaining in the solid products at this temperature.

Other Sodium Carboxylate Salts

Aside from those sodium carboxylate species shown in Figure 5.5, the other observed sodium carboxylate species in the alkaline thermal treatment of cellulose were tested for gas product formation up to 573 K. Sodium succinate was unreactive with and without NaOH at these reaction conditions. Sodium propionate produced negligible amounts of CH_4 and C_2H_6 when reacted with NaOH. Sodium oxalate, however, did produce H_2, both in the absence and presence of steam flow. However, because little sodium oxalate was found qualitatively in either the no steam or steam flow experiments, it was only considered to be a minor contributor to H_2 formation in the alkaline thermal treatment of cellulose.

It should be noted here that because the technique for measuring the sodium carboxylate salt concentrations in the intermediates was not *in situ*, the concentrations of the sodium carboxylate salt species reported here for each temperature should not be taken as total formation values upon reaching each intermediate temperature. Decreasing trends in sodium carboxylate

salt formation with increasing temperature do not necessarily imply that less of the sodium carboxylate salts were being formed. It is also possible that the sodium carboxylate salts were still forming, but the lower observed final concentrations in the intermediates with increasing temperature were due to the improved kinetics of the sodium carboxylate salt reactions. Indeed, rough carbon balances were done for the alkaline thermal treatment of cellulose reactions conducted up to the intermediate temperatures, and although closures improved with increasing temperature, they were still incomplete by the 573 K case, indicating that the breakdown of cellulose into the sodium carboxylate salts was either incomplete or other types of products were also forming. Thus, the observed concentration trends of the intermediates in the solids should be considered in concert with the gaseous formation rate data as a function of temperature for both the sodium carboxylate salt reactions with NaOH as well as the cellulose reaction with NaOH in order to elucidate reaction pathways.

5.3.3 Role of Sodium Glycolate in the Alkaline Thermal Treatment of Cellulose

As shown in Figure 5.5, the maximum concentrations of sodium glycolate in the intermediate solids in both the no steam flow and steam flow cases were several times higher than those of sodium formate and sodium acetate. Based on this as well as the formation rates for H_2 and CH_4 for the sodium glycolate and NaOH reaction still exhibiting increasing trends at 573 K, the sodium glycolate and NaOH reaction was studied out to 773 K and compared with the alkaline thermal treatment of cellulose to 773 K to see if any correlations existed in high temperature gaseous formation rates. Similar to the previous experiments with cellulose, cellulose and NaOH were mixed at a stoichiometric 12:1 molar ratio and placed into the quartz tube reactor. After a 1 h drying phase at 373 K, steam flow ($P_{H2O} = 38.8$ kPa) carried by the N_2 carrier was introduced into the reactor, which was then heated at a rate of 2 K/min to 773 K.

Throughout this period, the gas product stream was sampled via Micro GC, and gas analysis was also done on the total gaseous product collected in the tedlar bag. The same reaction parameters and analysis method were employed for a 3:1 molar mixture of NaOH and sodium glycolate. Experiments were only conducted in the presence of steam flow because steam flow was found to be necessary in promoting H_2 formation in both reactions. The comparison of the cellulose and sodium glycolate systems as a function of temperature is shown in Figure 5.6 for H_2 formation rates (Fig. 5.6a) and CH_4 and C_2H_6 formation rates (Fig. 5.6b).

Hydrogen

First, examining H_2 formation rates as a function of temperature, three peaks of H_2 formation are observed in the cellulose system. The first two have already been described for the experiments up to 573 K. After the maximum H_2 formation rate in the second peak region of 0.12 mol H_2/mol cellulose-min was observed, the H_2 formation rate declined until 645 K, where it was 4.6×10^{-3} mol H_2/mol cellulose-min, a decrease of about 25 times. The H_2 formation rate then began to slowly increase and essentially reached a steady state rate of about 10^{-2} mol H_2/mol cellulose-min until the reactor reached 723 K. After this temperature the H_2 formation rate declined until the end of the experiment at 773 K. Conversion to H_2 according to Reaction 5.1 was approximately 50%.

For sodium glycolate, its reaction with NaOH produced two H_2 formation rate peak regions. These peak regions were found to have good correspondence to the second and third peak regions in the cellulose system in terms of temperature. In the first region for the sodium glycolate system, the peak H_2 formation rate was 7.8×10^{-2} mol H_2/mol sodium glycolate-min, and it occurred at 586 K. This formation rate value was about 1.5 times lower than that of the maximum H_2 formation rate in the second region for the cellulose case, and both maximum

formation rates occurred at roughly the same temperature in both systems. After 586 K, the H_2 formation rate in the sodium glycolate system decreased until 635 K, where it was over two orders of magnitude lower than the peak formation rate at 586 K. The H_2 formation rate then began to increase, reaching a steady state value between 669 K and 706 K of about 1.8×10^{-3} mol H_2/mol sodium glycolate-min, about 5 times lower than the molar flow rate of H_2 from the cellulose reaction in this temperature region. After 706 K, the H_2 formation rate began to decrease until H_2 was undetected beyond 715 K. Total conversion of sodium glycolate to H_2 according to Reaction 5.5 was about 57%.

Comparing the H_2 formation rate trends between the cellulose and sodium glycolate systems, both were very similar starting around the second peak of H_2 formation for the cellulose reaction at 580 K until the end of the experiment at 773 K. As the temperature increased, however, the difference between the molar flow rates of H_2 per mole of cellulose and glycolate increased. This may indicate that sodium glycolate may be a more important source of H_2 in the secondary peak region for cellulose and more minor in the tertiary peak region.

Hydrocarbons

The comparison between the cellulose and sodium glycolate reactions also showed similarities in trends for both CH_4 and C_2H_6. The CH_4 formation rate for the cellulose case increased up to 666 K, reaching 3.2×10^{-2} mol CH_4/mol cellulose-min, after which the rate declined until the end of the experiment at 773 K. The total amount of CH_4 produced was 0.8 mol CH_4/mol cellulose, which accounted for 12% of the amount of the total gaseous product. For the sodium glycolate and NaOH reaction, two peak formation rate events were observed, a minor one at 595 K of 1.6×10^{-3} mol CH_4/mol sodium glycolate-min and a larger one at 678 K of 1.5×10^{-2} mol CH_4/mol sodium glycolate-min. After the peak at 678 K, the formation rate declined,

reaching a steady state value from 723 K – 773 K of approximately 3.6×10^{-4} mol CH_4/mol sodium glycolate-min. From about 580 K to 700 K, the CH_4 formation rate per mole of sodium glycolate followed a similar increasing trend to that of CH_4 from the cellulose system, consistently being about 2 – 3 times higher for the cellulose system than sodium glycolate system on a per mole of reactant basis. A similar magnitude difference was observed for cellulose and sodium glycolate with regard to H_2 formation rates between 580 K and 625 K. Both the CH_4 formation rates for the cellulose case and the sodium glycolate case peaked at similar temperatures, 666 K and 678 K, respectively. The concentration of CH_4 in the final gaseous product for the sodium glycolate reaction with NaOH was around 19%, similar to the 12% value found for the alkaline thermal treatment of cellulose.

For C_2H_6, the similarities in magnitude of the molar formation rates between cellulose and sodium glycolate were never as close as they were with H_2 or CH_4, being roughly 8 times higher per mole of cellulose than per mole of sodium glycolate. Both, however, did experience peak C_2H_6 formation rates at roughly 700 K, and the shapes of the overall formation rate trends as a function of temperature were similar in both cases. The concentration of C_2H_6 in the total gaseous product collected was about double for the cellulose case compared to the sodium glycolate case, 0.3% and 0.15%, respectively.

Sodium Carbonate

Finally, conversions to Na_2CO_3 were compared in both the alkaline thermal treatment of cellulose and the sodium glycolate and NaOH reactions up to 773 K. Conversion to Na_2CO_3 was about 93% in the sodium glycolate and NaOH reaction. Comparing IC analyses between the products made from the sodium glycolate and NaOH reaction at 573 K versus 773 K, residual sodium glycolate, as well as the formation of significant sodium acetate and Na_2CO_3 was

observed in the 573 K case, whereas in the 773 K case, only Na_2CO_3 was observed. This indicated that gaseous formation from the sodium glycolate and NaOH reaction also was concomitant with Na_2CO_3 formation, as hypothesized in the carboxylate intermediate pathway, and in particular, the CH_4 observed at higher temperatures may be coming from the reaction of sodium acetate and NaOH, given by Reaction 5.4. On the other hand, although the IC analysis of the final reaction products of the alkaline thermal treatment of cellulose reaction up to 773 K showed only Na_2CO_3 in the solids, TIC analysis showed approximately 50% conversion to Na_2CO_3. Thus carbon had ended up in products other than sodium carboxylate salts or Na_2CO_3, and further study is required to identify those products.

5.3.4 H_2 versus Na_2CO_3 Formation Behavior as a Function of Temperature

In the proposed sodium carboxylate pathways for H_2 formation as well as in the overall alkaline thermal treatment reaction given by Reaction 5.1, the carbon is ultimately directed into its lowest energy state, Na_2CO_3. Thus to gain further insight into the reaction pathways of the alkaline thermal treatment of cellulose, conversions to H_2 and Na_2CO_3 are compared as a function of temperature for the no steam flow and steam flow cases, and this comparison is shown in 5.7. First examining the no steam flow cases, at 473 K, Na_2CO_3 conversion was higher than H_2 conversion, 2.3% versus 0.7%. The low, but non-zero carbonation values obtained at lower reaction temperatures are believed to be due to CO_2 absorption from room air and not from a reaction in the alkaline thermal treatment system. As the temperature was increased beyond 498 K in the no steam flow cases, the difference between H_2 and Na_2CO_3 conversion decreased such that between 523 K and 548 K, Na_2CO_3 conversion surpassed H_2 conversion. At 548 K, H_2 conversion was about 25%, whereas Na_2CO_3 conversion was about 29%. Interestingly, the difference between Na_2CO_3 and H_2 conversion continued to increase up to 573 K, where H_2

conversion was 29% and Na_2CO_3 conversion was 38%, making the carbonation extent about 1.3 times higher than the measured H_2 conversion. From a previous study of the alkaline thermal treatment of cellulose, H_2 and Na_2CO_3 conversions were also compared for a sample heated to 573 K at a rate of 2 K/min, but then held isothermally at 573 K until the online H_2 concentration in the product gas stream fell below the GC's 0.1% detection limit. In this case, H_2 conversion did not significantly increase from the 29% value obtained in the 573 K immediate case. However, Na_2CO_3 conversion increased significantly, reaching 53%, an increase of about 1.4 times.

The steam flow cases, on the other hand, exhibited some different behaviors in conversions of H_2 and Na_2CO_3 as a function of temperature. Similar to the no steam flow cases, at lower temperatures up to 523 K, H_2 conversion was higher than Na_2CO_3 conversion; however the difference between the two conversions was larger than in the no steam cases. At 513 K, H_2 conversion was about 4.6 times larger than Na_2CO_3 conversion, compared to 2.5 times for the 513 K no steam flow case. At 523 K, H_2 conversion was about 3.3 times higher than Na_2CO_3 conversion, compared to 1.5 times for the 523 K no steam flow case. Increasing the temperature to 548 K, H_2 conversion was found to be higher by about 1.4 times, unlike the no steam case where carbonation was greater. At 573 K in the steam flow case, both Na_2CO_3 and H_2 conversion had similar values, with an H_2 conversion of 31% and an Na_2CO_3 conversion of 33%. Finally, comparing H_2 and Na_2CO_3 conversions for the 573 K isothermal case, both values increased from the 573 K intermediates case, but maintained similar values to each other, with an H_2 conversion of 47% and an Na_2CO_3 conversion of 52%.

A few insights can be made from the comparison between H_2 and Na_2CO_3 conversions. First, the similarity in H_2 and Na_2CO_3 conversions for the higher temperature steam flow cases

support the overall stoichiometry proposed in Reaction 5.1 for the alkaline thermal treatment of cellulose. At these same temperature conditions without steam flow, it was observed that the Na_2CO_3 conversion was significantly higher than the H_2 conversion. This showed that in the absence of steam flow, significant carbonation that does not relate to H_2 formation as given by the stoichiometry of Reaction 5.1 was taking place. Further study is needed to understand the H_2 and Na_2CO_3 conversion discrepancy in the no steam flow case.

A second insight that arises from both sets of data, but more so from the steam flow cases, is that the molar ratio of H_2 formation:Na_2CO_3 formation does not always adhere to the 2:1 stoichiometry proposed in Reaction 5.1. If the reaction proceeded according to Reaction 5.1 throughout the experiment, then trends for both H_2 and Na_2CO_3 conversions as a function of temperature should quantitatively match. However, in both the no steam flow and steam flow cases, at temperatures below 523 K H_2 conversion is greater than Na_2CO_3 conversion. That carbonation becomes nearly equivalent with H_2 conversion by 573 K in the steam flow case indicates that at these higher temperatures, H_2 formation is associated with proportionally greater Na_2CO_3 formation. These observations support the hypothesis of the alkaline thermal treatment reaction proceeding through a sodium carboxylate intermediate pathway, where the H_2 formation observed at lower temperatures corresponds to the alkaline thermal breakdown of cellulose into the sodium carboxylate salts, which at higher temperature can then react further with NaOH to produce more H_2 and Na_2CO_3.

5.4 Conclusions

Reaction pathways have been investigated for the alkaline thermal treatment reaction for cellulose. The sodium carboxylate salts hypothesized to be formed during the alkaline thermal treatment of cellulose reaction were identified and their concentrations were quantified at various

reaction temperatures. It was found that the concentration of sodium carboxylate salts in the solids changed as a function of reaction temperature, with concentrations typically decreasing with increasing temperature. On the other hand, the concentration of Na_2CO_3 in the solids was found to increase with increasing temperature, indicating that the decrease in the intermediate species may be due to sodium carboxylate salt reactions with NaOH posited in this study that lead predominantly to the formation of H_2 and Na_2CO_3. The reactions of sodium formate, sodium oxalate, and sodium glycolate with NaOH were all found to produce H_2, and the reactions of sodium acetate and sodium glycolate with NaOH were found to produce CH_4. In particular, sodium glycolate was found to be an abundant intermediate formed in the alkaline thermal treatment of cellulose and one whose gaseous formation rate trends at higher temperatures for H_2 and CH_4 matched well with those of the cellulose system. Steam flow was found to have a profound impact on the alkaline thermal treatment reaction for cellulose in terms of the gas products formed, the concentration of sodium carboxylate salt intermediates found as a function of temperature, and the reactions of the sodium carboxylate salts with NaOH.
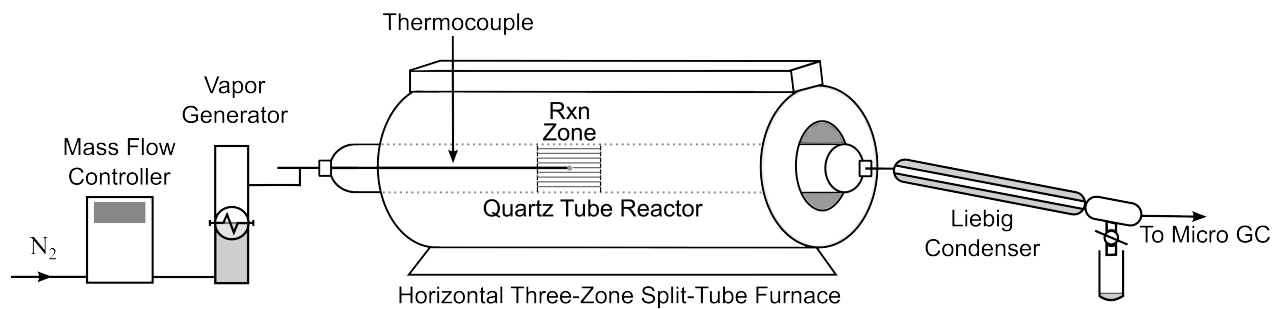
Figure 5.1 Experimental setup used in the studies of the alkaline thermal treatment of cellulose and the intermediate reactions.
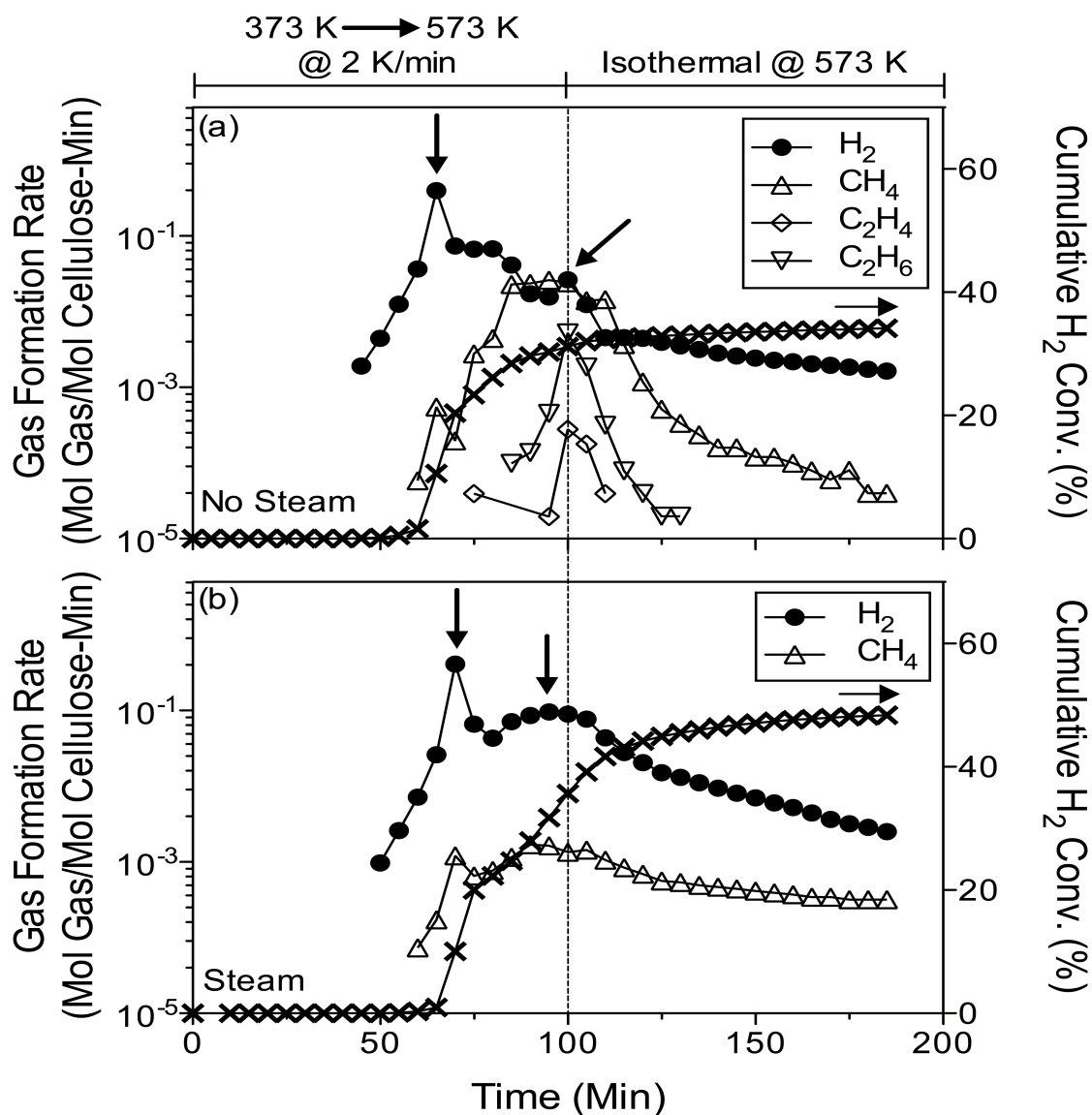
Figure 5.2 Comparison of online formation rate data from the alkaline thermal treatment of cellulose in a) the no steam flow and in the b) the steam flow cases (P_{H2O} = 38.8 kPa). In both experiments, a stoichiometric (12:1) NaOH:Cellulose molar ratio was used. Reactor temperature programming: reactants dried for 1 h at 373 K, 373 K → 573 K at 2 K/min and held isothermally at 573 K until [H_2] fell below GC's H_2 detection limit of 0.1%. Arrows associated with the H_2 formation rate curve denote apex of different peak H_2 formation rate events.
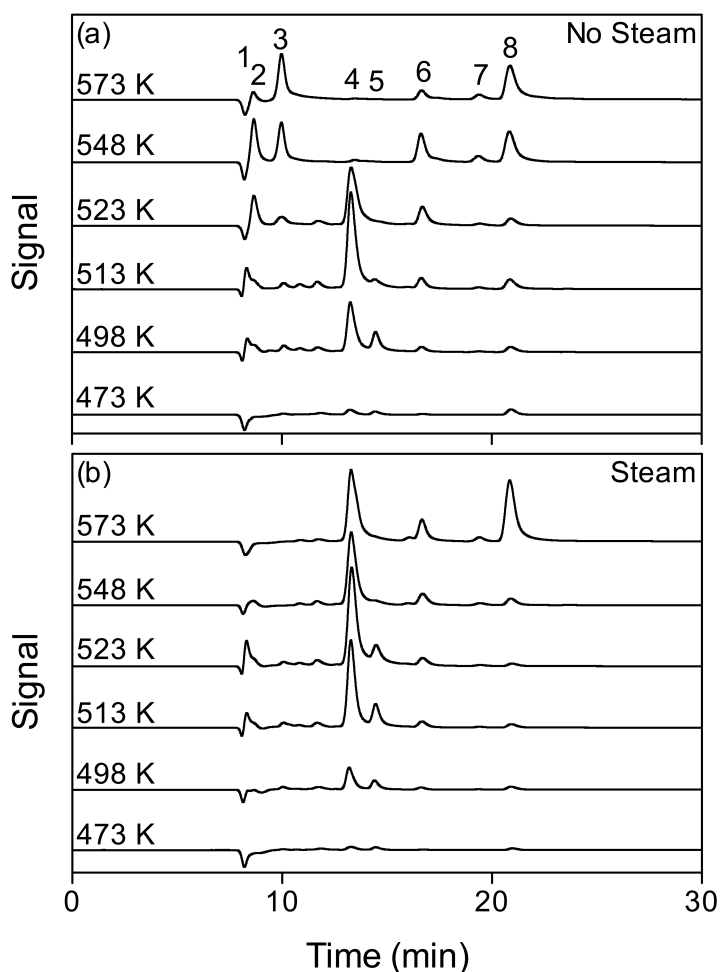
Figure 5.3 Ion chromatography (IC) analyses of the alkaline thermal treatment of cellulose system reacted to different temperatures for both a) the no steam flow and b) the steam flow cases (P_{H2O} = 38.8 kPa). A stoichiometric 12:1 molar mixture of NaOH:Cellulose was used in all experiments. The mixture was dried for 1 h at 373 K, and then heated to the experimental temperature at a rate of 2 K/min. Upon reaching the intermediate temperature, the reactor was immediately quenched. The solids were removed for IC analysis, which were prepared for each sample by dissolving 40 mg in 15 ml of DI water and passing this solution through a 0.45 μm filter. The anion peaks observed in order of retention time were: (1) Oxalate, (2) Unknown, (3) Unknown, (4) Glycolate, (5) Formate, (6) Acetate, (7) Propionate, (8) Carbonate.
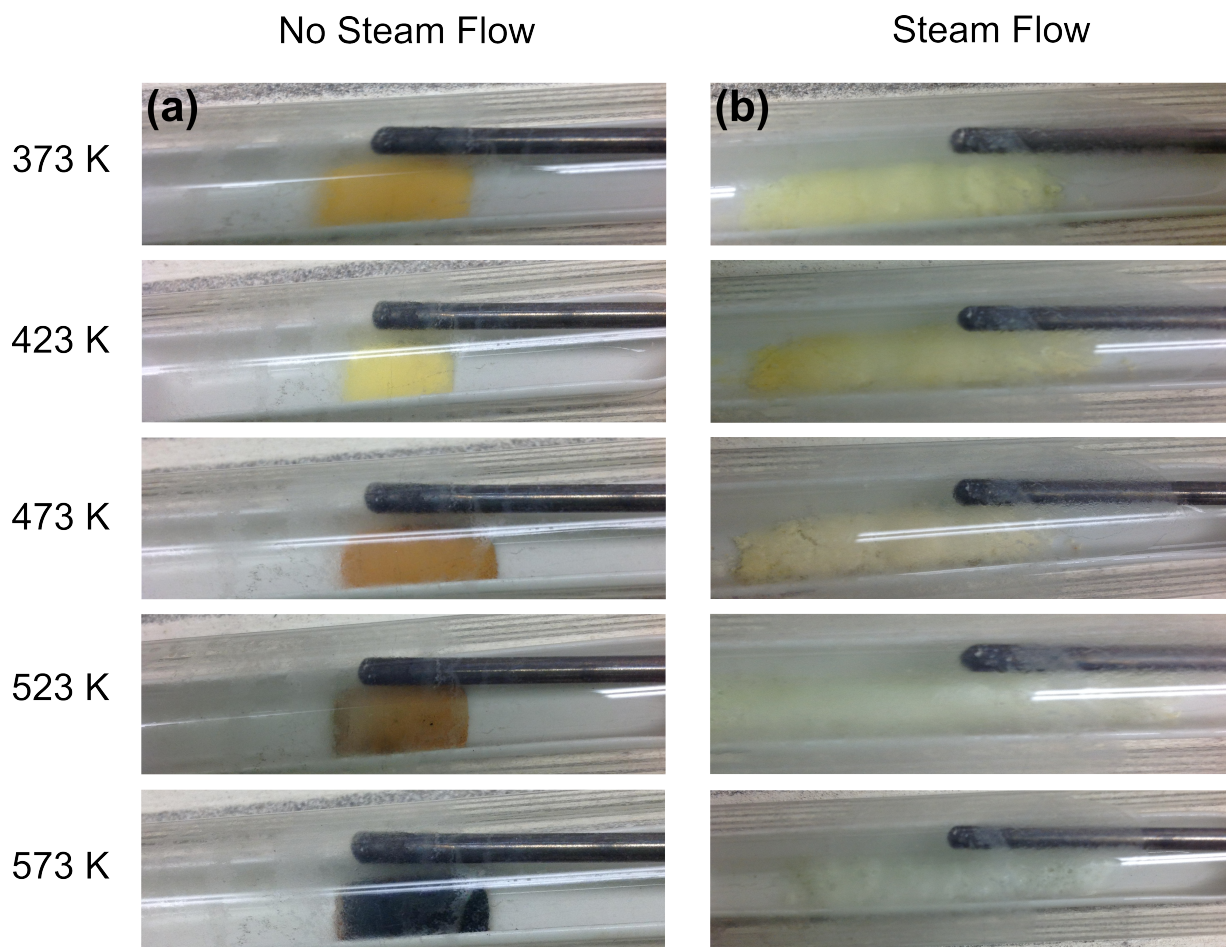
Figure 5.4 Qualitative evolution of the solid products of the alkaline thermal treatment of cellulose as a function of reactor temperature, both in a) the absence and b) the presence of steam flow (P_{H2O} = 38.8 kPa).
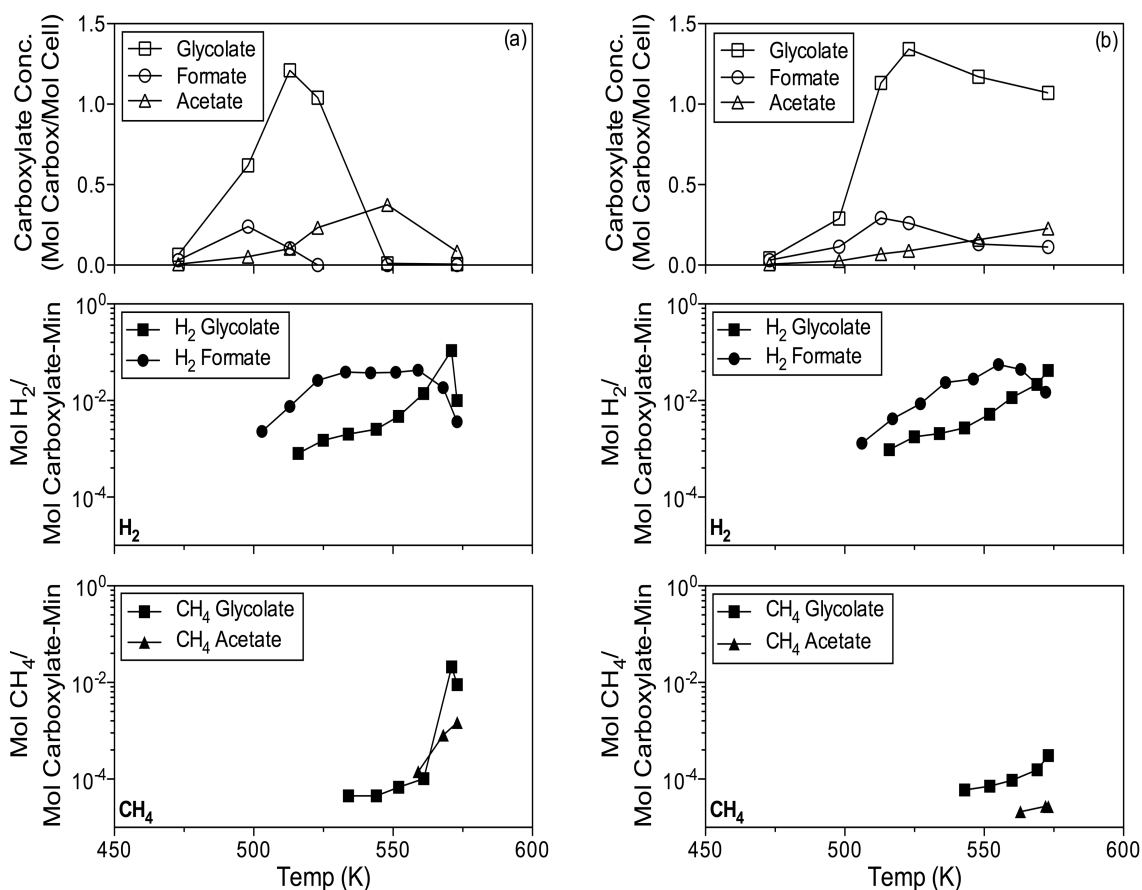
Figure 5.5 Comparison of the sodium formate, sodium acetate, and sodium glycolate concentrations in the solid products from the alkaline thermal treatment of cellulose reaction at different intermediate temperatures with the online H_2 and CH_4 gaseous formation rates from the reactions of sodium formate, sodium acetate, and sodium glycolate with NaOH, done in a) the absence of steam flow and b) the presence of steam flow ($P_{H2O} = 38.8$ kPa). Reactor temperature programming for the sodium carboxylate salt reactions with NaOH: reactants dried for 1 h at 373 K, 373 K $\rightarrow$ 573 K at 2 K/min. Stoichiometric mixtures of reactants were used in all of the sodium carboxylate salt reactions with NaOH.

124
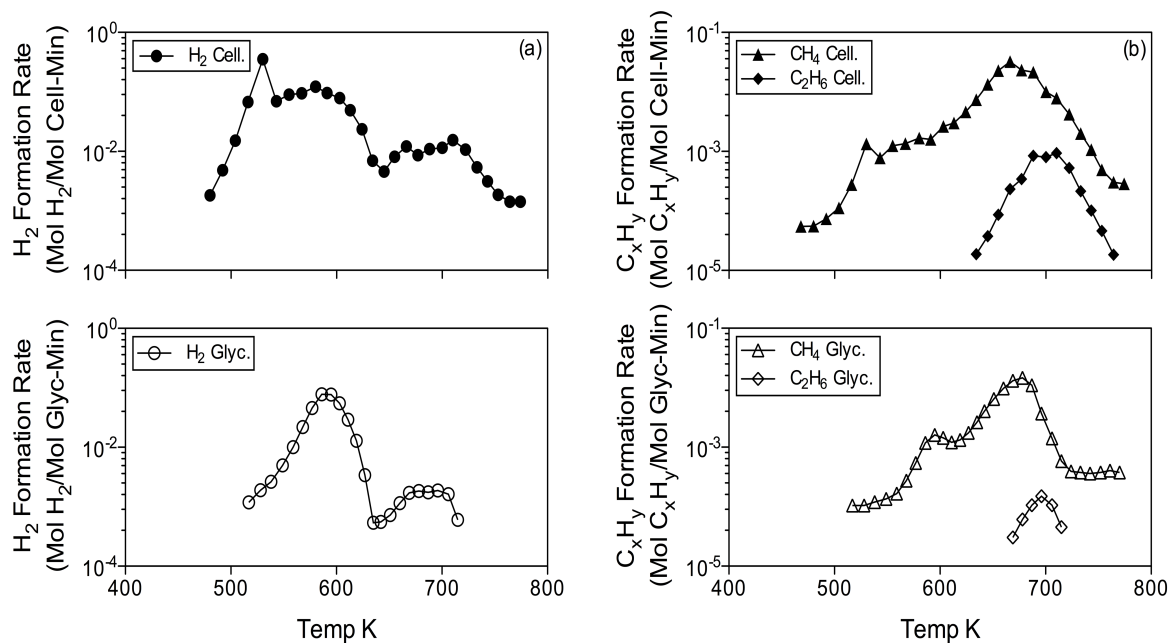
Figure 5.6 Comparison of the alkaline thermal treatment of cellulose with the reaction of sodium glycolate and NaOH for a) H_2 formation and b) CH_4 and C_2H_6 formation, up to 773 K under 38.8 kPa steam flow. Stoichiometric ratios of NaOH:Cellulose and NaOH:Sodium glycolate were used in both experiments. Reactor temperature programming: reactants dried for 1 h at 373 K, 373 K $\rightarrow$ 773 K at 2 K/min, with sampling done online throughout via Micro GC.
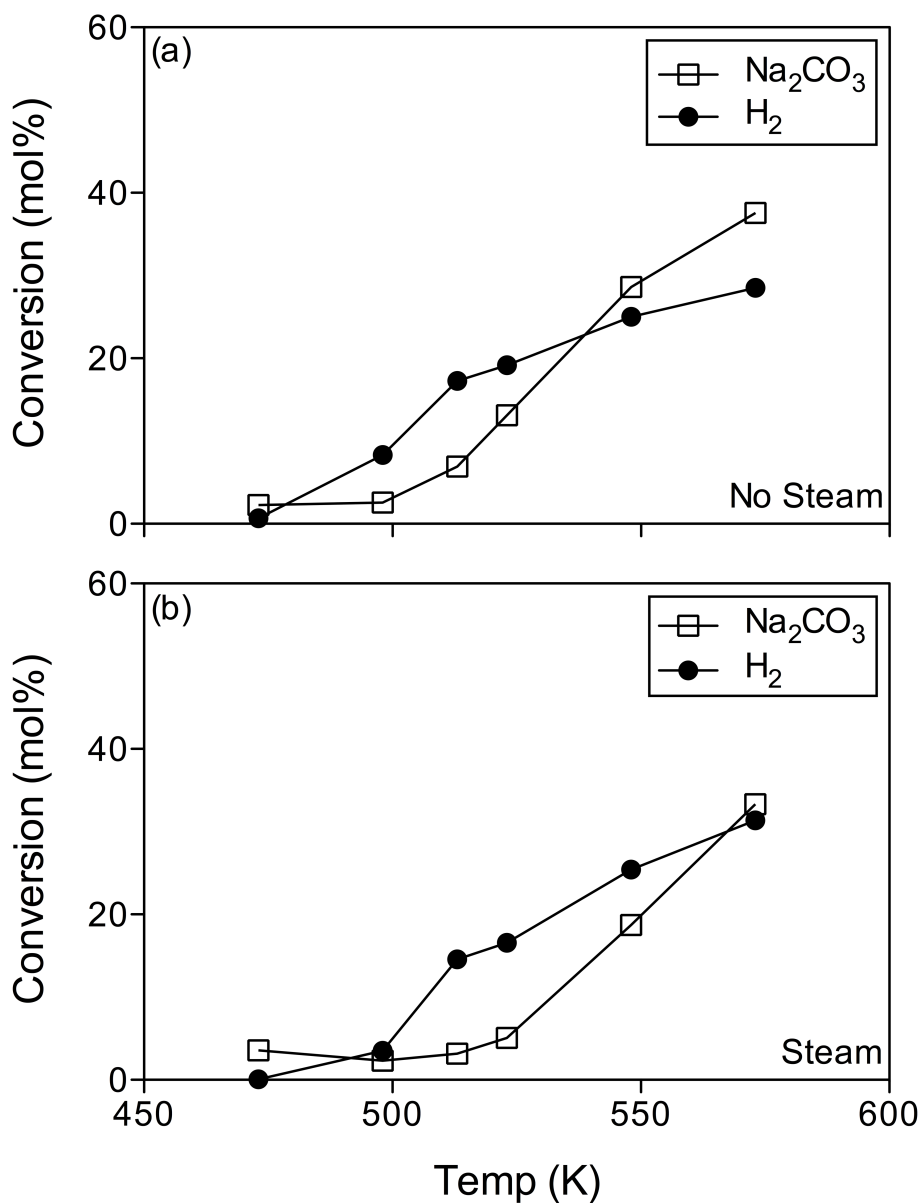
Figure 5.7 Comparison of conversions between H_2 and Na_2CO_3, based on the stoichiometry given by Reaction 5.1, for a) the no steam flow cases and b) the steam flow cases (P_{H2O} = 38.8 kPa). H_2 conversions were calculated based on total product gas collected in a tedlar bag for each intermediate temperature experiment. Na_2CO_3 conversions were calculated based on Total Inorganic Carbon (TIC) analysis of the solids formed from each intermediate temperature experiment.

CHAPTER 6

KINETIC STUDY OF ATT OF CELLULOSE AND ITS INTERMEDIATES FOR HYDROGEN PRODUCTION

The contents of this chapter are to be submitted to Industrial & Engineering Chemistry Research as an Article entitled "Kinetics of hydrogen formation from cellulose and reactive intermediates in the alkaline thermal treatment reaction" (Ferguson and Park 2014).

6.1   Introduction

Thermochemical conversion of biomass into energy and fuels has received wide attention as a means for mitigating societal dependence on fossil fuel resources and for improving the overall sustainability of the global energy economy. Through thermochemical conversion technologies such as gasification, pyrolysis, hydrothermal conversion and aqueous phase processing, biomass can be converted into a wide range of chemicals and fuels fungible with those derived from fossil fuels (Brown 2011, Huber et al. 2005, Huber et al. 2006, Alonso et al. 2012, Ni et al. 2006, Navarro et al. 2007, Bridgwater 2012, McKendry 2002b). A relatively new thermochemical biomass conversion technology, alkaline thermal treatment, has begun to be more thoroughly investigated due to unique benefits it confers. Alkaline thermal treatment is a method to produce high-purity H_2 from biomass at relatively low temperature, around 573 K, and atmospheric pressure. These relatively mild reaction conditions allow for the design of scalable reactors that can be used by unskilled operators. This is in contrast to the other thermochemical process, which due to the temperatures and/or pressure involved, are generally best run by skilled operators at larger scales.

The alkaline thermal treatment of biomass has mainly been studied on model compounds, such as glucose and cellulose, and their reactions are given below:

$$C_6H_{12}O_6 + 12NaOH = 6Na_2CO_3 + 12H_2; \qquad \Delta H^0 = \text{-404 kJ/mol} \qquad \text{(Rxn. 6.1)}$$

$$C_6H_{10}O_5 + 12NaOH + H_2O = 6Na_2CO_3 + 12H_2 \qquad \text{(Rxn. 6.2)}$$
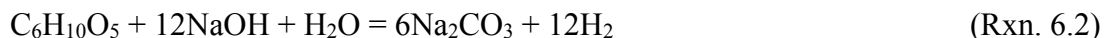
From the above reactions, it can be seen that the concept of the alkaline thermal treatment reaction is react the biomass with an alkali metal hydroxide, which acts to direct all of carbon and oxygen embodied in the reactants to Na_2CO_3, while releasing all of the hydrogen embodied in the reactants as H_2 gas. Because theoretically there is no associated CO_x emission from the alkaline thermal treatment reaction, the H_2 produced can be directly fed into a PEM fuel cell to produce electricity, without the need for CO cleanup in the product gas stream.

Previous study on alkaline thermal treatment by other groups focused on the effects of metal hydroxide type and, particularly, catalysis on the H_2 yield (Hsu and Hixson 1981, Ishida et al. 2005, Hansen et al. 2011, Tongamp et al. 2010, Zhang et al. 2009, Su et al. 2008, Su et al. 2010a, Su et al. 2010b). Less study has focused on the effects of the non-catalytic parameters of the alkaline thermal treatment reaction, such as NaOH:Biomass ratio, reaction temperature, and presence and concentration of steam flow. The effects of these variables on the alkaline thermal treatment reactions for both glucose and cellulose have been reported in previous studies by this group (Ferguson 2012). Briefly, NaOH was found to alter the usual pyrolysis pathways exhibited by glucose and cellulose subjugated to thermal treatment, suppressing CO_x formation while causing H_2 formation and enhancing hydrocarbon formation, particularly CH_4. The addition of steam flow enhanced H_2 formation in both feedstocks, but had a much greater impact on cellulose than it did on glucose. In contrast, steam flow acted to suppress the formation of hydrocarbons in both feedstocks.

Reaction pathways also began to be explored that could explain the observed gaseous products from alkaline thermal treatment. Based on the literature for the alkaline degradation of biomass (Othmer et al. 1942, Richards and Sephton 1957, Whistler and BeMiller 1958, Niemela and Sjostrom 1986, Krochta et al. 1987, Ponder and Richards 1993, Van Loon and Glaus 1997, Machell and Richards 1960, Mahood and Cable 1919, Philpot 1971), it was hypothesized that the H_2 released at lower temperatures was a result of the breakdown of cellulose into predominantly sodium carboxylate salts. H_2 produced after this breakdown at higher temperatures was then believed to be largely due to the reaction of these sodium carboxylate salts with additional NaOH, which would also produce Na_2CO_3 as a final product. The comparison of H_2 conversion versus Na_2CO_3 conversion, with calculations based on the stoichiometry of Reaction 6.2, supported this hypothesis, with conversion according to H_2 being higher at lower temperature than Na_2CO_3 conversion, while at higher temperatures H_2 and Na_2CO_3 conversions were quite similar. A similar H_2 formation pathway was proposed and confirmed for the alkaline hydrothermal gasification of biomass, which was conducted in an aqueous alkaline solution at high pressure (Onwudili et al. 2009, Onwudili et al. 2010).

Based on the formation of sodium carboxylate salts at intermediate temperatures from the alkaline thermal treatment of cellulose, the following H_2-producing reactions were proposed and explored:

$$NaCOOH + NaOH = Na_2CO_3 + H_2; \qquad \Delta H^0 = -39 \text{ kJ/mol} \qquad \text{(Rxn. 6.3)}$$

$$Na_2C_2O_4 + 2NaOH = 2Na_2CO_3 + H_2; \qquad \Delta H^0 = -95 \text{ kJ/mol} \qquad \text{(Rxn. 6.4)}$$

$$NaC_2H_3O_3 + 3NaOH = 2Na_2CO_3 + 3H_2; \qquad \Delta H^0 = -161 \text{ kJ/mol} \qquad \text{(Rxn. 6.5)}$$

Sodium glycolate was identified at the highest concentrations in the intermediate solid products, and its reaction with NaOH produced both H_2 and CH_4. The H_2 and CH_4 formation rate curves for the sodium glycolate system as a function of temperature above 573 K also exhibited similar trends to those generated in the alkaline thermal treatment of cellulose.

With potential reaction pathways identified, this study explores the kinetics of these sodium carboxylate salt reactions with NaOH and compares them to the kinetics of alkaline thermal treatment of cellulose reaction. For the kinetics of the sodium carboxylate salt reactions, those salts that were reactive to form H_2 were tested: sodium formate, sodium oxalate, and sodium glycolate. Each compound was tested isothermally at a series of temperatures to study the effect of temperature on H_2 formation rates and conversion, and to estimate activation energies. An understanding of the kinetics of H_2 formation in the alkaline thermal treatment reaction will inform engineering design as well as suggest directions for improvement of the technology.

6.2   Materials and Methods

6.2.1   Heating Rate Studies

The studies of the alkaline thermal treatment of cellulose and of the sodium carboxylate salt reactions with NaOH were conducted in a semi-batch reactor, shown in Figure 6.1. Cellulose (Acros), sodium formate (Sigma Aldrich), sodium acetate (Fisher Scientific), sodium oxalate (Fisher Scientific), and sodium glycolate (Acros) were used as feedstocks and mixed with a 50 wt% NaOH solution (Acros) to produce stoichiometric mixtures of the reactants: 12:1 NaOH:Cellulose, 1:1 NaOH:Sodium formate, 1:1 NaOH:Sodium acetate, 2:1 NaOH:Sodium oxalate, 3:1 NaOH:Sodium glycolate. The stoichiometric mixtures were loaded into a ceramic boat and centered in a quartz tube reactor, and this assembly was placed in a three-zone

horizontal furnace (Mellen Co.) The reactor was purged of air with N_2 at a flow rate of 50 ml/min (STP) prior to the experiment. After purging the reactor of air, it was raised to a temperature of 373 K, and the reactants were dried for 1 h. The experimental phase was then initiated, with the reactor being heated to 573 K at a rate of 2 K/min, and upon reaching this temperature, it was held isothermally for 20 min. Temperature was monitored inside the reactor using a thermocouple. Online gas sampling was accomplished throughout the experimental phase via Micro GC, with a sampling frequency of one sample taken every 5 min. For experiments involving steam flow, it was introduced after the reactant drying period at 373 K, and carried by the N_2 flow at a $P_{H2O} = 38.8$ kPa.

6.2.2 Isothermal Kinetic Studies

To perform the isothermal kinetic studies, the semi-batch reactor setup was modified. A manipulator rod with a hook on the end was inserted into a hole drilled through the lip on the end of the ceramic boat. This allowed for the ceramic boat to be slid into and out of the center zone of the three-zone horizontal furnace. Experimental samples were prepared in the same manner as previously described and loaded into the horizontal quartz tube reactor, which was placed in the three-zone furnace. As before, the reactor was purged of air under constant N_2 flow of 50 ml/min (STP) and the reactants dried at 373 K for 1 hr. Subsequently, the ceramic boat was pulled back from the center zone to an outer zone. For experiments involving steam flow, the flow ($P_{H2O} = 38.8$ kPa) was initiated at this point. The center zone was then brought to the desired temperature for the isothermal study, and the outer zones were brought to as high a temperature as possible to minimize the thermal gradient in the center zone without having any reaction occur in the ceramic boat. Temperature in the center zone was measured via a thermocouple, and once the temperature was shown to have equilibrated to the desired temperature, the ceramic boat was

pushed into the center zone and the Micro GC immediately started sampling the online gaseous product stream. The analytical method of the Micro GC was modified to only detect H_2 and the reference gas, N_2, which improved the sampling frequency from one sample taken every 5 min to one sample taken every 2 min. The experiments were terminated once the online H_2 concentration as measured by the Micro GC fell below the detection limit of 0.1%. The total gaseous product was also collected in a tedlar bag, which was sampled by the Micro GC to obtain total conversion data. In obtaining total gaseous conversion data, the previous 5 min full GC analytical method was used.

Those sodium carboxylate salts that reacted with NaOH to produce H_2, sodium formate, sodium oxalate, and sodium glycolate, were examined in this kinetic study. For each sodium carboxylate salt reaction with NaOH, a molar concentration of NaOH 5 times in excess of that required by the stoichiometry for each reaction was used: 5:1 NaOH:Sodium formate, 10:1 NaOH:Sodium oxalate, 15:1 NaOH:Sodium glycolate. Potential mass transfer issues were avoided in doing so. For the cellulose system, however, the stoichiometric ratio of NaOH:Cellulose of 12:1 was used. This was because experiments conducted in 5 times excess NaOH with cellulose were found to have different H_2 profiles than the stoichiometric reaction, whereas the H_2 production profiles for the sodium carboxylate salt reactions between the stoichiometric and excess NaOH mixtures were similar.

6.2.3 Ion Chromatography Analysis

A Metrohm 861 Advanced Compact IC equipped with a Metrosep Organic Acids 250/7.8 column for component separation was utilized for identifying carboxylates remaining in the solid products resulting from the alkaline thermal treatment reactions. The eluent used was 0.5 mM H_2SO_4, while the suppressor was 20 mM LiCl.

The samples were prepared for ion chromatography (IC) analysis using the following procedure. First, the solid products from the reaction were ground with a mortar and pestle to a fine powder. Next, 15 ml of deionized water was added to 40 mg of the powder, and this solution was well mixed. The solution was then passed through a 0.45 μm filter before being introduced to the ion chromatograph.

6.2.4 Total Inorganic Carbon Analysis

Total inorganic carbon (TIC) (UIC Inc. CM5130 Acidification Module) was quantified by acidifying the solid product formed from the reactions to evolve the inorganic carbon present, which for the alkaline thermal treatment reaction would be in the form of Na_2CO_3, as carbon dioxide. The carbon dioxide was then passed into a CO_2 coulometer for quantification.

6.3 Results and Discussion

6.3.1 Non-Isothermal Kinetics of the Alkaline Thermal Treatment of Cellulose and Reaction Intermediates

Previous study showed that the alkaline thermal treatment of cellulose does produce sodium carboxylate salt intermediates, and the reactions of some of these intermediates with NaOH produced H_2 (i.e. sodium formate, sodium oxalate, sodium glycolate) and CH_4 (i.e. sodium acetate, sodium glycolate), pointing to potential reaction pathways in the alkaline thermal treatment of cellulose reaction. In order to see if the sodium carboxylate salt reactions that have been studied are connected to the alkaline thermal treatment of cellulose reaction, gaseous trends from the cellulose reaction must be compared to those from the aforementioned reactions of the sodium carboxylate salt intermediates. These trends are compared in Figure 6.2, with the top plots depicting the online H_2 formation rates from the alkaline thermal treatment of cellulose and the bottom plots depicting the online H_2 formation rates from the reactions of the intermediate

species sodium formate, sodium acetate, sodium oxalate, and sodium glycolate with NaOH. The reactions were studied in the absence of steam flow (Fig. 6.2a) as well as in its presence (Fig. 6.2b). Stoichiometric ratios of reactants were used in all cases. The dashed lines in the figure represent the detection limit of the Micro GC for H_2. The solid black line gives the thermal profile used in the reactions, which was heating from 373 K to 573 K at 2 K/min and holding at 573 K isothermally for 20 min. The results for CH_4 are given in the Supporting Information.

First looking at the no steam flow cases in Fig. 6.2a, it was observed in the cellulose system that the maximum H_2 formation rate, which occurred at 511 K, occurred just as H_2 was being formed from the sodium formate reaction and before any H_2 was observed from the sodium glycolate or sodium oxalate reactions. The percentage of the total H_2 produced from the alkaline thermal treatment of cellulose in this first H_2 formation region to 511 K, where the H_2 formation rate from cellulose was at least an order of magnitude greater than H_2 formation rate from sodium formate, was approximately 31%. Thus it can be concluded that significant H_2 formation must be attributed to reactions other than those of the sodium carboxylate salts with NaOH. Perhaps the H_2 formed in this lower temperature region can be attributed to gaseous release from the thermal decomposition of cellulose into the observed sodium carboxylate salt products, similar to the scheme proposed by Onwudili for alkaline hydrothermal gasification of biomass (Onwudili and Williams 2009).

Beyond 511 K, attempting to quantitatively correlate the H_2 formation rates between the alkaline thermal treatment of cellulose and the sodium carboxylate salt reactions with NaOH is not valid because the *in situ* formation and consumption behavior of species in the alkaline thermal treatment system is not known. However, the correlation in the spike in H_2 formation rate seen in both the cellulose reaction and the sodium glycolate reaction around 573 K, which

was observed in repeated trials of both systems, may indicate that sodium glycolate does play a role in the production of H_2 in the alkaline thermal treatment of cellulose in the absence of steam flow.

Shown in Figure 6.2b are the analogous H_2 formation rate curves for the alkaline thermal treatment of cellulose case and the sodium carboxylate salt reactions with NaOH under steam flow. Up to the peak H_2 formation rate observed at 518 K, before the formation rate of H_2 from sodium formate became more significant, about 20% of the total H_2 from the cellulose system had been produced. This percentage was smaller than in the no steam flow case because relatively more H_2 is produced at higher temperature in the steam flow case than the no steam flow case.

After this peak at 518 K in the cellulose reaction, the broad secondary peak of H_2 formation correlated well with the three overlapping H_2 formation rate trends from the sodium formate reaction, the sodium oxalate reaction, and the sodium glycolate reaction. The closer match in trend between the cellulose case and the sodium formate case from roughly 538 K to 565 K could be explained by the fact that more sodium formate was likely formed in the steam flow cases than the no steam flow cases, as shown in the previous study. Although H_2 formation from sodium oxalate initiated at the highest temperature of the three sodium carboxylate salts, 524 K, it peaked at 563 K at 7.2×10^{-2} mol H_2/mol sodium oxalate-min, which was shortly after the peak H_2 formation rate observed for the sodium formate case and before the peak H_2 formation rate observed for the sodium glycolate case. The sodium glycolate H_2 formation rate trend began to correspond more closely to the H_2 formation rate trend from cellulose after 565 K, particularly in the isothermal period at 573 K. In the last 15 min of the measured period both H_2 formation rates for the cellulose case and the sodium glycolate case began to fall off similarly,

with the decrease in formation rate from the beginning to the end of the isothermal period being about 2.1 times for the cellulose case and 1.7 times for the sodium glycolate case. Both the cellulose and sodium glycolate reactions also had similar magnitudes of H_2 formation rates per mole of reactant in the isothermal region. These observations may point to the rate of H_2 formation in the 573 K isothermal region being limited by the kinetics of sodium glycolate conversion to H_2, and this will be explored subsequently in the isothermal kinetic studies.

6.3.2 Isothermal Kinetics of the Alkaline Thermal Treatment of Cellulose

Figure 6.3 shows the online H_2 formation rates for the alkaline thermal treatment of cellulose conducted at several isothermal temperature conditions. In Figure 6.3a, H_2 formation kinetics are compared between the no steam flow and steam flow cases at 573 K. In both cases, H_2 began to be observed by the second GC measurement at 2 min, and the formation rate then increased rapidly and peaked at 6 min in the no steam flow case and 8 min in the steam flow case. Both peak formation rates were quite similar, around 1.3 mol H_2/mol cellulose-min, and both cases produced similar amounts of H_2 in this initial period. This was consistent with the observation in previous studies that steam flow had a greater impact in secondary H_2 generation, and initial H_2 formation was relatively unaffected by steam flow. The H_2 formation rate then fell off much more rapidly in the no steam flow case than the no steam flow case, with detectable levels of H_2 being observed for 42 min in the no steam flow case versus 150 min in the steam flow case. As has also been observed previously, total H_2 conversion was much higher in the steam flow case than the no steam flow case, 30% versus 46%.

Figure 6.3b shows the H_2 formation kinetics for the first 30 min of the alkaline thermal treatment of cellulose reaction conducted isothermally at temperatures ranging from 473 K to 598 K, all in the presence of steam flow. In general, as the temperature at which the reaction was

conducted increased, the peak H_2 formation rate increased and the time at which this peak H_2 formation rate was observed decreased, pointing to improved kinetics and greater extent of reaction with increasing temperature. All kinetic experiments except for the 573 K and 598 K cases were run for 120 min, since H_2 was still being generated above the detection limit of the Micro GC after this time for the lower temperature cases. The 573 K and 598 K experiments were terminated once the online H_2 concentration in the product gas stream fell below the Micro GC's detection limit of 0.1%.

Relative to the rest of the experiments, the maximum H_2 formation rate observed for the 473 K case was quite low, 2.9×10^{-2} mol H_2/mol cellulose-min, and occurred 70 min into the experiment. For the 498 K case, the peak H_2 formation rate had increased by over an order of magnitude from that observed in the 473 K case, 0.37 mol H_2/mol cellulose-min, and occurred much earlier in the experiment, 26 min. The H_2 formation rate curve continued to be pushed toward earlier times as temperature was increased, with the peak H_2 formation rate occurring at 6 min and being 0.88 mol H_2/mol cellulose-min for the 548 K case.

The pattern of the peak H_2 formation rate occurring at earlier times with increasing temperature seemingly was broken for the 573 K case, where the peak H_2 formation rate was observed at 8 min into the experiment; however, the peak H_2 formation rate was larger than it was in the 548 K case, being 1.3 mol H_2/mol cellulose-min. The observed later time to reach the peak formation rate was believed to be due to the sampling limitations of Micro GC. As the temperature of the reaction was increased, reactions kinetics improve and more H_2-producing reactions were able to proceed. Each of the sodium carboxylate salts will not react with NaOH to produce detectable H_2 below certain temperatures; this will be shown later in this study. Thus, as kinetics and extent of reaction improved with increasing reactor temperature, the temporal

limitations of the gas sampling method made accurately observing the true H_2 formation rate trends more difficult. As the time difference between the observed peak H_2 formation rates for the 548 K case and the 573 K case was the same length as the sampling time of the Micro GC, it cannot be definitively said which temperature case actually experienced the earlier peak H_2 formation rate. A similar argument can be applied to explain the data from the 598 K case. Although the peak H_2 formation rate occurred at the earliest time of any of the cellulose trials, 4 min into the experiment, the magnitude of the observed H_2 formation rate was only 0.6 mol H_2/mol cellulose-min, nearly identical to the peak formation rate reported for the 533 K experiment. Again, this low observed peak formation rate value for 598 K is likely due to the sampling limitations of the Micro GC.

To further probe the mechanisms behind these kinetic studies, H_2 conversions were compared to Na_2CO_3 conversions, according to the stoichiometry of Reaction 6.2, for all of the alkaline thermal treatment of cellulose isothermal experiments. This comparison is depicted in Figure 6.4. Similar to what was observed in the previous study, at lower temperatures, H_2 conversion was greater than Na_2CO_3 conversion, and as temperature increased, both conversions were more similar in value. H_2 conversion for the 473 K case was 14%, 7 times higher than the Na_2CO_3 conversion of 2%. H_2 conversion increased for the 498 K case to 19%, and the Na_2CO_3 conversion increased more dramatically to 8%. Interestingly, both H_2 and Na_2CO_3 conversions did not significantly increase from the 498 K case to the 513 K case, with H_2 conversion for the 513 K case being 19% and the Na_2CO_3 conversion being 9%. As will be shown subsequently, the only sodium carboxylate intermediate that has been shown to significantly react to form H_2 at 513 K is sodium formate; therefore, the increase in extent of carbonation from 473 K to 513 K is likely coming from the conversion of sodium formate to H_2 and Na_2CO_3. Additionally, these

results show that significant H_2 formation can occur without the formation of Na_2CO_3 according to the 2:1 molar proportion given by Reaction 6.2. As has been hypothesized previously, this H_2 generation was believed to be a product of the alkaline degradation of cellulose to produce the sodium carboxylate salt intermediates.

By the 533 K case, both H_2 and Na_2CO_3 conversions had increased, Na_2CO_3 more dramatically, and both values were very similar, with the values being 32% and 30%, respectively. This represented an increase in H_2 conversion of 67% and an increase in Na_2CO_3 conversion of nearly 250% from the 513 K case. Thus the additional H_2 generated was accompanied by much greater Na_2CO_3 formation, perhaps indicative of the sodium carboxylate salt reactions with NaOH becoming more predominant. Beyond the 533 K case, Na_2CO_3 conversion was actually larger than H_2 conversion; however, the difference between the two values was much smaller than the differences observed in the low temperature cases. H_2 conversion increased slightly from the 533 K case to the 548 K case, increasing to 36%, and the Na_2CO_3 conversion increased more significantly to 41%. Both H_2 conversion and Na_2CO_3 conversion continued to increase in the 573 K case, with H_2 conversion being 46% and the Na_2CO_3 conversion being 52%. Further increasing the temperature to the 598 K case did not affect H_2 or Na_2CO_3 conversions, which at this temperature were 45% and 50%, respectively.

6.3.3   Isothermal Kinetics of the Sodium Carboxylate Salt and NaOH Reactions

After the investigation of the overall alkaline thermal treatment of cellulose kinetics, the kinetics of the H_2-producing sodium carboxylate salt reactions was explored. The H_2 formation rate curves for the first 30 min of the reactions of sodium formate, sodium oxalate, and sodium glycolate with NaOH are shown in Figure 6.5. The temperature range for each sodium carboxylate salt shown in Figure 6.5 was chosen based on the observable data and the

capabilities and limitations of the kinetic sampling method. The lowest temperature in each study was the temperature where kinetics for H_2 generation were quite slow and H_2 was being produced just above the detection limit of the Micro GC. At the highest temperature used in each study, kinetics for H_2 generation were very fast, and thus the likelihood of observing the actual fastest H_2 production rate, given the 2 min sampling time, decreased. Regarding the study of sodium oxalate, although the earlier alkaline thermal treatment of cellulose study showed that concentrations of sodium oxalate in the solid products were relatively low, it was analyzed in this kinetics study because varying the alkaline degradation conditions has been shown in other studies to influence the relative production of sodium oxalate as an alkaline degradation product from cellulose (Othmer et al. 1942, Krochta et al. 1987, Mahood and Cable 1919). Also, because the reaction of sodium oxalate with NaOH produces only H_2 as a gaseous product, sodium oxalate is a relevant product to attempt to select for in producing high-purity H_2 from alkaline thermal treatment. Thus knowledge of the kinetics of the sodium oxalate and NaOH reaction could be of importance.

As was the case with the isothermal studies of the alkaline thermal treatment of cellulose, as the isothermal temperature was increased, the maximum formation rates of H_2 occurred at earlier times and increased in magnitude for all of the sodium carboxylate salt systems studied. Figure 6.5a shows the results for the isothermal reactions of sodium formate with NaOH, which were conducted at temperatures ranging from 483 K to 548 K. Over the 50 K temperature range from 498 K to 548 K, the observed maximum formation rate of H_2 increased by about an order of magnitude, from 5.7×10^{-2} mol H_2/mol sodium formate-min to 0.6 mol H_2/mol sodium formate-min. For the sodium oxalate system, shown in Figure 6.5b, over the studied 50 K temperature range, the increase in the maximum formation rate of H_2 was more dramatic,

increasing by about 60 times from 6.5×10^{-3} mol H_2/mol sodium oxalate-min to 0.4 mol H_2/mol sodium oxalate-min. Finally, for the sodium glycolate system, shown in Figure 6.5c, over the studied 50 K temperature range, the magnitude of the maximum H_2 formation rate increased by nearly 20 times, from 8.7×10^{-3} mol H_2/mol sodium glycolate-min to 0.15 mol H_2/mol sodium glycolate-min.

For calculating rate constants and activation energies for these sodium carboxylate salt reactions with NaOH, the conventional power rate law, which assumes homogeneous reaction conditions, was employed first as a starting point. In terms of the reaction order applied to the power rate law model, both first order and derived non-integer orders were tested. However, the sodium carboxylate salts were not fully soluble in the excess NaOH solution; therefore, the salts existed as solids in a liquid NaOH solution prior to their isothermal reaction. This observation warranted the comparison of the homogeneous models to heterogeneous models.

Kinetic models that have been employed previously for solid-liquid reactions have compared extent of conversion of the solid product to the reaction time to derive rate constants and subsequently activation energies (Salmi et al. 2013, Dickinson 1999). The extent models are divided into categories based on proposed mechanisms including geometric contraction, diffusion, and nucleation. Identifying the category to which the reaction belongs can be accomplished by fitting a linear regression to the extent model versus time plot and finding which category of models exhibits the best linear fit; however, to differentiate among the models in a category is considerably more challenging, requiring detailed knowledge about transport phenomena and particle morphology (Salmi et al. 2013, Hancock and Sharp 1972, Khawam and Flanagan 2006). Thus the methodology employed in this study for choosing a model was to

identify the model category and then to choose a model within that category based on reasonable assumptions.

Of the extent models given by Dickinson et al., the geometric contraction models exhibited the best fits to the kinetic data. Reactions progressing according to geometric contraction models are controlled by the rate of contraction of the reaction interface toward the center of the solid particle. Within the category of geometric contraction models, the Contracting Volume model was chosen based upon the assumption that the sodium carboxylate salt particles were spherical:

$$1 - (1 - \alpha)^{1/3} = kt \qquad \qquad \text{(Eqn. 6.1)}$$

In Equation 6.1, α is the extent of conversion of the sodium carboxylate salt, k is the rate constant, and t is the reaction time. These extents of conversion of the sodium carboxylate salts at different times were determined by stoichiometrically relating H_2 generation with sodium carboxylate salt consumption. For the reactions of sodium formate and sodium oxalate with NaOH, these relationships were 1:1 molar, as given by the stoichiometries of Reactions 6.3 and 6.4, respectively. For the sodium glycolate reaction with NaOH, the ratio of molar H_2 generation to Sodium glycolate consumption was assumed to be 1.6:1, based on the estimated material balance of the sodium glycolate and NaOH reaction to be described in the subsequent section.

In performing a linear regression on the model given in Equation 6.1 as a function of time, the slope will yield the rate constant, k. The derived rate constants for all of the isothermal studies for each sodium carboxylate salt according to the Contracting Volume model are shown in Table 6.1, and the corresponding Arrhenius plots for the derivation of activation energies are shown in Figure 6.6. From Table 6.1, it can be observed that the H_2 formation rate from the

sodium carboxylate salt reactions with NaOH increases in the following order: sodium glycolate < sodium oxalate < sodium formate. In particular, at 548 K, the rate constant for the sodium formate reaction was estimated to be about 5 times greater than for the sodium oxalate reaction, and about 100 times greater than the sodium glycolate reaction. Thus if sodium formate formation during alkaline thermal treatment can be preferentially selected for, the overall H_2 formation kinetics from alkaline thermal treatment should dramatically improve. From the Arrhenius plots given in Figure 6.6, the highest activation energy was estimated for the sodium oxalate reaction with NaOH at about 206 kJ/mol, followed by the sodium glycolate and NaOH reaction at about 165 kJ/mol, and finally the sodium formate and NaOH reaction at about 138 kJ/mol. All of these values are indicative of kinetically controlled reactions. The linear fit for the sodium glycolate Arrhenius plot ($R^2 = 0.99$) was better than the fits for the sodium formate and sodium oxalate cases ($R^2 = 0.91$ and $R^2 = 0.94$, respectively), which was likely due to the rapid kinetics of the sodium formate and sodium oxalate reactions with NaOH at higher temperatures, limiting data collection in those cases and thus introducing more error into the estimation of the rate constants.

Interestingly, these activation energies were very similar to those derived assuming pseudo first order and non-integer power rate law models. From the Arrhenius plots, estimated activation energies for the sodium carboxylate salt reactions with NaOH based on a pseudo first order power rate law were: 201 kJ/mol for sodium oxalate, 160 kJ/mol for sodium glycolate, and 134 kJ/mol for sodium formate. Thus, homogeneous reaction kinetics may be able to approximate the sodium carboxylate salt reactions with NaOH. However, solid-liquid reaction kinetics are complicated by transfer issues, with some studies suggesting that derived parameters such as the rate constants and the activation energies have more empirical significance than

theoretical significance. Thus, an understanding of how heat and mass transfer and particle size and morphology may affect the measured kinetic parameters of the sodium carboxylate salt reactions with NaOH is necessary and requires future study (Salmi et al. 2012, Brown et al. 2008, Ninan 1985, Khawam and Flanagan 2006, White et al. 2011, Grenman et al. 2011).

Derivations of the kinetic parameters for the power rate law reaction models, as well as a more detailed discussion of the comparisons among the different kinetic models may be found in the Supporting Information.

6.3.4   Comparison of H_2 Kinetics Between the Alkaline Thermal Treatment of Cellulose and Intermediates

Having obtained all of the H_2 formation rate curves at different isothermal temperatures for each of the sodium carboxylate salt reactions with NaOH, these curves were compared with the H_2 formation rate curves generated for the alkaline thermal treatment of cellulose at the same isothermal temperature conditions. Two interesting results were observed in comparing the cellulose and sodium glycolate cases at 573 K and 598 K, and these H_2 formation rate curves are plotted against each other in Figure 6.7. First examining the 573 K cases in Figure 6.7a, the trends for both the cellulose system and the sodium glycolate system were very similar starting around 20 min into the experiments, with the H_2 formation rates on a per molar basis from cellulose being about 1.5 – 2 times higher than those from the sodium glycolate reaction with NaOH. A similar result can be observed in comparing the H_2 formation rate curves from the cellulose and sodium glycolate systems at 598 K, shown in Figure 6.7b. From 6 min into the experiments until their conclusions, the H_2 formation rates on a per molar basis from the cellulose system were about 1.2 – 2 times higher than those from sodium glycolate system, with

the difference in formation rates between the cellulose and sodium glycolate systems decreasing with increasing time.

The more significant differences in molar H_2 formation rates between the cellulose and sodium glycolate systems at earlier times was likely due to other H_2 formation pathways that are more kinetically favorable at lower temperatures. These may include the initial breakdown of the cellulose into the sodium carboxylate salts, which may release H_2 gas, as well as the reactions of sodium formate and sodium oxalate with NaOH. Coupling these kinetic results with the IC results, which showed that sodium glycolate was a major decomposition product from the alkaline thermal treatment of cellulose, indicated that the rate of H_2 formation from the alkaline thermal treatment of cellulose conducted isothermally at 573 K and at higher temperatures may have become limited by the rate of sodium glycolate conversion to H_2.

As the conversion of sodium glycolate into H_2 appeared to be a rate limiting step in the kinetic analyses, and previously it was shown that the H_2 and CH_4 formation rate trends between the sodium glycolate reaction with NaOH and the alkaline thermal treatment of cellulose corresponded well above 573 K and up to 773 K, the reaction of sodium glycolate with NaOH was studied in more detail. Although the proposed stoichiometry for the reaction of sodium glycolate NaOH to produce H_2 and Na_2CO_3 given by Reaction 6.5 shows that 3 moles of H_2 are produced for every mole of sodium glycolate consumed, the total amount of H_2 produced from this reaction was actually about half of this value. In examining the isothermal tests of this reaction conducted at 573 K both in the absence and presence of steam flow, very different final gaseous product distributions were observed. In the absence of steam flow, about 0.6 mol H_2/mol sodium glycolate were produced, corresponding to 20% conversion according to Reaction 6.5. Significant formation of CH_4 was also observed, with 0.3 mol CH_4/mol sodium glycolate being

produced, and a small amount of C_2H_6, 9×10^{-4} mol C_2H_6/mol sodium glycolate, was also observed. The sodium glycolate and NaOH reaction in the presence of steam flow, on the other hand, yielded much more H_2, 1.6 mol H_2/mol sodium glycolate, which corresponded to about 53% conversion according to Reaction 6.5, and much fewer hydrocarbons, 2.5×10^{-2} mol CH_4/mol sodium glycolate, and no detectable C_2H_6.

In order to ascertain the fate of the unconverted H_2 in the sodium glycolate and NaOH reaction, a material balance was calculated based on the concentrations of the identified side products in the remaining solids from the sodium glycolate and NaOH reaction conducted at the 573 K isothermal condition, and combined with the total gaseous product results. These non-gaseous compounds were identified and quantified using IC, with the exception of Na_2CO_3, which was quantified using TIC analysis. Due to the necessity of steam as a reactant in the alkaline thermal treatment of cellulose reaction, and the enhancement in H_2 production from the sodium glycolate reaction with the addition of steam flow, only the steam case was considered.

From the analysis of the gaseous and solid products of the reaction, the following approximate material balance for the sodium glycolate and NaOH reaction was found:

$$NaC_2H_3O_3 + 3NaOH \rightarrow 1.6H_2 + 0.025CH_4 + 0.25NaC_2H_3O_2 + 0.01NaC_3H_5O_2 + 1.6Na_2CO_3$$
$$+ (Na_{0.5}O_{0.7}H_{1.9}) \qquad\qquad \text{(Rxn. 6.6)}$$
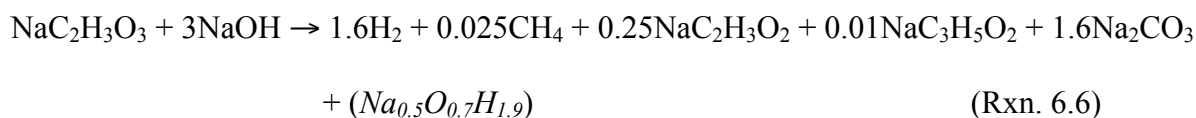
Steam was shown to have a major effect on the reaction of sodium glycolate with NaOH; however, because it is unknown exactly how steam influences the reaction, it was not included in the reactants side of the stoichiometry. It can be immediately observed that the reaction of sodium glycolate and NaOH under steam flow produced other sodium carboxylate salts, namely sodium acetate and sodium propionate. Thus the reaction of sodium glycolate with NaOH may

account for some of the sodium acetate and sodium propionate that was also observed in the alkaline thermal treatment of cellulose products. The observed sodium acetate in both the cellulose and sodium glycolate systems could react with NaOH under steam flow to produce CH_4 at temperatures above 573 K, which would explain the observed CH_4 formation above 573 K in both of these systems.

For the estimated material balance of the sodium glycolate reaction with NaOH under steam flow shown in Reaction 6.6, the carbon balance between reactants and products was found to be nearly closed, with the products side having less than 10% more carbon than the reactants side. For the other elements, about 87% of the sodium is accounted for on the products side, 89% of the oxygen, and 68% of the hydrogen. The unaccounted for compounds in the products are represented by the empirical formula shown in parentheses in Reaction 6.6. From this approximate mole balance, it can be observed that over 10% of the hydrogen embodied in the reactants ended up in sodium acetate, and smaller amounts in sodium propionate and CH_4. Regarding other potential sources of H_2 to close out the attempted material balance for the sodium glycolate reaction, it was also possible that water was being abstracted from the reactants, which would explain why there is a deficiency in the products side in hydrogen and oxygen. In the alkaline hydrothermal gasification of biomass studies, Onwudili et al. also argued for abstraction of water from the reaction medium as an explanation for the elemental composition of their solid products (Onwudili et al. 2009). Complete characterization of all of the products from the sodium glycolate and NaOH reaction, including the potential abstraction of water from the system, requires further study.

A similar material balance was attempted for the alkaline thermal treatment reaction of cellulose in the presence of steam flow. Based on the quantitation of the gaseous and solid products from the 573 K isothermal test, the following approximate material balance was found:

$$C_6H_{10}O_5 + 12NaOH + H_2O \rightarrow 5.5H_2 + 0.05CH_4 + 0.5NaC_2H_3O_2 + 0.09NaC_3H_5O_2 + 3.1Na_2CO_3$$

$$+ (C_{1.6}Na_{5.2}O_{7.5}H_{11}) \hspace{2cm} \text{(Rxn. 6.7)}$$
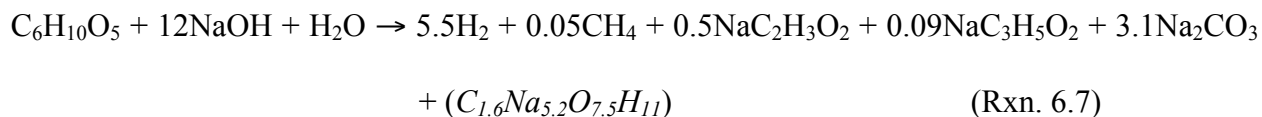
The molar balance for the alkaline thermal treatment of cellulose did not close as well as it did in the sodium glycolate and NaOH reaction. The carbon balance on the products side was about 74% of the original carbon in the reactants, about 57% for sodium, 54% for hydrogen, and 58% for oxygen. The unaccounted for compounds in the products are represented by the empirical formula shown in parentheses in Reaction 6.7. That the carbon balance was closer than any of the other elements may indicate that there was significant unreacted NaOH left in the products and/or that water had been abstracted from the reactants. As with the case of sodium glycolate, further investigation is required to explain the differing mole balances.

6.4   Conclusions

The kinetics of H_2 formation from the alkaline thermal treatment reaction for cellulose as well as those sodium carboxylate salts identified which were reactive with NaOH to form H_2 have been reported. As was found in the previous 2 K/min heating rate studies, the addition of steam flow to the alkaline thermal treatment reaction of cellulose conducted isothermally at 573 K enhanced H_2 production. The magnitude of the enhancement observed in this kinetic study was similar to that observed in the heating rate study, indicating that heating rate does not significantly impact H_2 production.

The reactivity of the three H_2-producing sodium carboxylate salts studied as a function of temperature was found to be as follows: sodium formate, then sodium oxalate, and then sodium glycolate. Sodium formate and sodium oxalate both had the best selectivities toward H_2 formation, producing only H_2 and Na_2CO_3 as products. Sodium glycolate, on the other hand, exhibited maximum H_2 conversions of around 50%, co-producing other sodium carboxylate salts, CH_4, and perhaps abstracting water from the reaction medium, leading to H_2 loss. Comparing the kinetics of H_2 formation for the cellulose system and the sodium glycolate system revealed that the alkaline thermal treatment of cellulose reaction to produce H_2 appeared to be limited by the rate of sodium glycolate conversion to H_2 at 573 K and higher temperatures.

Thus one potential avenue for improving H_2 yields from the alkaline thermal treatment of cellulose would be to improve the selectivity toward H_2 formation of the sodium glycolate and NaOH reaction, which could be accomplished through catalysis. Catalysis may also be able to influence the relative concentrations of the sodium carboxylate salts formed, with preferential formation of sodium formate not only eliminating the formation of the unwanted side products that were observed, but also lowering the temperature required for H_2 conversion. Research into these areas is currently ongoing.
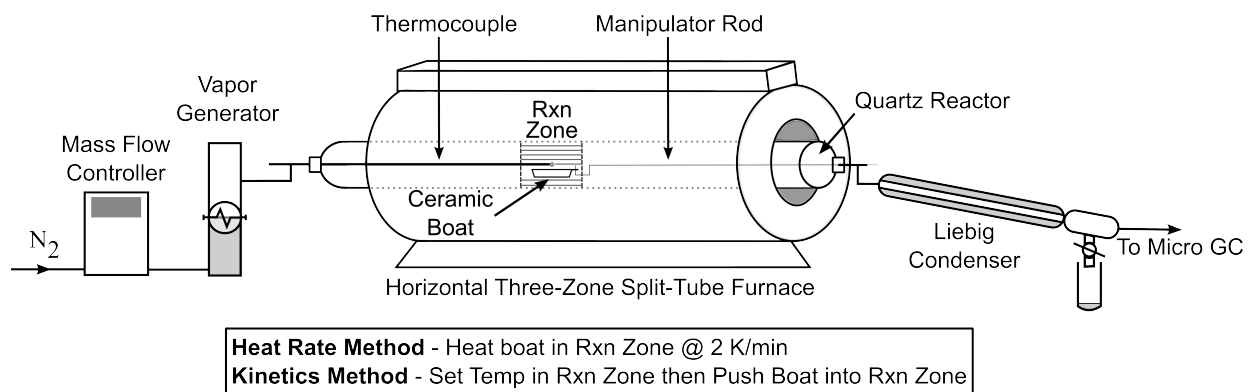
Figure 6.1 Experimental setup used in the kinetic studies of the alkaline thermal treatment of cellulose and of the sodium carboxylate salt intermediate reactions with NaOH.
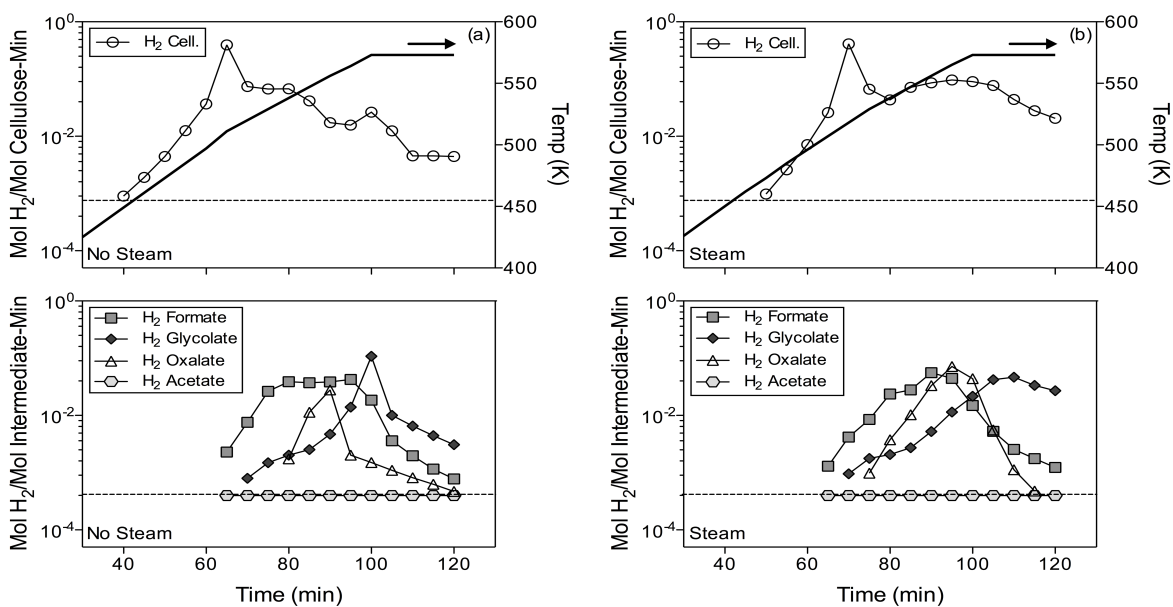
Figure 6.2 Online gaseous formation rates of H_2 for the alkaline thermal treatment of cellulose and the reactions of sodium formate, sodium oxalate, sodium acetate, and sodium glycolate with NaOH in a) the no steam flow and b) the steam flow cases (P_{H2O} = 38.8 kPa). Reactor temperature programming: reactants dried for 1 h at 373 K, 373 K $\rightarrow$ 573 K at 2 K/min and held isothermally at 573 K for 20 min. Stoichiometric ratios of reactants were used in all reactions.
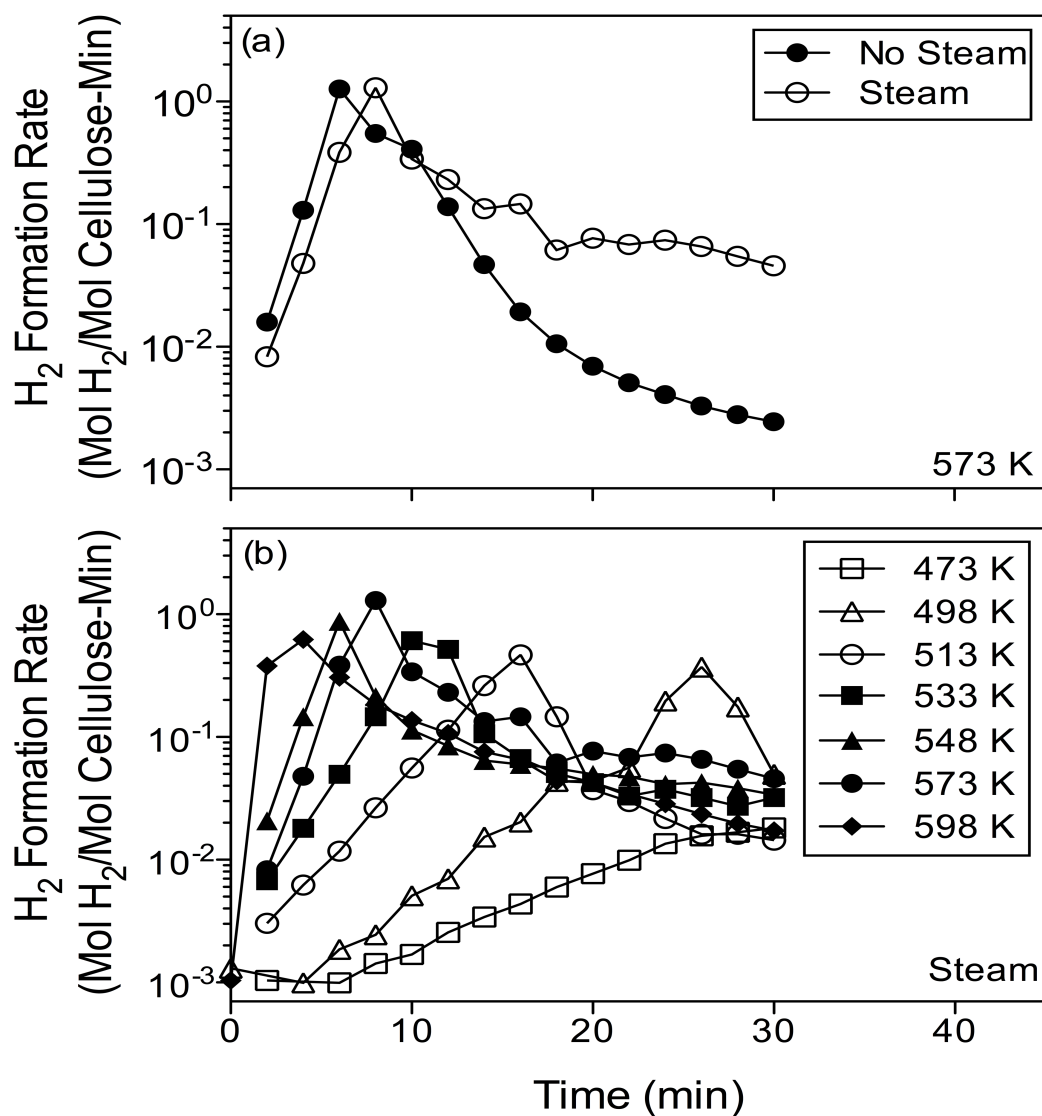
Figure 6.3 The first 30 min of H_2 formation kinetics from the alkaline thermal treatment of cellulose as a function of time a) in the absence and presence of steam flow (P_{H2O} = 38.8 kPa), conducted isothermally at 573 K, and b) conducted in the presence of steam flow isothermally at various isothermal temperatures.
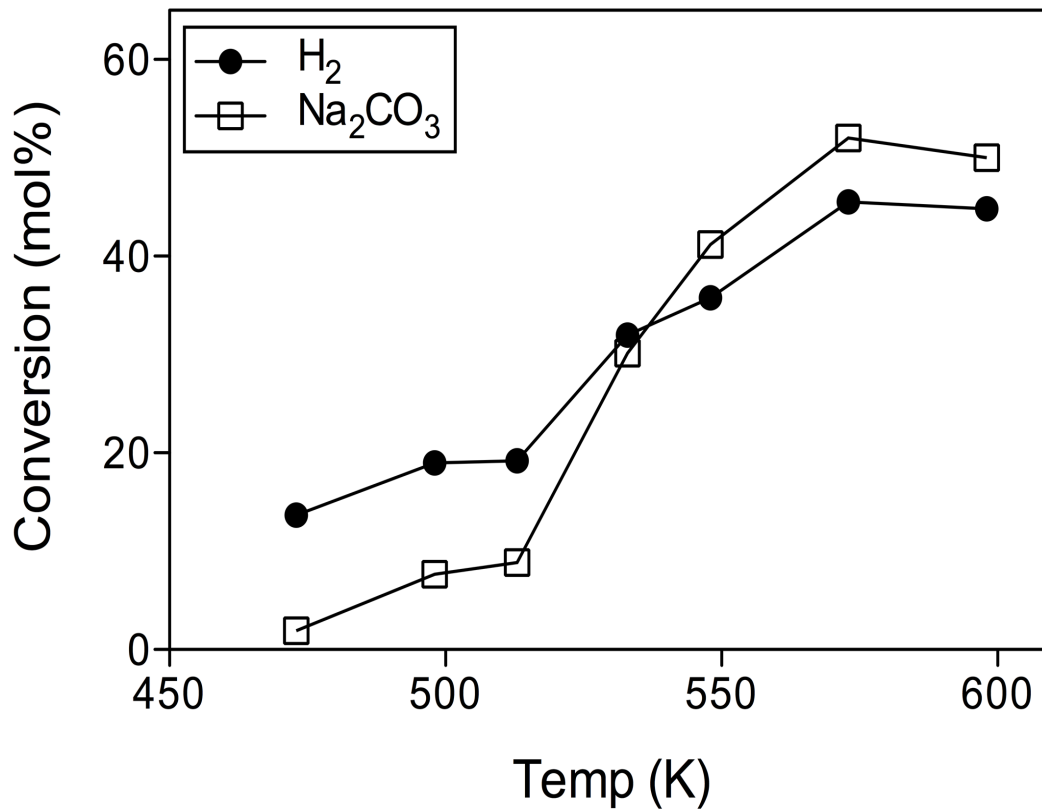
Figure 6.4 Comparison of H_2 conversion (gas analysis) to Na_2CO_3 conversion (solid analysis), based on the stoichiometry of Reaction 6.1, for the alkaline thermal treatment of cellulose experiments conducted isothermally at different temperatures in the presence of steam flow ($P_{H2O} = 38.8$ kPa).
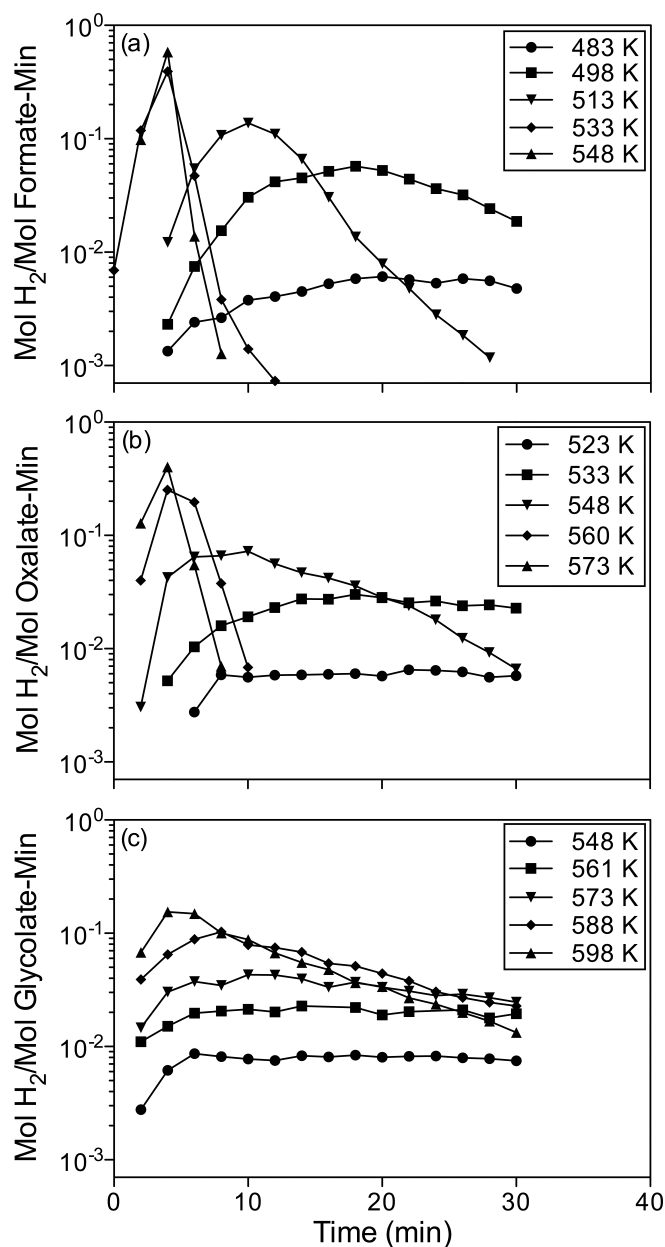
Figure 6.5 First 30 min of H_2 formation kinetics from the reactions of a) sodium formate and NaOH, b) sodium oxalate and NaOH, and c) sodium glycolate and NaOH, all in the presence of steam flow (P_{H2O} = 38.8 kPa), conducted isothermally at different temperatures. Reactions of each sodium carboxylate salt and NaOH were run in five times molar excess NaOH.

154

Table 6.1 Estimates of the rate constants for the reactions of the sodium carboxylate salts with

NaOH at different isothermal temperatures, based on the Contracting Volume model.

Sodium Formate		Sodium Oxalate		Sodium Glycolate	
T (K)	k (min^{-1})	T (K)	k (min^{-1})	T (K)	k (min^{-1})
483	2.4×10^{-3}	523	1.9×10^{-3}	548	1.8×10^{-3}
498	2.3×10^{-2}	533	1.2×10^{-2}	560	5.2×10^{-3}
513	4.3×10^{-2}	548	3.3×10^{-2}	573	9.9×10^{-3}
533	1.2×10^{-1}	560	9.6×10^{-2}	588	2.5×10^{-2}
548	1.8×10^{-1}	573	1.3×10^{-1}	598	3.9×10^{-2}
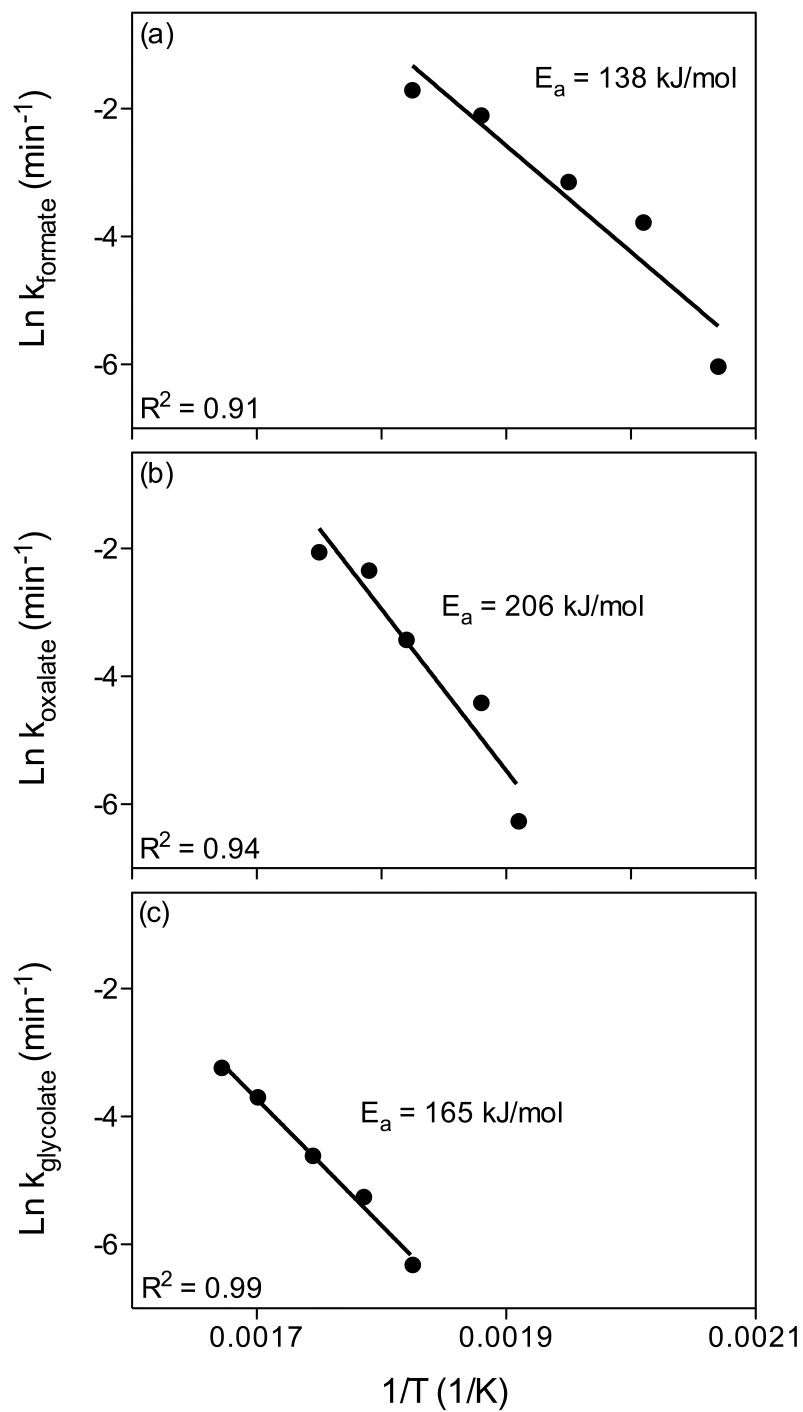
Figure 6.6 Arrhenius plots for the determination of the activation energies of the reactions of a) sodium formate with NaOH, b) sodium oxalate with NaOH, and c) sodium glycolate with NaOH.
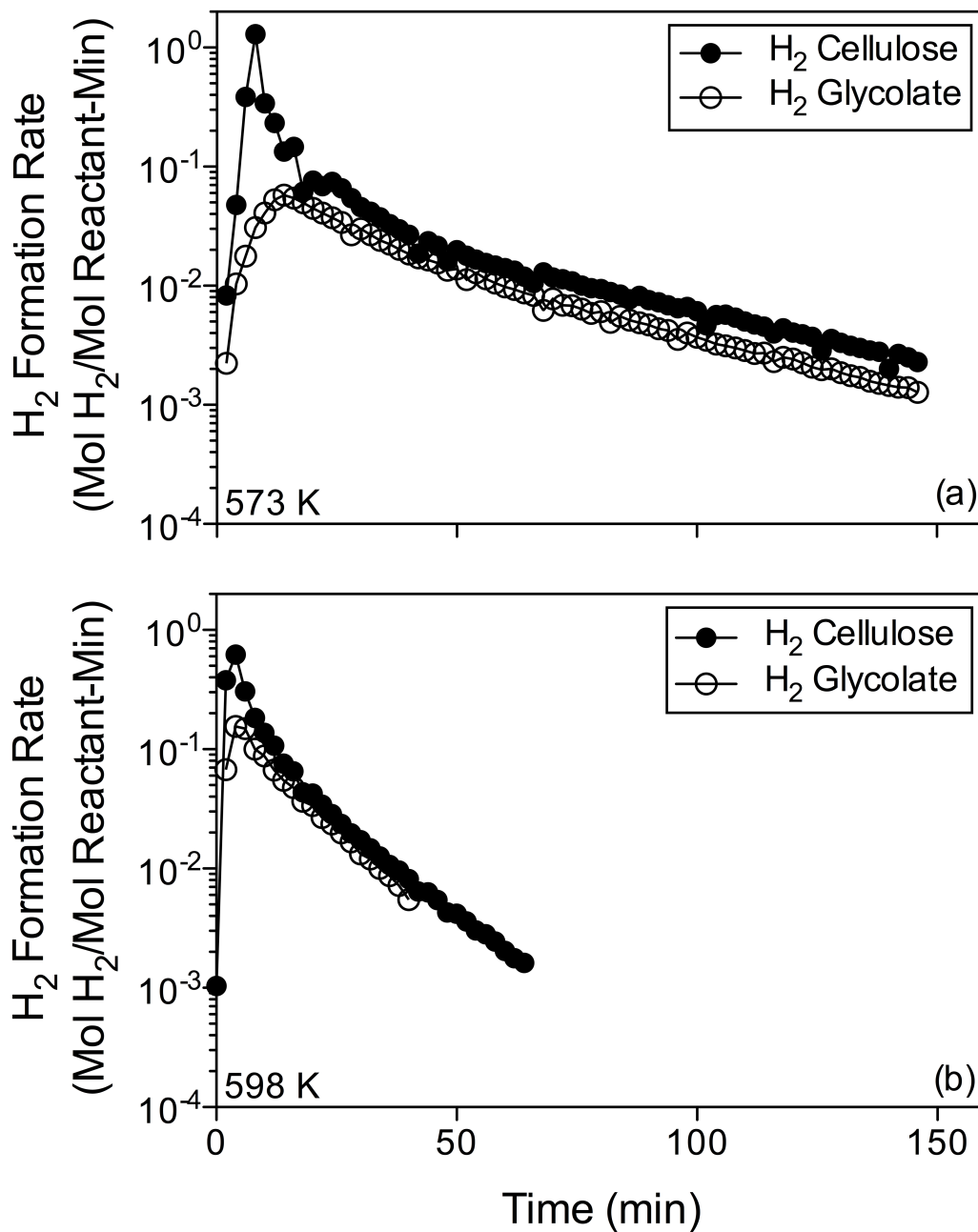
Figure 6.7 Comparison of the H_2 formation kinetics from the alkaline thermal treatment of cellulose and the reaction of sodium glycolate with NaOH, conducted at a) 573 K and b) 598 K, both in the presence of steam flow (P_{H2O} = 38.8 kPa).

6.5   Supporting Information

6.5.1   Non-isothermal Kinetics of CH_4 formation from the Alkaline Thermal Treatment of Cellulose and Reactive Intermediates

A comparison of the CH_4 formation rates for the alkaline thermal treatment of cellulose versus the formation rates for the sodium carboxylate intermediate reactions is shown in Figure 6.8. The reactions of sodium formate and sodium oxalate with NaOH did not produce CH_4. In both the no steam flow and steam flow cases, the reaction of sodium glycolate with NaOH was a much more significant source of CH_4 than the analogous sodium acetate reaction. In the no steam flow case, prior to 573 K, CH_4 formation rates from the cellulose reaction were at least 2 orders of magnitude higher than the formation rates from the sodium acetate and sodium glycolate reactions. Therefore the reaction of sodium carboxylate intermediates to form CH_4 prior to the 573 K isothermal period could only negligibly contribute to CH_4 formation in the alkaline thermal treatment of cellulose reaction; the same can be said of the steam flow cases.

In the steam flow case, the CH_4 formation rate from the sodium glycolate reaction was about an order of magnitude greater than that from the sodium acetate reaction throughout the experiment. Examining the final 15 min of the isothermal period, the rates of decline in formation rates of CH_4 between the cellulose case and the sodium glycolate case were similar. The CH_4 formation rate from the cellulose system in this isothermal period was consistently about twice the CH_4 formation rate from the sodium glycolate reaction, which was also about the magnitude difference observed between the cellulose and sodium glycolate systems for the H_2 formation rates. Overall, the addition of steam flow lowered the CH_4 formation rates for all of the biogenic compounds considered: cellulose, sodium acetate, and sodium glycolate. It is clear that steam plays a role in CH_4 suppression from organic species that are undergoing alkaline degradation.
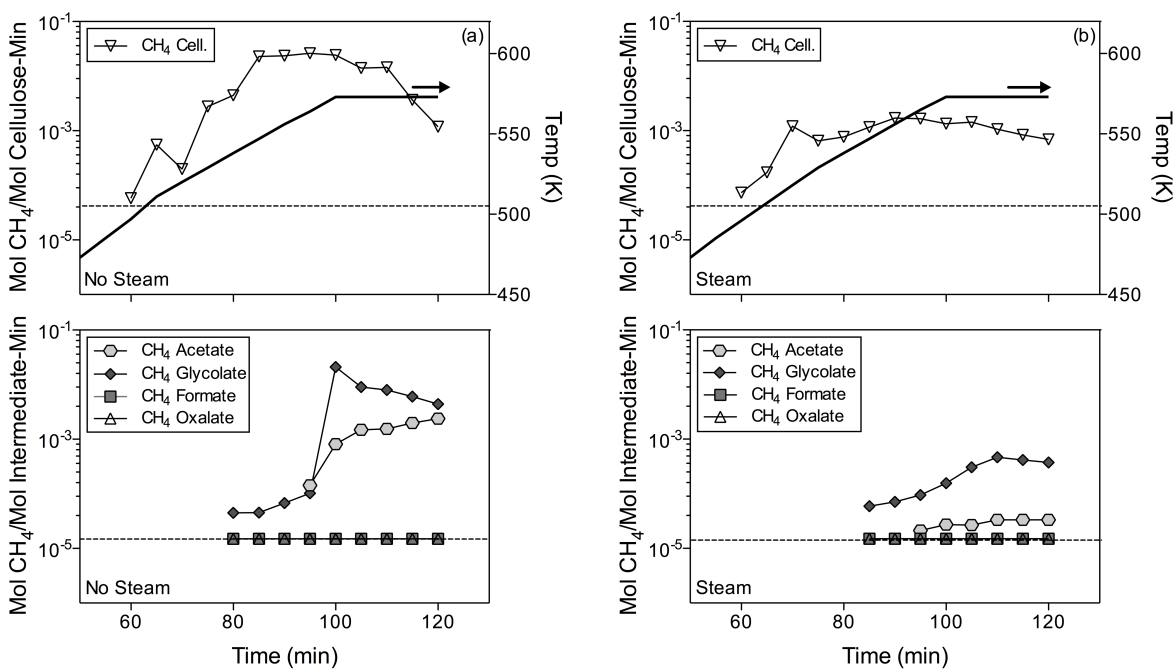
Figure 6.8 Online gaseous formation rates of CH$_4$ for the alkaline thermal treatment of cellulose and the reactions of sodium formate, sodium oxalate, sodium acetate, and sodium glycolate with NaOH in a) the no steam flow and b) the steam flow cases. Reactor temperature programming: reactants dried for 1 h at 373 K, 373 K → 573 K at 2 K/min and held isothermally at 573 K for 20 min.

6.5.2 Comparison of Heterogeneous Reaction Models to Homogeneous Reaction Models for the Sodium Carboxylate Salt Reactions

Assuming Homogeneous, Pseudo First Order Power Rate Law

A first order homogeneous reaction with respect to the sodium carboxylate salt, assuming

an excess of NaOH as was used in these studies, takes on the form:

$$-r_a = k'_a C_a \qquad \text{(Eqn. 6.2)}$$

$-r_a$ = rate of sodium carboxylate salt consumption (mol/min)
k'_a = pseudo rate constant which included the concentration of NaOH, held in excess (min^{-1})
C_a = Concentration of sodium carboxylate salt (mol)

Since only H_2 formation data was obtained, formation of H_2 was related to consumption of

carboxylate based on the reaction stoichiometries to obtain values for $-r_a$. The C_a used was the

concentration of carboxylate existing prior to measurement of $-r_a$.

Assuming Homogeneous nth order Reactions: Calculation of Orders for Each Sodium Carboxylate Salt Reaction

Sodium Glycolate Reaction with NaOH

The stoichiometry of the sodium glycolate and NaOH reaction, assuming complete

conversion to H_2 and Na_2CO_3, is given by the following:

$$NaC_2H_3O_3 + 3NaOH = 2Na_2CO_3 + 3H_2 \qquad \text{(Rxn. 6.5)}$$

However, the results of this reaction showed that only 1.6 mol H_2 were generated at the expense

of the formation of other side products; thus this 1.6:1 relationship was used in relating H_2

generation with sodium glycolate consumption.

The rate of reaction can be expressed as:

$$(-dC_{NaC2H3O3}/dt) = k'_{NaC2H3O3}C^n_{NaC2H3O3} \qquad \text{(Eqn. 6.3)}$$

Then, taking the natural log of both sides yields:

$$\ln(-dC_{NaC2H3O3}/dt) = \ln k'_{NaC2H3O3} + n \ln C_{NaC2H3O3} \qquad \text{(Eqn. 6.4)}$$

Taking the slope of the $\ln(-dC_{NaC2H3O3}/dt)$ versus $\ln C_{NaC2H3O3}$ plot will give the reaction order for sodium glycolate. To obtain $C_{NaC2H3O3}$ at different times, H_2 generation was related to loss of the starting sodium glycolate in the 1.6:1 molar ratio. To obtain $-dC_{NaC2H3O3}/dt$, the Finite Difference Method as discussed in the *Elements of Chemical Reaction Engineering* by Fogler was employed. The initial time used in the Finite Difference Method was defined as the time when the maximum H_2 formation rate was observed, which was believed to be greater than zero due to an induction period. An example $\ln(-dC_{NaC2H3O3}/dt)$ versus $\ln C_{NaC2H3O3}$ plot is shown in Figure 6.9. The orders for sodium glycolate obtained for each of the 5 isothermal temperature experiments ranged from $0.53 - 0.71$, with an average order of 0.62, giving the rate law:

$$-r_{NaC2H3O3} = k'_{NaC2H3O3}C^{0.62}_{NaC2H3O3} \qquad \text{(Eqn. 6.5)}$$

Sodium Formate Reaction with NaOH

The reaction of sodium formate with NaOH is given:

$$NaCOOH + NaOH = Na_2CO_3 + H_2 \qquad \text{(Rxn. 6.3)}$$

The molar ratio of H_2 generation to sodium formate consumption was assumed to be 1:1. The order for sodium formate was obtained using the same analysis method as was used to obtain the

order for sodium glycolate. The range of orders obtained was $0.4 - 0.65$, with an average order of 0.53, giving a rate law:

$$-r_{NaCOOH} = k'_{NaCOOH} C^{0.53}_{NaCOOH} \qquad \text{(Eqn. 6.6)}$$

Sodium Oxalate Reaction with NaOH

The reaction of sodium oxalate with NaOH is given:

$$Na_2C_2O_4 + 2NaOH = 2Na_2CO_3 + H_2 \qquad \text{(Rxn. 6.4)}$$

The molar ratio of H_2 generation to sodium oxalate consumption was assumed to be 1:1. The order for sodium oxalate was obtained using the same analysis method as was used to obtain the order for sodium glycolate and sodium formate. The range of orders obtained was $0.47 - 0.63$, with an average order of 0.56, giving a rate law:

$$-r_{Na2C2O4} = k'_{Na2C2O4} C^{0.56}_{Na2C2O4} \qquad \text{(Eqn. 6.7)}$$

Calculation of Rate Constants and Activation Energies for Pseudo First Order and nth Order Cases

The calculated rate constant values in the pseudo first order and non-integer order cases are shown in Table 6.2 for each sodium carboxylate salt. For each intermediate, two rate constant values are shown. One is based on the fastest rate of carboxylate salt consumption, denoted as 'Fastest', and the other is the average rate constant for sodium carboxylate salt conversions between $0.15 - 0.50$, denoted as 'Average'. The conversion range of $0.15 - 0.50$ was chosen based on recommendation in the literature for reactions involving a solid phase (Hancock and Sharp 1972).

With the rate constants obtained, Arrhenius plots for each of the sodium carboxylate salt reactions were made to find the activation energy for each reaction. These plots are shown for both the pseudo first order and non-integer order cases in Figures 6.10 – 6.12, and the activation energies are summarized in Table 6.3. For the sodium glycolate reaction with NaOH, the linear fits to the data were all very good, with R^2 above 0.98 in all cases. Additionally, the activation energies were similar in comparing the Fastest and Average methods, as well as in comparing the assumptions of pseudo first order kinetics and non-integer order kinetics, with all activation energies falling between 150 – 160 kJ/mol.

Agreement in activation energies between the Fastest and Average methods for the sodium formate and sodium oxalate systems, however, were not as good. For both systems, the activation energies derived from the Average method were about 30 kJ/mol lower than when using the Fastest method. The linear fits were also not as good for the Average method compared to the Fastest method, in both the pseudo first order and non-integer order cases. The reason for both of these discrepancies was due to the lack of data collection for the higher temperature isothermal experiments. Both the sodium formate and sodium oxalate systems reacted quickly at higher temperatures, in some cases only generating 3 data points during reaction as a result of the Micro GC's 2 min sampling time. This caused the value of the Average rate constants obtained in these experiments to be significantly different from those obtained using the Fastest rate of carboxylate consumption, affecting both the integrity of the linear fit as well as the resulting activation energy calculation. Thus, k values obtained at higher temperatures and activation energies for the sodium formate and sodium oxalate systems have more uncertainty associated with them than for the sodium glycolate system.

Regarding the comparison between the pseudo first order and non-integer order power rate law models, examining the activation energies obtained in the Fastest method, both order assumptions produced similar values for activation energies. The rate constants, however, were about 20 – 35 times lower in the non-integer order cases than the pseudo first order cases. The rate constants obtained with non-integer orders in the power rate law models for each of the sodium carboxylate salts were about an order of magnitude lower than the rate constants obtained using the Contracting Volume model based on extent of reaction. Given that the reactions of the sodium carboxylate salts are not likely homogeneous, and the rate constants were significantly different than those given by the Contracting Volume model and other heterogeneous extent models, assuming a homogeneous power rate law with derived non-integer orders is likely underestimating the rate constants for the reactions.

Comparison of Homogeneous Kinetic Model to Heterogeneous Contracting Volume Model

Finally, in each of the sodium carboxylate salt reactions, the rate constants for the pseudo first order power rate law models were about 2 – 4 times higher than those given by the Contracting Volume models. Interestingly, there was about a factor 4 difference between the lowest estimated rate constant and the highest estimated rate constant among the heterogeneous extent models for all of the sodium carboxylate salt systems. These differences between the models were within differences reported among models in the literature (Al-Raqom and Klausner 2013, Lee et al. 2005), indicating that homogeneous kinetics may be able to approximate kinetic parameters for these sodium carboxylate salt reactions. However, in order to more accurately derive kinetic parameters, especially the rate constants, which were found to differ more significantly among models than activation energies, further study is required to physically understand how the reaction is proceeding, which will allow for more accurate modeling.
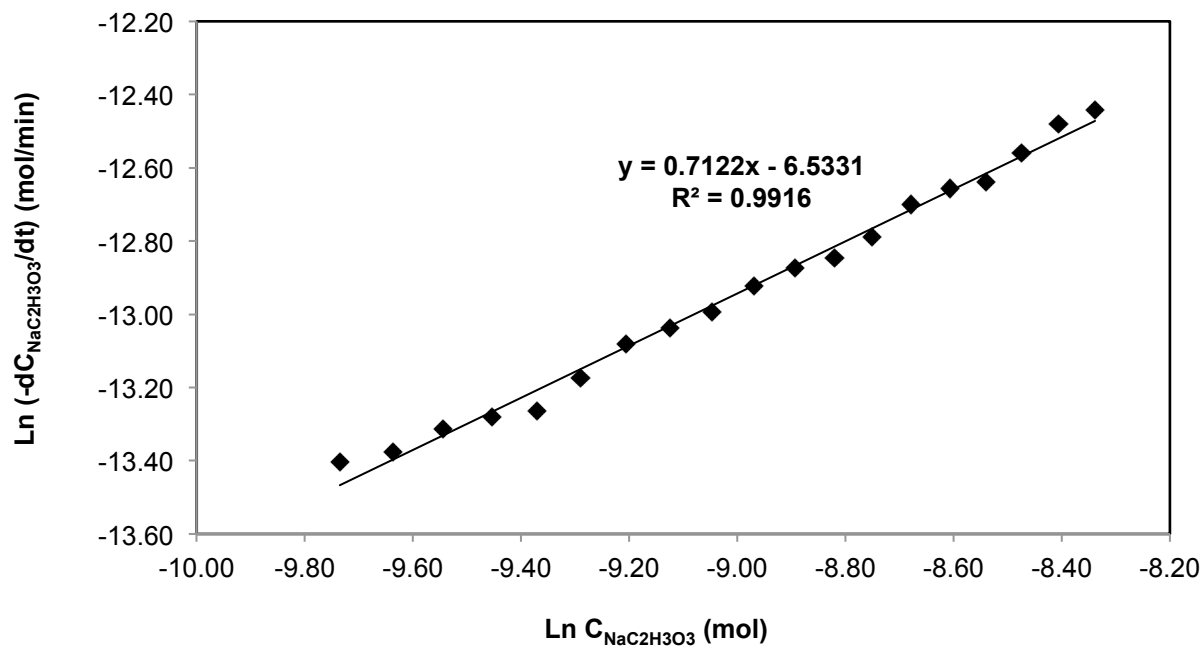
Figure 6.9 Derivation of reaction order for sodium glycolate, reacted in excess NaOH isothermally at 573 K.

Table 6.2 Calculated rate constants for sodium carboxylate salt reactions with NaOH using Power Law Models.

Temp (K)	Sodium Formate					
	Assuming Pseudo First Order Kinetics[a]			Assuming 0.53 Order Kinetics[b]		
	Fastest	Average	Fastest:Average	Fastest	Average	Fastest:Average
483	9.7×10^{-03}	8.4×10^{-03}	1.2	3.5×10^{-04}	2.7×10^{-04}	1.3
498	8.6×10^{-02}	8.0×10^{-02}	1.1	2.8×10^{-03}	2.8×10^{-03}	1.0
513	1.8×10^{-01}	1.7×10^{-01}	1.1	6.2×10^{-03}	5.6×10^{-03}	1.1
533	4.5×10^{-01}	2.3×10^{-01}	1.9	1.7×10^{-02}	1.1×10^{-02}	1.6
548	6.5×10^{-01}	2.7×10^{-01}	2.4	2.4×10^{-02}	9.6×10^{-03}	2.5

Temp (K)	Sodium Oxalate					
	Assuming Pseudo First Order Kinetics[a]			Assuming 0.56 Order Kinetics[c]		
	Fastest	Average	Fastest:Average	Fastest	Average	Fastest:Average
523	7.1×10^{-03}	5.7×10^{-03}	1.2	2.3×10^{-04}	1.7×10^{-04}	1.3
533	3.9×10^{-02}	4.1×10^{-02}	1.0	1.2×10^{-03}	1.1×10^{-03}	1.0
548	1.0×10^{-01}	9.6×10^{-02}	1.1	3.0×10^{-03}	2.7×10^{-03}	1.1
560	2.6×10^{-01}	1.9×10^{-01}	1.4	8.3×10^{-03}	5.1×10^{-03}	1.6
573	4.6×10^{-01}	2.5×10^{-01}	1.8	1.4×10^{-02}	7.0×10^{-03}	2.0

Temp (K)	Sodium Glycolate					
	Assuming Pseudo First Order Kinetics[a]			Assuming 0.62 Order Kinetics[d]		
	Fastest	Average	Fastest:Average	Fastest	Average	Fastest:Average
548	5.5×10^{-03}	5.9×10^{-03}	0.9	2.7×10^{-04}	2.6×10^{-04}	1.0
560	1.7×10^{-02}	1.8×10^{-02}	0.9	6.8×10^{-04}	6.6×10^{-04}	1.0
573	3.1×10^{-02}	3.3×10^{-02}	0.9	1.3×10^{-03}	1.3×10^{-03}	1.0
588	7.9×10^{-02}	7.9×10^{-02}	1.0	3.1×10^{-03}	2.9×10^{-03}	1.1
598	1.0×10^{-01}	1.1×10^{-01}	0.9	4.3×10^{-03}	4.0×10^{-03}	1.1

[a] k has units of min^{-1}
[b] k has units of $mol^{0.47}min^{-1}$
[c] k has units of $mol^{0.44}min^{-1}$
[d] k has units of $mol^{0.38}min^{-}$
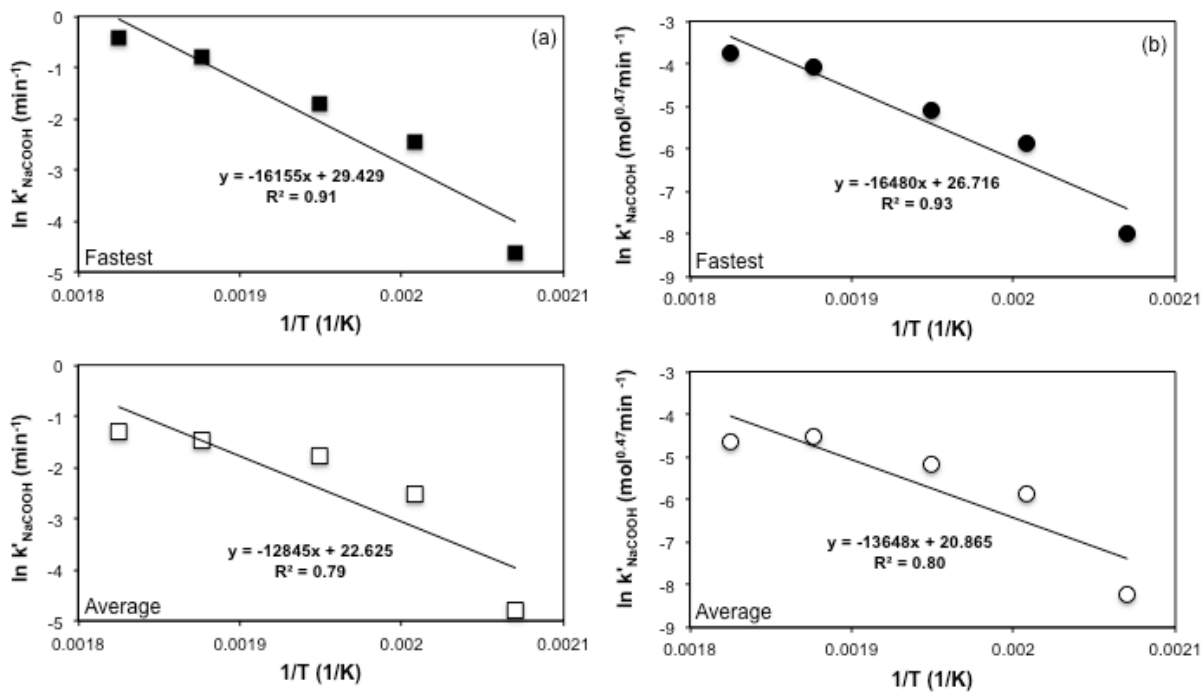
Figure 6.10 Arrhenius plots for determining the activation energy for the reaction of sodium formate with NaOH, assuming a) pseudo first order kinetics and b) a reaction order of 0.53 for sodium formate. Both the fastest rate constants (top plots) and average rate constants (bottom plots) are shown for comparison.
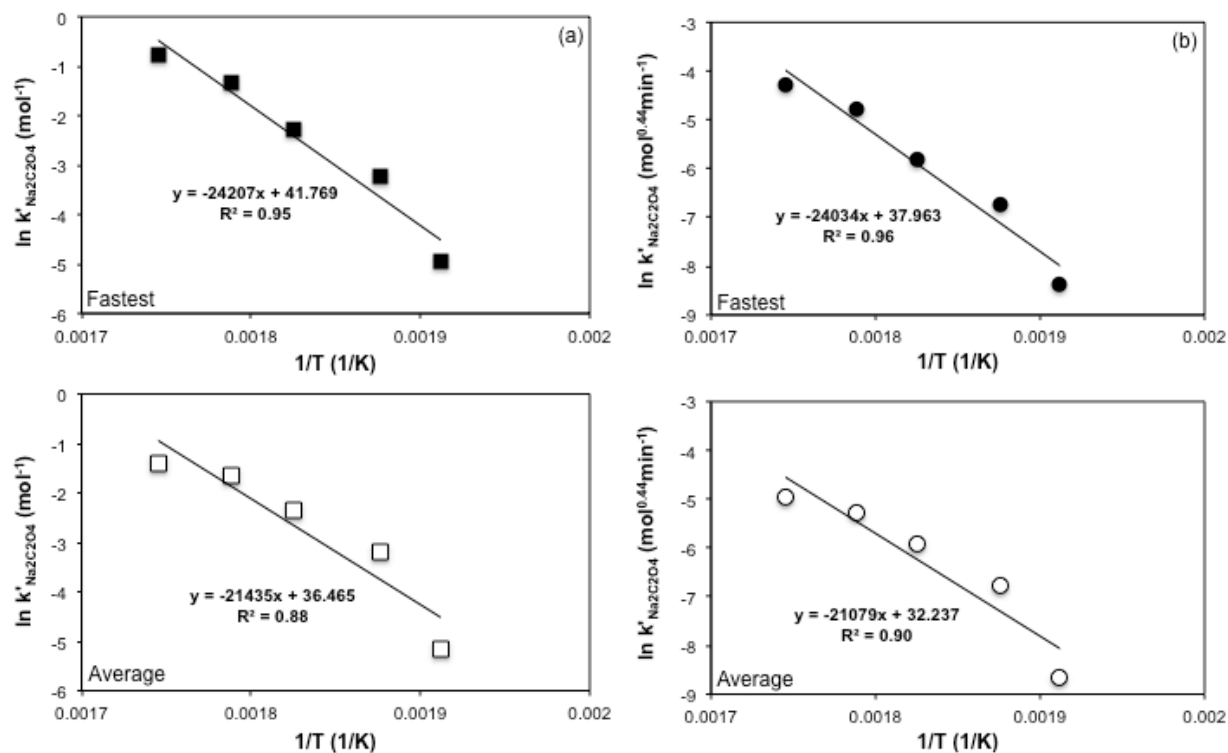
Figure 6.11 Arrhenius plots for determining the activation energy for the reaction of sodium oxalate with NaOH, assuming a) pseudo first order kinetics and b) a reaction order of 0.56 for sodium oxalate. Both the fastest rate constants (top plots) and average rate constants (bottom plots) are shown for comparison.
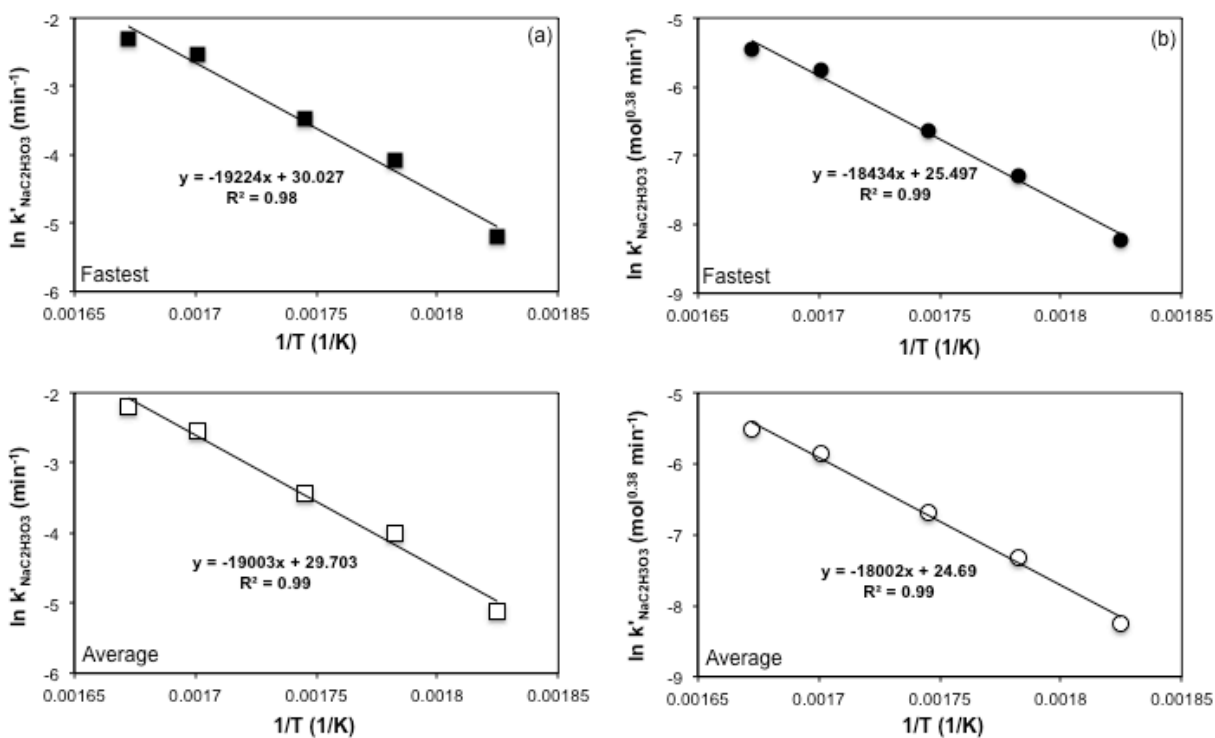
Figure 6.12 Arrhenius plots for determining the activation energy for the reaction of sodium glycolate with NaOH, assuming a) pseudo first order kinetics and b) a reaction order of 0.62 for sodium glycolate. Both the fastest rate constants (top plots) and average rate constants (bottom plots) are shown for comparison.

Table 6.3 Activation energies derived from Arrhenius plots for the sodium carboxylate salt reactions with NaOH.

Activation Energy (kJ/mol)		
Sodium Formate		
Order	Fastest	Average
1	134	107
0.53	137	113
Sodium Oxalate		
Order	Fastest	Average
1	201	178
0.56	200	175
Sodium Glycolate		
Order	Fastest	Average
1	160	158
0.62	153	150

CHAPTER 7

PRELIMINARY LIFE CYCLE AND ECONOMIC ASSESSMENTS OF A CASE STUDY OF THE CONVERSION OF HOUSEHOLD WASTE TO HYDROGEN VIA ALKALINE THERMAL TREATMENT

Hydrogen Generation Potential from Household Municipal Solid Waste

In order to begin to evaluate the potential impact of the alkaline thermal treatment technology, an estimation for the energy potential from the process was made for the case of household waste. Household waste was chosen because it represents a feedstock that can be used on site and thus has no associated transportation costs, and converting a waste product into energy would be beneficial to the environment. The following analysis includes many assumptions and rough estimates.

First, it was assumed that the alkaline thermal treatment reactor, fuel cell, and other ancillary equipment were already in place. Also not included in this analysis were the potential energy and environmental costs associated with separation of different types of wastes and any other pre-processing of the wastes that may be necessary prior to charging the alkaline thermal treatment reactor with the reactants. Also not considered here was any energy that would be required to remove or separate the solid end products from the alkaline thermal treatment reactor.

Figure 7.1 shows the breakdown of municipal solid waste (MSW) by waste type in 2012 for the United States (EPA 2014). The data were aggregated from households, schools, hospitals, and businesses; however, for the purposes of this estimation, it was assumed that the percentages given for each category shown in Figure 7.1 are representative for households. The fractions considered for alkaline thermal treatment included: paper, yard trimmings, and wood. These were considered because these fractions have significant cellulose content, and cellulose was the

171

main feedstock studied in this dissertation. Paper was assumed to be 100% cellulose, and yard trimmings and wood assumed to be 40% cellulose. It is possible that the results from the cellulose study may not exactly translate to a heterogeneous lignocellulosic feedstock, perhaps to due interactions among the different lignocellulosic fractions and from inorganic content; however, such effects were not considered in this estimation.

According to the Environmental Protection Agency, an individual generates about 2 kg of MSW per day; assuming 2.6 people per household (U.S. Census Bureau 2014) and that all waste generated by the individual was at the household as a simplifying assumption, each household generates 5.2 kg of MSW per day. Combining this with the percentage of cellulose in MSW from the three aforementioned waste fractions yields a total of 11 mol of cellulose per day from MSW:

$$((0.274*1)+(0.135*0.4)+(0.063*0.4)) * 5.2 \text{ kg/day} = 1.8 \text{ kg cell/day} = 11 \text{ mol cell/day}$$

Assuming complete conversion of the cellulose to H_2 via alkaline thermal treatment, a total of 133 moles of H_2 can be generated per household per day. According to a report by the National Renewable Energy Laboratory, a fuel cell operating at maximum power output can generate 154 kJ/mol H_2 consumed (Harrison 2010); thus, in the average household, about 20,500 kJ/day, or 5.7 kWh/day can be produced from the alkaline thermal treatment of the cellulosic fraction of MSW. From the Energy Information Administration, in 2012 the average household consumed about 30 kWh/day of electricity (EIA 2014). Thus, assuming complete conversion of the cellulose, alkaline thermal treatment from MSW could supply about 20% of the daily electricity demand for the average household.

In the non-catalytic study of the alkaline thermal treatment of cellulose, conversion to H_2 was approximately 50%; thus, without catalysis, alkaline thermal treatment could supply about 10% of the daily electricity demand for the average household. Additionally, if the electricity

demand required to heat the reactants to 573 K is included, the efficiency is further reduced. In making this estimation, the heat capacity used for cellulose was 2.5 kJ/kg-K (Boutin 1998), 2.15 kJ/kg-K for NaOH (NIST 2011), and 4.2 kJ/kg-K for water, also taking into account the heat of vaporization of water. Starting with the 1.8 kg of cellulose produced per day from MSW, and then adding the amount of NaOH and water required by the stoichiometry of the alkaline thermal treatment reaction for cellulose, the total energy required to raise the reactants to 573 K would be approximately 5,000 kJ, or about 24% of the 20,500 kJ daily energy output from the alkaline thermal treatment of cellulose process. Including these losses, alkaline thermal treatment from MSW could supply about 14% of the daily electricity demand for the average household assuming 100% conversion to H_2, or 7% assuming 50% conversion in the non-catalytic scheme. However, improvements to these numbers could be had if heat recovery were included. The alkaline thermal treatment process is exothermic, with the enthalpy change for the alkaline thermal treatment of glucose being -404 kJ/mol glucose. Depending on the recovery system and the quality of the heat, this heat could be recovered and either be used to reduce the heat demand of the reactor or be used in different household applications, improving the overall efficiency of the process.

The non-cellulosic fractions of the lignocellulose were not considered here because further study is necessary to understand their reactivity in alkaline thermal treatment; however, preliminary results have shown that hemicellulose and lignin can also produce H_2 when reacted with NaOH, and thus the MSW conversions reported here could be improved. Additionally, this analysis did not include the rubber, leather & textiles fraction, the plastics fraction, or the food waste fraction; these fractions also have the potential to be converted to H_2 using the alkaline thermal treatment technology (Ishida et al. 2005, Tongamp et al. 2010).

Cost of Hydrogen from Household Municipal Solid Waste

The cost of H_2 from the alkaline thermal treatment of cellulosic MSW was also estimated. The simplifying assumptions utilized in the estimation of H_2 generation potential from MSW were also used in this cost estimation analysis. Based on the alkaline thermal treatment of cellulose reaction, in order to produce 1 kg of H_2, 6.75 kg of cellulose, 20 kg of NaOH, and 0.75 kg of water are necessary. In addition to producing the 1 kg of H_2, 26.5 kg of Na_2CO_3 are produced. This Na_2CO_3 can be used to regenerate the NaOH through a double replacement reaction, such as the one with $Ca(OH)_2$ used in the Kraft recovery process given by Reaction 1.3. Or the Na_2CO_3 can sold as a value-added product. For the purposes of this economic analysis, it was assumed that the Na_2CO_3 produced was sold as a value-added product.

The raw material inputs are cellulose, NaOH, and water. Because the cellulose is being derived from waste, there are no costs associated with it aside from any separation and pre-treatment costs, which were not considered in this analysis. NaOH costs $0.42/kg (Saxena et al. 2008), and water costs $1.26 x 10^{-3}/kg (NYC 2014). Heat is also an input to the process. The amount of energy necessary to generate the heat input was assumed to be that calculated above for the H_2 generation from MSW estimation, and the source of energy used was assumed to be a coal-fired plant, with an associated energy cost of $95.60/MWh (EIA 2014).

Regarding the outputs, the cost of Na_2CO_3 is $0.31/kg (Kostick 2013). A summary of associated costs with each input and output of the alkaline thermal treatment of cellulose is given in Table 7.1. With the knowledge of the amount of each input needed and amount of output generated during the formation of 1 kg of H_2, as well as the associated costs in raw materials and heat input with each, the cost of H_2 generation was calculated to be about $0.68/kg H_2. As a point of comparison, the DOE's goal for the generation cost of H_2 for H_2-powered vehicles is $2

– \$3/kg H_2. Also, given that H_2 has an energy density of 120 MJ/kg, this H_2 cost is equivalent to an energy cost of \$20.40/MWh. As calculated in the previous section, the amount of energy that can be produced in this alkaline thermal treatment scheme, taking into account energy required for heat without the exothermic heat recovery, is 5.7 kWh/day. The energy savings for alkaline thermal treatment as compared to electricity generation from coal is \$75.20/MWh. This translates to an energy savings of \$0.38/day, or about \$11/month.

Based solely on this input and output-based cost estimate, about 98% of the H_2 generation cost is due to the NaOH. The production of NaOH is both an expensive and energy intensive process. CO_2 emissions from the production of NaOH, which is produced primarily from the chlor-alkali process, are also significant. A life cycle analysis for the chlor-alkali process found that in the production of a 50% NaOH solution, 0.81 kg CO_2/kg NaOH solution are emitted (Leimkühler 2010). Applying this emission factor to the daily NaOH requirement for the alkaline thermal treatment of cellulosic MSW of 10.67 kg of 50% NaOH solution, 8.64 kg CO_2/day are embodied in the NaOH requirement. However, as the alkaline thermal treatment process captures carbon from biomass, 2.93 kg of CO_2 are sequestered from the 1.8 kg of starting cellulose, which would decrease the embodied CO_2 from alkaline thermal treatment to about 5.7 kg CO_2/day. Given that 5.7 kWh/day can be produced from the alkaline thermal treatment of cellulosic MSW, assuming 100% conversion, the CO_2 intensity would be 1 kg CO_2/kWh. For the United States, the average CO_2 intensity for electricity generation is 0.61 kg CO_2/kWh (Metz 2005). Given that the CO_2 intensity calculated for alkaline thermal treatment only includes that amount due to the production of NaOH and no other aspects of the process that would require energy, it is clear that NaOH management is a key factor in determining the overall sustainability of the alkaline thermal treatment technology. For these reasons, alkaline thermal treatment

schemes where the NaOH demand can be reduced either through regeneration, through partial or full substitution with another hydroxide, such as $Ca(OH)_2$, or through catalysis, are under investigation.

Given the assumptions and simplifications of this estimation, the estimated H_2 cost of $0.68/kg H_2 would be below the actual cost. Additional costs would depend on how the alkaline thermal treatment technology is implemented, but could include: separation and pretreatment of MSW prior to alkaline thermal treatment, cost of alkaline thermal treatment reactor, which would have to be built to withstand a very alkaline environment, removal and separation of solid products, hydroxide regeneration, cost of H_2 storage if not all of the H_2 generated is immediately being converted to electricity, cost of fuel cell stack, and any O&M that may be required during the life of the system. However, additional cost and energy reductions could result from the integration of a heat recovery system, and if renewable energy could be used in aspects of the process such as reactor heating and NaOH production and/or recovery, this would improve the overall sustainability of the alkaline thermal treatment technology.

Finally, although the alkaline thermal treatment reactor can be operated at relatively low temperature and atmospheric pressure conditions, safety considerations in designing the process must be made for handling the significant NaOH content of the alkaline thermal treatment reactor, as well as for the generated H_2 from the reaction, especially if the system were to be deployed as a distributed energy generation system to be used by unskilled operators.
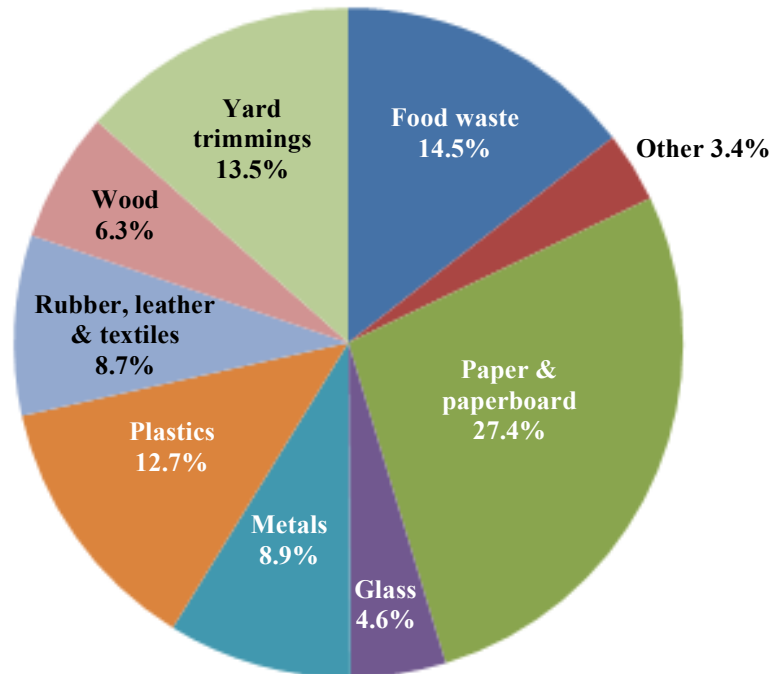
Figure 7.1 Breakdown of total Municipal Solid Waste Generation by waste type in 2012. A total of 251 million tons of MSW was generated. From EPA.

Table 7.1 Costs associated with the alkaline thermal treatment reaction for cellulose to produce

H_2. Na_2CO_3, a value added product, is a benefit and is bolded in the table.

Input	Cost		Amount Needed or Created (kg)
	Material ($/kg)	Electricity ($/kg)	
Cellulose	0	0.018	6.75
NaOH	0.42	0.016	20
Water	0.0013	0.075	0.75
Na_2CO_3	**-0.31**	**0**	**26.5**

CHAPTER 8

CONCLUSIONS AND FUTURE WORK

8.1   Conclusions

This study on the alkaline thermal treatment of biomass has shown that by adding NaOH to the model biomass feedstocks of glucose and cellulose, the degradation pathways observed in biomass pyrolysis that lead to CO_x formation are suppressed, while H_2 with purity as high as 99% is formed, along with gaseous hydrocarbon side products. In comparing the results of this study of the non-catalytic alkaline thermal treatment to those in the literature, important similarities and differences were observed.

Regarding the similarities, the peak H_2 formation rates in both glucose studies occurred around 550 K, and both studies reported conversions to H_2, according to Reaction 1.1, of around 40%. The trends in H_2 and CH_4 formation rates as a function of temperature for the alkaline thermal treatment of cellulose were also quite similar in both studies. Up to 773 K, both studies showed three peak regions of H_2 formation. The highest H_2 formation rate occurred around 523 K in the first peak period, between 500 – 543 K. The second peak period, between 543 – 645 K, was broader than the first but had a smaller peak H_2 formation rate around 580 K. The third peak period, from 645 K – 773 K, had the lowest maximum H_2 formation rate of the three peaks, and this occurred around 710 K. In both this cellulose study and the one found in the literature, the CH_4 formation rate surpassed the H_2 formation rate beyond ~650 K, and the maximum formation rate of CH_4 observed in both studies was around 670 K.

However, the H_2 conversion reported in this cellulose study for the non-catalytic cellulose case was ~50%, whereas in the Ishida cellulose study it was reported as 62%. As

posited in Chapter 4, this difference in conversion was believed to be due to the different methods of conversion calculation employed between this study and the Ishida study. In this study, calculation of conversion by integration of the H_2 formation rate curve, which was the method employed in the Ishida study, yielded more significant variations in the conversion value in repeated trials than the more consistent results obtained from the calculation from the total gas product collected in the tedlar bag. Another difference between the studies was that CO_x and C_2 hydrocarbon gas formation was reported in this study in some cases at temperatures beyond 573 K, whereas none of these gases were reported in the Ishida study. The likely reason for this discrepancy was the improved gas chromatography detection limits for these gases in this study as opposed to the Ishida study (Ishida et al. 2005, Ishida et al. 2006).

Establishing the similarities in H_2 production between this study and previous studies was important in establishing the alkaline thermal treatment technology as a biomass-to-H_2 conversion method, as no other investigations of this reaction had been previously reported. With established base cases for glucose and cellulose, in-depth investigations into the non-catalytic parameters of the alkaline thermal treatment reactions, including temperature, NaOH:Biomass ratio, method of NaOH and biomass mixing, presence of the flow of steam, and steam flow concentration, were conducted. In these studies, which were detailed in Chapters 3 and 4, gas and solid analyses were more comprehensive than were reported in previous studies, which mainly focused on H_2 formation and reported no quantitative information on the solid products formed.

For both glucose and cellulose, increasing the NaOH:Biomass ratio from 0 to the stoichiometric amount, which was 12:1 molar for both feedstocks, decreased CO_x formation to negligible or undetectable levels, and caused H_2 formation and enhanced hydrocarbon formation,

especially CH_4. Increasing the NaOH:Biomass ratio to create a system that was in excess of NaOH lead to a small increase in H_2 conversion from the stoichiometric case for both the glucose and cellulose systems, and the formation of CO_x and hydrocarbon gases were similar to what was observed in the stoichiometric case. These results indicated that conversion of the biomass was not limited by NaOH concentration beyond the stoichiometric ratio, according to Reactions 1 and 2 for glucose and cellulose, respectively, proposed by Ishida.

With the addition of steam flow to the alkaline thermal treatment reactor, both the glucose and cellulose systems experienced increases in H_2 conversion and decreases in hydrocarbon gas formation. The differences between the no steam flow and steam flow cases were more pronounced in the cellulose system, where H_2 conversion nearly doubled. On the other hand, the glucose system experienced a 32% increase in H_2 conversion from the no steam flow case. Similarly, total CH_4 formation decreased by 5 times from the no steam flow to the steam flow case for glucose, but decreased by 35 times for the cellulose case upon the addition of steam flow. These results were also reflected in the GC/MS analysis of the total gaseous product, showing that the addition of NaOH shifted the gas products formed from CO_x compounds and oxygenated hydrocarbons to light hydrocarbons, and the further addition of steam flow acted to increase H_2 formation and suppress hydrocarbon formation. Increasing the concentration of steam flow in the carrier gas from 4.3 kPa to 38.8 kPa did not impact H_2 conversion or hydrocarbon formation as much as going from 0 kPa to 4.3 kPa did; however, slight increases in H_2 conversion and slight decreases in CH_4 formation were observed with increasing steam concentration.

Regarding the formation of Na_2CO_3, it was observed in both of the alkaline thermal treatment of glucose and cellulose studies. Interestingly, when comparing conversions on

Na_2CO_3 and H_2 bases for the cellulose system at 573 K, Na_2CO_3 conversion was significantly higher than H_2 conversion in the no steam flow cases, but both conversions were similar in the steam flow cases. The similarities in final H_2 and Na_2CO_3 conversions in the steam flow cases supported the overall stoichiometry of Reaction 1.2 proposed by Ishida et al., whereas the higher Na_2CO_3 conversion in the absence of steam flow indicated that other reaction pathways were occurring that favored greater carbonation relative to H_2 production.

With a more comprehensive understanding of how the different non-catalytic parameters affected the alkaline thermal treatment reaction, a more in-depth investigation of reaction pathways for the alkaline thermal treatment of cellulose reaction was undertaken. Cellulose was chosen because it is the predominant component of lignocellulosic biomass, the cheapest and most abundant form of biomass, which is being targeted as the feedstock source for second generation biofuels. From the literature, it was reported that the degradation of cellulose with concentrated alkali metal hydroxides additives such as NaOH lead to fragmentation of the polysaccharide into smaller carboxylate compounds such as sodium formate, sodium acetate, and sodium glycolate; thus, these potential pathways were chosen for investigation. A stoichiometric ratio of NaOH:Cellulose was used throughout this study, and all experiments were done in the presence and absence of steam flow to explore its effect in greater detail. The results, detailed in Chapter 5, revealed that these sodium carboxylate salts were indeed forming as the temperature inside the alkaline thermal treatment reactor increased, and that in most cases peak concentrations of these compounds were found in the solids at temperatures lower than 573 K, and as the temperature was increased to 573 K, the concentrations of these compounds in the solids decreased.

Reactions of these sodium carboxylate salts with NaOH were then performed, and gaseous formation in many of the reactions was reported. H_2 was produced from the reactions of sodium formate, sodium oxalate, and sodium glycolate with NaOH, and CH_4 was formed from the reactions of sodium acetate and sodium glycolate with NaOH. In general, the initiation temperature of gaseous formation from each sodium carboxylate salt reaction corresponded to the temperature at which the peak concentration of that sodium carboxylate salts was identified in the alkaline thermal treatment of cellulose, indicating that the decrease in the salt concentration as the reaction temperature increased may be due to the reaction of that sodium carboxylate salt with NaOH. On the other hand, Na_2CO_3 formation was relatively low until the reactor neared 573 K, where its concentration in the solids significantly increased. That the increase in Na_2CO_3 formation from the cellulose system was not observed until temperatures at which the sodium carboxylate salts reacted with NaOH to form gases and Na_2CO_3 also pointed to these potential sodium carboxylate salt reaction pathways in the alkaline thermal treatment reaction.

Sodium glycolate was observed in the largest concentrations, and the H_2 and CH_4 formation rate trends from the sodium glycolate reaction and for the cellulose reaction, both in the presence of steam flow, matched well during the 573 K isothermal period. For this reason, sodium glycolate was reacted with NaOH to 773 K under steam flow and compared to the analogous alkaline thermal treatment of cellulose experiment. From 573 K to 773 K, the formation rate trends for both gases for both systems matched well, indicating that the sodium glycolate reaction with NaOH played an important role in the alkaline thermal treatment of cellulose at higher temperatures.

As shown in Chapter 4, steam flow in the alkaline thermal treatment reactor was shown to have a significant effect on the gaseous products formed. Similarly, steam flow had a significant impact on the formation and consumption of the intermediate sodium carboxylate salts in the cellulose system, as well as on the reactions of the sodium carboxylate salts with NaOH. In particular, the absence of steam flow in the cellulose system caused much more dramatic consumption rates of sodium glycolate at higher temperatures, as well as the formation of unidentified compounds that were not observed in the steam flow studies. H_2 formation from the sodium glycolate and NaOH reaction decreased in the absence of steam flow while CH_4 formation increased, which was similar to what was found in the alkaline thermal treatment of cellulose system.

Finally, comparing Na_2CO_3 conversion to H_2 conversion, based on the stoichiometry of Reaction 1.2, at lower temperatures, H_2 conversion was significantly higher than Na_2CO_3 conversion. As the temperature was increased, Na_2CO_3 conversion surpassed H_2 conversion by 548 K in the no steam flow case, and was about equivalent to H_2 conversion by 573 K for the steam flow case. These results for the intermediate temperature experiments were very similar to what was observed in the cellulose study presented in Chapter 4. Regarding the steam flow cases, greater H_2 formation at lower temperatures compared to carbonation supports the hypothesis that H_2 formation at lower temperatures is associated with the degradation of cellulose, and H_2 formation at higher temperatures is more associated with the reactions of the sodium carboxylate salt intermediate degradation products with NaOH, which for these latter reactions are have Na_2CO_3 formation.

Qualitative analysis of the alkaline thermal treatment of cellulose as a function of reactor temperature revealed significant differences between the no steam flow and steam flow cases. In

the absence of steam flow, no major melting was observed in the system, and the products became progressively darker with increasing temperature, eventually turning black by 573 K. This was in stark contrast to the steam flow system, where around the temperature where the peak H_2 formation rate occurred, around 518 K, a white melt had formed and bubbling was observed. This behavior and color was observed as well at higher temperatures. The formation of a melt indicated that NaOH had degraded the cellulose, which is normally insoluble in water, into water soluble compounds, such as the observed sodium carboxylate salts. Thus, in addition to the different chemistry observed for the alkaline thermal treatment of cellulose in the presence of steam flow, steam flow also acted to improve the mixing and mass transfer of the system through the formation of a melt.

With potential H_2-production reaction pathways identified, isothermal H_2 formation kinetic studies were performed on the cellulose system as well as on the H_2-producing sodium carboxylate salt systems, and these results were presented in Chapter 6. Comparing the isothermal H_2 formation kinetic trends between the cellulose system and the sodium glycolate system at 573 K and 598 K, both trends fell off in a very similar manner, which indicated that conversion of H_2 at these temperatures may be limited by the conversion of sodium glycolate into H_2, pointing again to the potential importance of sodium glycolate as a key intermediate in the alkaline thermal treatment of cellulose system. The H_2 formation kinetics were favored from each intermediate in the following order: sodium formate, sodium oxalate, sodium glycolate. Additionally, sodium formate and sodium oxalate were able to be converted to just H_2 and Na_2CO_3, whereas the maximum conversion achieved for sodium glycolate to H_2 was ~50%, and other species such as CH_4 and sodium acetate were also produced as side products. Thus, if the selectivity of the sodium glycolate reaction could be improved, H_2 conversion in the alkaline

thermal treatment of cellulose may also be improved. Alternatively, if sodium formate or sodium oxalate could be more selectively formed during the alkaline thermal degradation of cellulose, both the selectivity for H_2 and Na_2CO_3 generation would increase and the required temperature for operation could be decreased due to the improved kinetics of these reactions. Variation of non-catalytic parameters, as well as the incorporation of catalysts, could help enable either of these scenarios. Additionally, if increased H_2 generation were observed due to either the alteration of the alkaline degradation products or by improving the selectivity of the sodium glycolate reaction, this could further confirm the proposed sodium carboxylate salt pathways for the alkaline thermal treatment system.

8.2   Future Work

The alkaline thermal treatment technology is a relatively unexplored biomass conversion process, with only a few studies (Ishida et al. 2005, Ishida et al. 2006, Hansen et al. 2011) and this dissertation having explored the process. Thus, there is still much that is unknown and many potential future research directions.

The formation and consumption of the sodium carboxylate salt intermediate species related to the proposed H_2-producing pathways was reported here at discrete temperature and thus discrete time intervals. In order to better understand the mechanisms behind the alkaline thermal treatment reaction as well as to better assess the importance of the proposed sodium carboxylate salt pathways in terms of their contributions to overall H_2 production, an *in situ* monitoring technique is necessary. *In situ* monitoring of biomass thermal degradation processes is just beginning to be reported in the literature, with the first study of the real-time changes in surface functional groups during biomass pyrolysis being published in 2013. In this study, Uchimiya et al. utilized the Diffuse Reflectance Infrared Fourier Transform (DRIFTs) technique

186

to monitor *in situ* surface changes of different biomass compounds as they were pyrolyzed up to 773 K in order to estimate optimal conditions for producing biochar as well as to gain improved mechanistic understanding of biomass pyrolysis (Uchimiya et al. 2013). Applying such a technique to the alkaline thermal treatment system would not only give much more detailed information on the formation and consumption of the sodium carboxylate salts, but could also provide insight into the low temperature H_2 formation that was observed at temperatures below which the sodium carboxylate salts were shown to react with NaOH. However, NaOH could be an issue for the DRIFTs cell, meaning that modifications to the technique would need to be made in order to be applicable to the study of the alkaline thermal treatment system (Orlov, Personal Communication).

From the literature on the alkaline degradation of biomass, there are a number of variables reported to influence the degradation process. These parameters and how they have been reported to influence the degradation products formed were discussed in Chapters 5 and 6, and include concentration of the metal hydroxide, the type of metal hydroxide, the reaction medium (e.g. aqueous, steam flow), air flow over the reactants, temperature of degradation, duration of degradation, and incorporation of non-catalytic or catalytic additives.

In particular, favoring the formation of sodium formate would not only improve the selectivity of the alkaline thermal treatment reaction, as its reaction with NaOH goes completely to H_2 and Na_2CO_3, but it would also lower the necessary temperature for operation, as sodium formate had the best kinetics of any of the H_2-producing intermediates. In a process aimed at converting glucose into formic acid, Jin et al. found that the addition of both NaOH and H_2O_2 to a hydrothermal reaction system yielded 75% formic acid from glucose (Jin et al. 2008). Similarly, Onwudili et al., who conducted several studies on H_2 generation from the alkaline

187

hydrothermal treatment of biomass using NaOH, found that the addition of H_2O_2 to the alkaline hydrothermal system further enhanced H_2 generation (Muangrat et al. 2010). A few studies have also looked at the alkaline degradation of cellulose under more dilute NaOH conditions and found that as NaOH concentration was decreased, formation of sodium formate increased and sodium glycolate formation decreased (Krochta et al. 1988, Machell and Richards 1960, Richards and Sephton 1957). Although the above studies did report improved formate selectivity, as many of the conditions of these studies were different from those in alkaline thermal treatment studies detailed in this dissertation, experiments would need to be conducted to evaluate the efficacy of any changes made in terms of alkaline thermal treatment process. For example, improving sodium formate generation may not translate to more H_2 generation at lower temperatures if other H_2-producing pathways become significantly suppressed; for example, less H_2 associated with the alkaline degradation of cellulose into sodium carboxylate salt intermediates may form, or a larger proportion of intermediates which are unreactive to generate H_2 may form. Investigation of other non-catalytic parameters, as well as investigation into catalysts that may favor greater formate formation is also warranted.

One catalyst-assisted direction that is currently being investigated is using alkaline earth metal hydroxides as opposed to alkali metal hydroxides in the alkaline thermal treatment system. The alkaline earth metal hydroxides have the advantages of being much cheaper than the alkali metal hydroxides, and can be derived from waste material such as steel slag, whereas NaOH is made through the energy intensive chlor-alkali process. However, the alkaline earth metal hydroxides are much less soluble in water, which may mean that mass transfer may play a bigger role with these hydroxides than with the alkali metal hydroxides, as the formation of a melt under steam flow may be less likely. Additionally, as was discussed in Chapter 5, previous study

has found that the alkaline degradation of cellulose with alkaline earth metal hydroxides favors rearrangement reactions as opposed to the fragmentation reactions that are favored when using an alkali metal hydroxide. Thus breaking the cellulose down is more difficult with alkaline earth metal hydroxides, which may also make H_2 generation more difficult. By incorporating catalysts into the alkaline earth metal hydroxide system, the cellulose may be able to be further fragmented, which may improve H_2 generation. Preliminary results have shown that without catalyst, H_2 conversion from $Ca(OH)_2$ is over an order of magnitude much lower than was found from the non-catalytic NaOH system. Also, the non-catalytic $Ca(OH)_2$ system required higher reaction temperatures to generate H_2 than the non-catalytic NaOH system, with H_2 generation beginning around 600 K for the $Ca(OH)_2$ system. The addition of a 10% Ni/ZrO_2 catalyst at 20% loading was able to improve conversion as well as lower the initial H_2 formation temperature for the $Ca(OH)_2$ system. H_2 conversion increased by nearly 25 times from the non-catalytic $Ca(OH)_2$ system to 29%, and H_2 formation was observed below 550 K. These catalytic studies and the potential reaction pathways associated with them continue to be investigated.

Heterogeneous feedstocks must also be investigated in the future, as these will be the real biomass feedstocks fed into any potential alkaline thermal treatment process. The study of the alkaline thermal treatment of cellulose provides a good starting point for lignocellulosic biomass studies, as about 50% of lignocellulosic biomass is comprised of cellulose, with hemicellulose (20-40%) and lignin (10-15%) being the other components (Yang et al. 2007). Converting lignin and hemicellulose into fuels is a less studied aspect of bioenergy, but the field is rapidly growing, with lignocellulosic materials being researched for the second generation of biofuels, as they make up non-edible bioresources and are an important part to the EPA's Renewable Fuels Standard (Alonso et al. 2012). Two studies have shown that interactions occur among the three

lignocellulosic fractions, with one supercritical gasification study showing that H_2 generation decreased with increasing lignin content in the feed (Hosoya et al. 2007, Yoshida and Matsumaura 2001). Thus the study of the alkaline thermal treatment of lignocellulosic biomass would include studies of model hemicellulose and lignin feedstocks individually, as well as mixtures of each of the components with NaOH to test for potential interactive effects. This would then need to be compared to a real lignocellulosic biomass feedstock, where inorganic content and unique structural characteristics could also play roles in the reaction.

A final example of an important direction for future investigation would be to perform comprehensive life cycle and economic analyses of the alkaline thermal treatment process. The alkaline thermal treatment process flow diagram is shown in Figure 2.2. In this dissertation, only the alkaline thermal treatment reaction was considered. As there are numerous ways the alkaline thermal treatment process could be implemented, a quick screening should be done to select those applications most promising for more in-depth analysis. A few applications that may be particularly interesting are: energy generation from household waste, energy generation for farmers from agricultural waste, and energy generation in paper mills. Household and agricultural waste would allow for on-site energy generation from waste materials under a distributed energy generation framework, meaning there would be no cost associated with obtaining the feedstock, and waste could be converted into energy. Paper mills may be an interesting niche application of the alkaline thermal treatment technology because mills already have the infrastructure in place to handle biomass and NaOH. Hemicellulose and lignin are two of the major byproducts of the Kraft Process, which is used in mills to convert wood into pulp consisting of pure cellulose. In particular, lignin is usually just burned to produce energy (Alonso

et al. 2012). Thus the byproducts of the Kraft Process may be able to be used in an alkaline thermal treatment scheme integrated into the paper mill to produce energy.

If the alkaline thermal treatment technology were to be used with NaOH, then the expense and energy needed to generate NaOH would need to be major considerations in life cycle and economic analyses. For example, CO_2 emissions from the production of NaOH, which is produced primarily from the chlor-alkali process, are significant. A life cycle analysis for the chlor-alkali process found that in the production of a 50% NaOH solution, 0.81 kg CO_2/kg NaOH solution are emitted (Leimkuhler 2010). Thus if NaOH were to be used in the alkaline thermal treatment process, its management would be a crucial.

NaOH could be recovered from the Na_2CO_3 formed through a double replacement reaction, such as the one with $Ca(OH)_2$ used in the Kraft recovery process given in Reaction 1.3, or perhaps through electrodialysis. NaOH dependence could also be curbed by partial or full substitution with an alkaline earth metal hydroxide, such as $Ca(OH)_2$, or through incorporation of catalysis. Many other aspects would need to be considered in developing life cycle and economic models, including the construction and maintenance of process components (e.g. alkaline thermal treatment reactor, fuel cell stack), integration of heat recovery from the exothermic alkaline thermal treatment reaction, steam delivery and recovery system, any pre-treatment that may need to be done prior to charging the alkaline thermal treatment reactor with the feed, any separation of undesired byproducts, and recovery and regeneration of catalysts, if used. As previously stated, because of the numerous potential inputs and deployment applications, relevant case studies should be chosen for in-depth feasibility and sustainability analyses.

REFERENCES

Alonso, D.M., Wettstein, S.G., Dumesic, J.A., 2012. Bimetallic catalysts for upgrading of biomass to fuels and chemicals. Chemical Society Reviews 41, 8075–8097.

Al-Raqom, F., Klausner, J. F., 2013. Fluidized bed kinetics for hydrogen production through steam iron oxidation. Proceedings of the ASME 2013 7th International Conference on Energy Sustainability, 1-7.

Amigun, B., Sigamoney, R., Blottnitz, von, H., 2008. Commercialisation of biofuel industry in Africa: A review. Renewable and Sustainable Energy Reviews 12, 690–711.

Asadullah, M., Ito, S.-I., Kunimori, K., Tomishige, K., 2002. Role of catalyst and its fluidization in the catalytic gasification of biomass to syngas at low temperature. Industrial & Engineeirng Chemistry Research 41, 4567–4575.

Asadullah, M., Miyazawa, T., Ito, S.-I., Kunimori, K., Tomishige, K., 2003. Demonstration of real biomass gasification drastically promoted by effective catalyst. Applied Catalysis A: General 246, 103–116.

Asadullah, M., Miyazawa, T., Ito, S.-I., Kunimori, K., Yamada, M., Tomishige, K., 2004. Gasification of different biomasses in a dual-bed gasifier system combined with novel catalysts with high energy efficiency. Applied Catalysis A: General 267, 95–102.

Balat, M., Balat, M., 2009. Political, economic and environmental impacts of biomass-based hydrogen. International Journal of Hydrogen Energy 34, 3589–3603.

Bassilakis, R., Carangelo, R.M., Wojtowicz, M.A., 2001. TG-FTIR analysis of biomass pyrolysis. Fuel 80, 1765–1786.

Boutin, O., Ferrer, M., Lede, J., 1998. Radiant flash pyrolysis of cellulose—Evidence for the formation of short life time intermediate liquid species. Journal of Analytical and Applied Pyrolysis 47, 13–31.

Brazilian Energy Balance 2013. Publisher: Empresa de Pesquisa Energetica, Brazil.

Bridgwater, A.V., 2012. Review of fast pyrolysis of biomass and product upgrading. Biomass and Bioenergy 38, 68–94.

Bridgwater, A.V., Peacocke, G.V.C., 2000. Fast pyrolysis processes for biomass. Renewable and Sustainable Energy Reviews 4, 1–73.

Brown, R.C., 2011. Thermochemical Processing of Biomass: Conversion Into Fuels, Chemicals and Power. Wiley, Hoboken, NJ.

Brown, W.E., Dollimore, D., Galway, A.K., 2008. Theory of Solid State Reaction Kinetics, in:

Bamford, C.H., Tipper, C.F.H. (Eds.), Comprehensive Chemical Kinetics. Elsevier, New York, pp. 41–113.

Cross, C.F., Bevan, K.J., Isaac, J.F.V., 1892. On the production of acetic acid from the carbohydrates. Journal of the Society of Chemical Industry 966–969.

Cushion, E., Whiteman, A., Dieterle, G., 2010. Bioenergy Development: Issues and Impacts for Poverty and Natural Resource Management. Publisher: The World Bank.

Demirbas, A., 2002. Gaseous products from biomass by pyrolysis and gasification: effects of catalyst on hydrogen yield. Energy Conversion and Management 43, 897–909.

Demirbas, A., 2005. Hydrogen Production from Biomass via Supercritical Water Extraction. Energy Sources 27, 1409–1417.

Demirel, Y., 2012. Energy and Energy Types, in: Green Energy and Technology. Springer London, London, 27–70.

Dickinson, C.F., Heal, G.R., 1999. Solid-liquid diffusion controlled rate equations. Thermochimica Acta 340-341, 89–103.

Energy Information Administration Annual Energy Outlook 2011; DOE/EIA-0383; U.S. Department of Energy: Washington, DC, 2011.

Energy Information Administration Annual Energy Outlook 2013; DOE/EIA-0484; U.S. Department of Energy: Washington, DC, 2013.

Ferguson, T.E., Park, Y., Petit, C., Park, A.-H.A., 2012. Novel Approach to Hydrogen Production with Suppressed CO_x Generation from a Model Biomass Feedstock. Energy & Fuels 26, 4486–4496.

Florin, N.H., Harris, A.T., 2008. Enhanced hydrogen production from biomass with in situ carbon dioxide capture using calcium oxide sorbents. Chemical Engineering Science 63, 287–316.

Giddey, S., Ciacchi, F.T., Badwal, S.P.S., 2005. Fuel quality and operational issues for polymer electrolyte membrane (PEM) fuel cells. Ionics 11, 1–10.

Grénman, H., Salmi, T., Murzin, D.Y., 2011. Solid-liquid reaction kinetics – experimental aspects and model development. Reviews in Chemical Engineering 27, 53–77.

Haas, D.W., Hrutfiord, B.F., Sarkanen, K.V., 1967. Kinetic study on the alkaline degradation of cotton hydrocellulose. Journal of Applied Polymer Science 11, 587–600.

Hanaoka, T., Yoshida, T., Fujimoto, S., Kamei, K., Harada, M., Suzuki, Y., Hatano, H., Yokoyama, S.-Y., Minowa, T., 2005. Hydrogen production from woody biomass by steam

gasification using a CO_2 sorbent. Biomass and Bioenergy 28, 63–68.

Hancock, J.D., Sharp, J.H., 1972. Method of comparing solid-state kinetic data and its application to the decomposition of kaolinite, brucite, and BaCO3. Journal of the American Ceramic Society 55 (2), 74–77.

Hansen, N.S., Ferguson, T.E., Panels, J.E., Park, A.-H.A., Joo, Y.L., 2011. Inorganic nanofibers with tailored placement of nanocatalysts for hydrogen production via alkaline hydrolysis of glucose. Nanotechnology 22, 1–14.

Harrison, K.W., Remick, R., Martin, G.D., Hoskin, A., 2010. Hydrogen Production: Fundamentals and Case Study Summaries. U. S. Department of Energy.

Heck, R.M., Farrauto, R., Gulati, S.T., 2002. Catalytic Air Pollution Control, 2nd ed. Wiley, New York.

Hosoya, T., Kawamoto, H., Saka, S., 2007. Cellulose–hemicellulose and cellulose–lignin interactions in wood pyrolysis at gasification temperature. Journal of Analytical and Applied Pyrolysis 80, 118–125.

Hsu, C.C., Hixson, A.N., 1981. C_1 to C_4 oxygenated compounds by promoted pyrolysis of cellulose. Industrial & Engineering Chemistry Product Research and Development 20, 109–114.

Huber, G.W., Chheda, J.N., Barrett, C.J., Dumesic, J.A., 2005. Production of liquid alkanes by aqueous-phase processing of biomass-derived carbohydrates. Science 308, 1446–1450.

Huber, G.W., Iborra, S., Corma, A., 2006. Synthesis of transportation fuels from biomass: chemistry, catalysts, and engineering. Chemical Reviews 106, 4044–4098.

IPCC, 2013: Summary for Policymakers. In: *Climate Change 2013: The Physical Science Basis. Contribution of Working Group I to the Fifth Assessment Report of the Intergovernmental Panel on Climate Change* [Stocker, T.F., D. Qin, G.-K. Plattner, M. Tignor, S.K. Allen, J. Boschung, A. Nauels, Y. Xia, V. Bex and P.M. Midgley (eds.)]. Cambridge University Press, Cambridge, United Kingdom and New York, NY, USA.

Ishida, M., Otsuka, K.Y., Takenaka, S., Yamanaka, I., 2005. One-step production of CO- and CO_2-free hydrogen from biomass. Journal Chemical Technology Biotechnology 80, 281–284.

Ishida, M., Takenaka, S., Yamanaka, I., Otsuka, K., 2006. Production of CO_x-free hydrogen from biomass and NaOH mixture: effect of catalysts. Energy & Fuels 20, 748–753.

Ishida, M., Toida, M., Shimizu, T., Takenaka, S., Otsuka, K.Y., 2004. Formation of hydrogen without CO_x from carbon, water, and alkali hydroxide. Industrial & Engineering Chemistry Research 43, 7204–7206.

Jin, F., Yun, J., Li, G., Kishita, A., Tohji, K., Enomoto, H., 2008. Hydrothermal conversion of carbohydrate biomass into formic acid at mild temperatures. Green Chemistry 10, 612–615.

Kalinci, Y., Hepbasli, A., Dincer, I., 2009. Biomass-based hydrogen production: A review and analysis. International Journal of Hydrogen Energy 34, 8799–8817.

Khawam, A., Flanagan, D.R., 2006. Solid-state kinetic models: Basics and mathematical fundamentals. Journal of Physical Chemistry B 110, 17315–17328.

Knill, C.J., Kennedy, J.F., 2003. Degradation of cellulose under alkaline conditions. Carbohydrate Polymers 51, 281–300.

Kostick, D.S., 2013. Soda ash. U.S. Geological Survey, Mineral Commodity Summaries.

Krochta, J.M., Hudson, J.S., 1985. Alkaline thermochemical degradation of rice straw to organic acids. Agricultural Wastes 14, 243–254.

Krochta, J.M., Tillin, S.J., Hudson, J.S., 1987. Degradation of polysaccharides in alkaline solution to organic acids: Product characterization and identification. Journal of Applied Polymer Science 33, 1413–1425.

Krochta, J.M., Tillin, S.J., Hudson, J.S., 1988. Thermochemical conversion of polysaccharides in concentrated alkali to glycolic acid. Applied Biochemistry and Biotechnology 17, 23–32.

Kruse, A., 2009. Hydrothermal biomass gasification. The Journal of Supercritical Fluids 47, 391–399.

Kumar, A., Jones, D.D., Hanna, M.A., 2009. Thermochemical biomass gasification: A review of the current status of the technology. Energies 2, 556–581.

Lee, H. -J., Ni, H., Wu, D.T., Ramirez, A.G., 2005. Experimental determination of kinetic parameters for crystallizing amorphous NiTi thin films. Applied Physics Letters 87, 114102-1–114102-3.

Leimkuhler, H.-J. (Ed.), 2010. Managing CO_2 Emissions in the Chemical Industry. Wiley, Weinheim.

Lenihan, P., Orozco, A., O'Neill, E., Ahmad, M.N.M., Rooney, D.W., Walker, G.M., 2010. Dilute acid hydrolysis of lignocellulosic biomass. Chemical Engineering Journal 156, 395–403.

Levelized Cost and Levelized Avoided Cost of New Generation Resources in the Annual Energy Outlook 2014, 2014. U.S. Energy Information Administration, Washington, DC.

Levin, D.B., Chahine, R., 2010. Challenges for renewable hydrogen production from biomass.

International Journal of Hydrogen Energy 35, 4962–4969.

Lin, S., Harada, M., Suzuki, Y., Hatano, H., 2004. Gasification of organic material/CaO pellets with high-pressure steam. Energy & Fuels 18, 1014–1020.

Lin, S.-Y., Suzuki, Y., Hatano, H., Harada, M., 2002. Developing an innovative method, HyPr-RING, to produce hydrogen from hydrocarbons. Energy Conversion and Management 43, 1283–1290.

Liu, J., Chu, X., Zhu, L., Hu, J., Dai, R., Xie, S., Pei, Y., Yan, S., Qiao, M., Fan, K., 2010. Simultaneous aqueous-phase reforming and KOH carbonation to produce CO_x-free hydrogen in a single reactor. ChemSusChem 3, 803–806.

Machell, G., Richards, G.N., 1960. Mechanism of saccharinic acid formation. Part I. Competing reactions in the alkaline degradation of 4-O-methyl-D-glucose, maltose, amylose, and cellulose. Journal of the Chemical Society 1924–1931.

Mahood, S.A., Cable, D.E., 1919. Reaction products of alkali-sawdust fusion acetic, formic, and oxalic acids and methyl alcohol. The Journal of Industrial and Engineering Chemistry 11, 651–655.

McKendry, P., 2002a. Energy production from biomass (part 1): overview of biomass. Bioresource Technology 83, 37–46.

McKendry, P., 2002b. Energy production from biomass (part 2): conversion technologies. Bioresource Technology 83, 47–54.

Meier, D., Faix, O., 1999. State of the art of applied fast pyrolysis of lignocellulosic materials - a review. Bioresource Technology 68, 71–77.

Metz, B., Kuijpers, L., Solomon, S., Anderson, S.O., Davidson, O., Pons, J., de Jager, D., Kestin, T., Manning, M., Meyer, L. (Eds.), 2005. Safeguarding the Ozone Layer and the Global Climate System. Cambridge University Press.

Mohan, S.V., Mohanakrishna, G., Ramanaiah, S.V., Sarma, P.N., 2008. Simultaneous biohydrogen production and wastewater treatment in biofilm configured anaerobic periodic discontinuous batch reactor using distillery wastewater. International Journal of Hydrogen Energy 33, 550–558.

Muangrat, R., Onwudili, J. A., & Williams, P. T., 2010. Reaction products from the subcritical water gasification of food wastes and glucose with NaOH and H_2O_2. Bioresource Technology 101 (17), 6812–6821.

Navarro, R.M., Pena, M.A., Fierro, J.L.G., 2007. Hydrogen production reactions from carbon feedstocks: Fossil fuels and biomass. Chemical Reviews 107, 3952–3991.

New York City Water Board Rates & Regulations. The City of New York. URL http://www.nyc.gov/html/nycwaterboard/html/rate_schedule/index.shtml (accessed 7.22.14).

Ni, M., Leung, D.Y.C., Leung, M.K.H., Sumathy, K., 2006. An overview of hydrogen production from biomass. Fuel Processing Technology 87, 461–472.

Niemela, K., 1990. The formation of hydroxy monocarboxylic acids and dicarboxylic acids by alkaline thermochemical degradation of cellulose. Journal of Chemical Technology and Biotechnology 48, 17–28.

Niemela, K., Sjostrom, E., 1986. The conversion of cellulose to carboxylic acids by a drastic alkaline treatment. Biomass 11, 215–221.

Ninan, K.N., 1985. Kinetics of solid state thermal decomposition reactions. Journal of Thermal Analysis 35, 1267–1278.

Nishikawa, J., Nakamura, K., Asadullah, M., Miyazawa, T., Kunimori, K., Tomishige, K., 2008. Catalytic performance of $Ni/CeO_2/Al_2O_3$ modified with noble metals in steam gasification of biomass. Catalysis Today 131, 146–155.

Oefner, P.J., Lanziner, A.H., Bonn, G., Bobleter, O., 1992. Quantitative studies on furfural and organic acid formation during hydrothermal, acidic and alkaline degradation of *D*-Xylose. Monatshefte fur Chemie Chemical Monthly 123, 547–556.

Olah, G.A., 2005. Beyond Oil and Gas: The Methanol Economy. Angewandte Chemoe International Edition 44, 2636–2639.

Onsager, O.-T., Brownriggi, M.S.A., Lodeng, R., 1996. Hydrogen production from water and CO via alkali metal formate salts. International Journal of Hydrogen Energy 21, 883–885.

Onwudili, J.A., Williams, P.T., 2009. Role of sodium hydroxide in the production of hydrogen gas from the hydrothermal gasification of biomass. International Journal of Hydrogen Energy 34, 5645–5656.

Onwudili, J.A., Williams, P.T., 2010. Hydrothermal reactions of sodium formate and sodium acetate as model intermediate products of the sodium hydroxide-promoted hydrothermal gasification of biomass. Green Chemistry 12, 2214–2224.

Othmer, D.F., Gamer, C.H., Jacobs, J.J., Jr, 1942. Oxalic acid from sawdust. Industrial and Engineering Chemistry 34, 252–257.

Patwardhan, P.R., Satrio, J.A., Brown, R.C., Shanks, B.H., 2010. Influence of inorganic salts on the primary pyrolysis products of cellulose. Bioresource Technology 101, 4646–4655.

Phanphanich, M., Mani, S., 2011. Impact of torrefaction on the grindability and fuel characteristics of forest biomass. Bioresource Technology 102, 1246–1253.

Philpot, C.W., 1971. The pyrolysis products and thermal characteristics of cottonwood and its components (No. INT-107). USDA Forest Service.

Ponder, G.R., Richards, G.N., 1993. Pyrolysis of inulin, glucose, and fructose. Carbohydrate Research 244, 341–359.

Pretsch, E., Buhlmann, P., & Badertscher, M. 2009. Structure Determination of Organic Compounds, 4 ed. Springer, London.3

Radlein, D., Piskorz, J., Scott, D.S., 1991. Fast pyrolysis of natural polysaccharides as a potential industrial process. Journal of Analytical and Applied Pyrolysis 19, 41–63.

Richards, G.N., Sephton, H.H., 1957. The alkaline degradation of polysaccharides. Part I. Soluble products of the action of sodium hydroxide on cellulose. Journal of the Chemical Society 4492–4499.

Rolin, A., Richard, C., Masson, D., Deglise, X., 1983. Catalytic Conversion of Biomass by Fast Pyrolysis. Journal of Analytical and Applied Pyrolysis 5, 151–166.

Roswell, M.C., Dickson, J.V., 1918. The action of sodium hydroxide on carbon monoxide, sodium formate and sodium oxalate. Journal of the American Chemical Society 40, 1779–1786.

Saeman, J.F., 1945. Kinetics of wood saccharification: Hydrolysis of cellulose and decomposition of sugars in dilute acid at high temperature. Industrial and Engineering Chemistry 37, 43–52.

Salmi, T., Grénman, H., Wärnå, J., Murzin, D.Y., 2013. New modelling approach to liquid–solid reaction kinetics: From ideal particles to real particles. Chemical Engineering Research and Design 91, 1876–1889.

Saxena, R.C., Adhikari, D.K., Goyal, H.B., 2009. Biomass-based energy fuel through biochemical routes: A review. Renewable and Sustainable Energy Reviews 13, 167–178.

Saxena, S., Kumar, S., Drozd, V., 2011. A modified steam-methane-reformation reaction for hydrogen production. International Journal of Hydrogen Energy 36, 4366–4369.

Saxena, S.K., 2003. Hydrogen production by chemically reacting species. International Journal of Hydrogen Energy 28, 49–53.

Saxena, S.K., Drozd, V., Durygin, A., 2008. A fossil-fuel based recipe for clean energy. International Journal of Hydrogen Energy 33, 3625–3631.

Schmieder, H., Abeln, J., Boukis, N., Dinjus, E., Kruse, A., Kluth, M., Petrich, G., Sadri, E., Schacht, M., 2000. Hydrothermal gasification of biomass and organic wastes. Journal of Supercritical Fluids 17, 145–153.

Seo, J.G., Kwon, J.T., Kim, J., Kim, W.S., Jung, J.T., 2007. Impurity effect on proton exchange membrane fuel cell. Presented at the International Forum on Strategic Technology, Ulaanbaatar, pp. 484–487.

Shafizadeh, F., Bradbury, A.G.W., 1979. Thermal degradation of cellulose in air and nitrogen at low temperatures. Journal of Applied Polymer Science 23, 1431–1442.

Shafizadeh, F., Lai, Y.Z., 1972. Base catalyzed, pyrolystic rearrangement of some monosaccharides. Carbohydrate Research 26, 83–89.

Smil, V., 2005. Energy at the Crossroads. The MIT Press, Cambridge.

Socrates, G., 2004. Infrared and Raman Characteristic Group Frequencies: Tables and Charts, 3rd ed. Wiley, Hoboken, NJ.

Solid Phase Heat Capacity - Sodium Hydroxide, 2011. National Institute of Standards and Technology. URL http://webbook.nist.gov/cgi/cbook.cgi?ID=C1310732&Units=SI&Mask=3FFF&Type=JAN AFS&Plot=on#JANAFS (accessed 7.22.14).

Srirangan, K., Akawi, L., Moo-Young, M., Chou, C.P., 2012. Towards sustainable production of clean energy carriers from biomass resources. Applied Energy 100, 172–186.

Stambouli, A.B., 2011. Fuel cells: The expectations for an environmental-friendly and sustainable source of energy. Renewable and Sustainable Energy Reviews 15, 4507–4520.

Su, S., Li, W., Bai, Z., Xiang, H., 2008. A preliminary study of a novel catalyst $Al_2O_3 \cdot Na_2O \cdot xH_2O/NaOH/Al(OH)_3$ for production of hydrogen and hydrogen-rich gas by steam gasification from cellulose. International Journal of Hydrogen Energy 33, 6947–6952.

Su, S., Li, W., Bai, Z., Xiang, H., Bai, J., 2010a. Effects of ionic catalysis on hydrogen production by the steam gasification of cellulose. International Journal of Hydrogen Energy 35, 4459–4465.

Su, S., Li, W., Bai, Z.-Q., Xiang, H.-W., Bai, J., 2010b. Production of hydrogen by steam gasification from lignin with $Al_2O_3 \cdot Na_2O \cdot xH_2O/NaOH/Al(OH)_3$ catalyst. Journal of Fuel Chemistry and Technology 38, 270–274.

Sutton, D., Kelleher, B., Ross, J.R.H., 2001. Review of literature on catalysts for biomass gasification. Fuel Processing Technology 73, 155–173.

Tongamp, W., Zhang, Q., Saito, F., 2010. Generation of H_2 gas from polystyrene and poly(vinyl alcohol) by milling and heating with $Ni(OH)_2$ and $Ca(OH)_2$. Fuel Processing Technology 91, 272–276.

Toor, S.S., Rosendahl, L., Rudolf, A., 2011. Hydrothermal liquefaction of biomass: A review of subcritical water technologies. Energy 36, 2328–2342.

U. S. Energy Information Administration Frequently Asked Questions, 2014. U. S. Department of Energy. URL http://www.eia.gov/tools/faqs/faq.cfm?id=97&t=3 (accessed 7.22.14).

U.S. Environmental Protection Agency, 2014. Municipal solid waste generation, recycling, and disposal in the United States: Facts and Figures for 2012. United States Environmental Protection Agency, Washington, DC.

Uchimiya, M., Orlov, A., Ramakrishnan, G., Sistani, K., 2013. In situ and ex situ monitoring of biochar's surface functional groups. Journal of Analytical and Applied Pyrolysis 102, 53–59.

USA State & Country QuickFacts, 2014. U.S. Census Bureau. URL http://quickfacts.census.gov/qfd/states/00000.html (accessed 7.22.14).

Van Loon, L.R., Glaus, M.A., 1997. Review of the kinetics of alkaline degradation of cellulose in view of its relevance for safety assessment of radioactive waste repositories. Journal of Environmental Polymer Degradation 5, 97–109.

Wantanabe, M., Inomata, H., Arai, K., 2002. Catalytic hydrogen generation from biomass (glucose and cellulose) with ZrO_2 in supercritical water. Biomass and Bioenergy 22, 405–410.

Whistler, R.L., BeMiller, J.N., 1958. Alkaline Degradation of Polysaccharides. Advances in Carbohydrate Chemistry 13, 289–329.

White, J.E., Catallo, W.J., Legendre, B.L., 2011. Biomass pyrolysis kinetics: A comparative critical review with relevant agricultural residue case studies. Journal of Analytical and Applied Pyrolysis 91, 1–33.

Xu, Y., Tian, Z., Wen, G., Xu, Z., Qu, W., Lin, L., 2006. Production of CO_x-free hydrogen by alkali enhanced hydrothermal catalytic reforming of biomass-derived alcohols. Chemistry Letters 35, 216–217.

Yang, B.Y., Montgomery, R., 2007. Alkaline degradation of invert sugar from molasses. Bioresource Technology 98, 3084–3089.

Yang, H., Yan, R., Chen, H., Lee, D.H., Zheng, C., 2007. Characteristics of hemicellulose, cellulose and lignin pyrolysis. Fuel 86, 1781–1788.

Yeh, T.M., Dickinson, J.G., Franck, A., Linic, S., Thompson, L.T., Jr, Savage, P.E., 2012. Hydrothermal catalytic production of fuels and chemicals from aquatic biomass. Journal of Chemical Technology and Biotechnology 88, 13–24.

Yoshida, T., Matsumura, Y., 2001. Gasification of cellulose, xylan, and lignin mixtures in

supercritical water. Industrial & Engineering Chemistry Research 40, 5469–5474.

Yu, J., Savage, P.E., 1998. Decomposition of formic acid under hydrothermal conditions. Industrial & Engineering Chemistry Research 37, 2–10.

Zhang, J., Datta, R., 2002. Sustained potential oscillations in proton exchange membrane fuel cells with PtRu as anode catalyst. Journal of the Electrochemical Society 149, A1423–A1431.

Zhang, Q., Kang, I., Tongamp, W., Saito, F., 2009. Generation of high-purity hydrogen from cellulose by its mechanochemical treatment. Bioresource Technology 100, 3731–3733.

APPENDIX A

LIST OF PUBLICATIONS AND PATENTS

<u>Published</u>

Ferguson, T.E., Park, Y., Petit, C., Park, A.-H.A., 2012. Novel approach to hydrogen production with suppressed CO_x generation from a model biomass feedstock. Energy & Fuels 26, 4486–4496.

Hansen, N.S., **Ferguson, T.E.**, Panels, J.E., Park, A.-H.A., Joo, Y.L., 2011. Inorganic nanofibers with tailored placement of nanocatalysts for hydrogen production via alkaline hydrolysis of glucose. Nanotechnology 22, 1–14.

<u>In Review</u>

Ferguson, **T.E.**, Park, A.-H.A., 2014. Non-catalytic conversion of cellulose to high-purity hydrogen at mild reaction conditions via alkaline thermal treatment. International Journal of Hydrogen Energy (*In Review*).

Ferguson, T.E., Park, A.-H.A., 2014. Production of high-purity hydrogen from cellulose through a carboxylate intermediate pathway via alkaline thermal treatment. Energy & Environmental Science (*In Review*).

Ferguson, T.E., Park, A.-H.A., 2014. Kinetics of hydrogen formation from cellulose and reactive intermediates in the alkaline thermal treatment reaction. Industrial & Engineering Chemistry Research (*In Review*).

Stonor, M.R.A., **Ferguson, T.E.**, Chen, J., Park, A.-H.A. Hydrogen production using $Mg(OH)_2$ and $Ca(OH)_2$ as replacements for NaOH in the alkaline thermal treatment of cellulose. Energy & Environmental Science (*In Review*).

<u>Patents</u>

Park, A.-H.A., **Ferguson, T.E.** Methods and systems for the co-generation of gaseous fuels and fertilizer from biomass and biogenic wastes. U.S. Patent Application 14/237,701, 2014.